EXPRESSION OF ECDYSONE AND RETINOID X RECEPTORS IN THE IXODID TICK, *Amblyomma americanum* (L.)

By

XIAOJING JIN

Bachelor of Science

Zhejiang University

Hangzhou, Zhejiang, P. R. China

1989

Submitted to the Faculty of the
Graduate College of the
Oklahoma State University
in partial fulfillment of
the requirement for
the Degree of
MASTER OF SCIENCE
December, 1998

EXPRESSION OF ECDYSONE AND RETINOID X RECEPTORS IN THE IXODID TICK, *Amblyomma americanum* (L.)

Thesis Approved:

Melanie J. Palmer
Thesis Adviser

John R. Sauer

Jack W. Dillwith

James Maly

Wayne B. Powell
Dean of the Graduate College

ACKNOWLEDGMENTS

I would like to have this opportunity to express my gratitude to all who have given me great help during the years of my graduate study in Entomology Department in Oklahoma State University.

First of all, I wish to express my sincere appreciation to my major advisor, Dr. Melanie Palmer for her constructive guidance, intelligent suggestion and constant support. She taught me as many things as she could like molecular techniques, how to solve problems in experiments, how to keep record of experiment results and scientific writing. I have got valuable experience working in Dr. Palmer laboratory.

I thank my committee member Dr. John Sauer for his instruction in regarding of tick salivary gland morphology. I thank my committee member Dr. Jack Dillwith for his encouragement when I gave my first seminar. I thank my committee member Dr. Jerry Malayer for his instruction in regarding of *in situ* hybridization.

I thank Dr. Katherine Kocan for her intelligent suggestions in tissue preparation including fixation, embedding, and sectioning for *in situ* hybridization. Dr. Stephen Wikel also gave me good suggestions in *in situ* hybridization techniques.

I particularly thank Xiaoping Guo in our laboratory, who is always ready to help and gives advice. From her, I learn a lot of hands-on molecular

techniques. I will never forget the help Xiaoping and her husband, Dr. Yinghua Huang, give to my family.

I thank Jim Tucker, who works in Dr. Sauer's laboratory, Robin Madden, who works in Dr. Dillwith's laboratory and Ms. Ginger Baker. who worked in EM laboratory, for giving me many technical assistance.

I thank the Department of Entomology, Oklahoma State University for supporting me during my Master's program.

I give my special appreciation to my parents, who have strong believe in education, who sacrifice so much time and energy for our education and my younger brother and my younger sister, who give me all their loves and supports, and my husband Xiaogang Chen, who influences me with his strength and encouragement and optimist attitude about life.

Finally, with deepest love and appreciation, I dedicated this thesis to my grandmother, Jiasheng Liu.

TABLE OF CONTENTS

LIST OF TABLES

Table Page

LIST OF FIGURES

Figure Page

Figure Page

NOMENCLATURE

20-OH ecdysone	20-hydroxy ecdysone
amol	attomole (10^{-18} moles)
AaEcR	*Aedes aegypti* ecdysone receptor
AaUSP	*Aedes aegypti* ultraspiracle
AamEcR	*Amblyomma americanum* ecdysone receptor
AamRXR	*Amblyomma americanum* retinoid X receptor
ACTH	adrenocorticotropic hormone
AF-1	activation function domain-1
AF-2	activation function domain-2
ATP	adenosine triphosphate
BmCF1	*Bombyx mori* RXR-type receptor
BmEcR	*Bombyx mori* ecdysone receptor
BmUSP	*Bombyx mori* ultraspiracle
BSA	bovine serum albumin
cDNA	complementary DNA
CfEcR	*Choristoneura fumiferana* ecdysone receptor
CtEcR	*Chironomus tentans* ecdysone receptor
DBD	DNA binding domain
DEPC	diethyl pyrocarbonate
DmEcR	*Drosophila melanogaster* ecdysone receptor
DMSO	dimethyl sulfoxide
DmUSP	*Drosophila melanogaster* ultraspiracle
DNA	deoxyribonucleic acid
dNTP	deoxyribonucleoside triphosphate
DR	direct repeat
DTT	Dithiothreitol
EDTA	disodium ethylenediamine tetraacetate
EcR	ecdysone receptor
EcRE	ecdysone response element
HBD	hormone binding domain

HRE	hormone response element
IR	inverted repeat
KCl	potassium chloride
KOAc	potassium acetate
KOH	potassium hydroxide
LBD	ligand binding domain
LcEcR	*Lucilia cuprina* ecdysone receptor
$MgCl_2$	magnesium chloride
$Mg(OAc)_2$	magnesium acetate
mM	milli molar (10^{-3} molar)
MOPS	morpholinopropane sulphonic acid
mRNA	messenger RNA
mRXRα	murine retinoid X receptor alpha
MsEcR	*Manduca sexta* ecdysone receptor
MsUSP	*Manduca sexta* ultraspiracle
MurA	muristerone A
ng	nanogram (10^{-9} gram)
nM	nanomolar (10^{-9} molar)
pg	picogram (10^{-12} gram)
pM	picomolar (10^{-12} molar)
Poly(A)	polyadenylate
Pu	purine
Py	pyrimidine
RAR	retinoic acid receptor
PPAR	peroxisome proliferator-activated receptor
PTTH	prothoacicotropic hormone
RNA	ribonucleic acid
RXR	retinoid X receptor
RT-PCR	reverse transcription-polymerase chain reaction
SDS	sodium dodecyl sulfate
SDS-PAGE	sodium dodecylsulfatepolyacrylamide gel electrophoresis
SR	steroid hormone
SSC	sodium saline citrate
ssDNA	salmon sperm DNA
TmEcR	*Tenebrio molitor* ecdysone receptor

TR	thyroid hormone receptor
Tris-HCl	Trishydroxymethylaminomethane-hydrochloric acid
VDR	vitamin D receptor
μg	microgram (10^{-6} gram)
μM	micromolar (10^{-6} molar)

CHAPTER I

INTRODUCTION

Background and Significance

Ticks are obligate blood sucking arthropods that transmit a wide variety of pathogens. These pathogens, including viruses, rickettsiae, spirochetes, bacteria, fungi, protozoa and filarial nematodes, cause several life threatening diseases to livestock and humans (Hoskins, 1991).

There are 825 species of ticks that fall into two major families. Ixodidae, with 650 species, are also called hard ticks because of the hardened dorsal scutum. Argasidae, with 170 species, are referred to as soft ticks because they lack this hard cover (Hoskins, 1991). All ixodid ticks have four developmental stages: embryo, larva, nymph and adult (Hoskins, 1991).

The ixodid tick *Amblyomma americanum* (L.), commonly known as the lone star tick because of the silver spot on its scutum, transmits pathogens that cause *Tremia coxiella* infection (Q fever) and babesiosis in the central and southeastern regions of the United States, Mexico, Central and South America (Hoskins, 1991). *A. americanum* has a three-host life cycle and the host range includes livestock, dogs, deer, humans and birds. This multi-host feature increases the chances of dissemination of pathogens between hosts and ticks and among hosts.

A. americanum feeds slowly in both immature and adult stages. Larvae and nymphs feed for 3-5 days while adult females feed for 9-14 days and imbibe a large quantity of blood. The ratio of fed to unfed body weight at repletion may

exceed 100 in adult females and the reproductive potential is high enough to produce thousands of eggs following a single blood meal (Hair and Bowman, 1986; Hoskins, 1991). An important step in controlling ticks and tick-borne diseases is uncovering the basic molecular mechanisms that govern tick development, feeding and reproduction.

Steroid Hormone Action

Steroid hormones are a large class of lipid-soluble hormones that regulate complex events in development, differentiation and in physiological responses in both vertebrates and invertebrates (Voet and Voet, 1990). In mammals, the major steroid hormones are the adrenocortical hormones, the sex hormones (androgens and estrogens) and vitamin D-derived hormones (Lehninger et al., 1993). In arthropods, the principal steroid hormones are ecdysteroids. Ecdysone and 20-OH ecdysone are the best characterized ecdysteroids in ticks (Sonenshine, 1991).

In insects, the natural sources of ecdysteroids have been found in prothoracic or corresponding glands in immature stages (Chino et al., 1974; King et al., 1974; Rees, 1985). However, in the immature stages of some holometabolous insects where the prothoracic glands degenerate before the pupal/adult ecdysteroid peak, the epidermis and oenocytes may be the alternative sources of ecdysteroid synthesis (Dai and Gilbert, 1991; Delbecque et al., 1986; Sakurai et al., 1991). In the adult stages of most insects except Apterygota, where the prothoracic glands are absent, the ovary, the epidermis and possibly oenocytes are sources of ecdysteroid synthesis (Delbecque et al., 1990; Koolman, 1990).

A number of tissues have been proposed as sites for ecdysteroid synthesis in ticks. In the argasid tick *Ornithodoros parkeri* , the epidermis has been found to

be the main source of ecdysone synthesis and the fat body the site for conversion of ecdysone to 20-OH ecdysone (Zhu et al., 1991). Ecdysteroid synthesis has also been demonstrated in whole integumental tissue (epidermis and fat body included) in the ixodid tick *Amblyomma hebraeum* (Lomas et al., 1997), suggesting that ecdysteroid synthesis occurs in analogous tissues in both argasid and ixodid ticks. Since both prothoracic glands and epidermis originate from ectoderm, this may reflect an evolutionary division between primitive arthropods, where the epidermis serves both as a source and target of ecdysteroids, and more advanced arthropods, where the epidermal tissue responsible for producing ecdysteroids has specialized into a gland.

The prothoacicotropic hormone (PTTH) is secreted by the corpora cardiaca and stimulates the production of ecdysone in the prothoracic glands in insects. This is similar to vertebrates, where adrenocorticotropic hormone (ACTH) triggers the adrenal cortical steroidogenesis. However, ticks lack the classical neuroendocrine and endocrine structures of insects: the corpora cardiaca, corpora allata and prothoracic glands. The central nervous system is condensed into a periesophageal synganglion. There has been evidence that implies the existence of a neuropeptide produced by the synganglion that stimulates integumental tissue ecdysteroidogenesis in *A. hebraeum* (Lomas et al., 1997). Other presumed neuropeptides in the synganglion are proposed to regulate diapause and vitellogenesis in various ixodid and argasid ticks (Ioffe, 1964; Khalil, 1976; Oliver et al., 1984; Sonnenshine, 1991; Schriefer, 1991). Thus, the brain-prothoracic gland axis of insects might be analogous to the vertebrate pituitary-adrenal axis and tick synganglion-epidermis axis.

The action of ecdysteroids in insects is best known for controlling the processes of molting and metamorphosis. The molting process consists of generation of a new exoskeleton and separation (apolysis) and loss (ecdysis) of

the old one. During metamorphosis, ecdysteroids induce imaginal tissues to generate adult structures and larval tissues to undergo apoptosis (Jiang et al., 1997). In the tobacco hornworm *Manduca sexta* , ecdysteroids stimulate both larval-larval and larval-pupal molts (Bollenbacher et al., 1981). In *Drosophila melanogaster*, molts of the first and second larval instars are triggered by a pulse of ecdysone. A higher titer ecdysone pulse at the end of third larval instar triggers metamorphosis (Nijhout, 1994). In both processes, ecdysteroid titers show a temporal pattern that corresponds to physiological and morphological changes. Ecdysteroids have also been shown to stimulate ovarian and embryonic development in some insects (Bollenbacher et al., 1978; Bulliere et al., 1979). In dipterans, ecdysteroids control puffing of polytene chromosomes, the morphological manifestation of transcription (Ashburner et al., 1974).

Steroid Hormone Receptors

All steroid hormones share a common mode of action. The lipid-soluble steroid hormones readily pass through the plasma membrane of target cells by passive diffusion. They either bind to their specific receptors in the cytosol and then are translocated to the nucleus or they enter the nucleus directly and bind to their receptors. Upon hormone binding, the receptor undergoes a conformational change to facilitate DNA binding and the hormone-receptor complex binds to hormone response elements (HREs) in target genes which either activates or represses gene transcription (Voet and Voet, 1990).

The steroid hormone receptors belong to a superfamily of nuclear receptors that encode transcription factors, many of which are ligand-activated. Most of the nuclear receptors share a highly conserved structure that consists of six functional domains (Figure 1). The amino- terminal domain (A/B domain), which is involved in the transcriptional activation, varies in length and amino

acid composition. The central DNA binding domain (C domain), which consists of 66-68 amino acids, is the most conserved domain among steroid receptors. Twenty out of 66-68 amino acids are invariant. Among the invariant residues, eight cysteine residues fold into two "zinc finger" motifs, in which four cysteines are coordinated with a zinc atom. The proximal (P) box in the first zinc finger determines the DNA binding site specificity and distal (D) box in the second zinc finger determines half-site spacing specificity (Umesono and Evans, 1989). The ligand binding domain (E domain) binds the ligand and participates in dimerization, nuclear translocation and hormone-dependent transcriptional activation. Within the ligand binding domain, a set of nine conserved hydrophobic heptad repeats is proposed to form the dimerization interface between receptor monomers. Another highly conserved structure, a hydrophobic cavity consisting of two β-strands and two-three α-helices, is proposed to form the ligand binding pocket (Bourguet et al., 1995; Renaud et al., 1995; Wagner et al., 1995). Domain D provides a hinge between the DNA and ligand binding domain. In the thyroid-hormone and retinoic-acid receptors, the hinge region also contributes to ligand-independent repression (Baniahmad, 1993; Baniahmad, 1995). The function of the carboxy-terminal domain F, which is absent in some members, is unknown (Evans, 1988).

Within the nuclear receptor superfamily, there are six subfamilies: (i) a large one containing the thyroid hormone receptors (TRs), retinoic acid receptors (RARs), peroxisome proliferator-activated receptors (PPARs), vitamin D receptors (VDRs) and ecdysone receptors (EcRs) as well as numerous orphan receptors; (ii) one containing retinoid X receptors (RXRs) and some orphan receptors; (iii) one containing steroid receptors (SRs); (iv) one containing the NGFIB orphan receptors; (v) one containing FTZ-F1 orphan receptors; and (vi) one containing the GCNF1 orphan receptor (Laudet, 1997) (Figure 2).

Among the members of the nuclear receptor superfamily, RXR is a unique member that appears to be a pleiotropic regulator of hormone response pathways in both vertebrates and invertebrates (Mangelsdorf and Evans, 1995). In contrast to steroid hormone receptors, which function as homodimers, RXR pairs with other nuclear receptors to form heterodimers. In vertebrates, it pairs with RAR, TR, VDR and PPAR as a silent partner that does not bind ligand. It can also form homodimers that bind 9 cis-retinoic acid (Mangelsdorf and Evans, 1995). In addition, it pairs with LXR, a novel member of the nuclear receptor superfamily, to form a RXR/LXR heterodimer which can be activated by the RXR ligand (9 cis-retinoic acid) (Willy et al., 1995), the LXR ligand (oxysterols), or both ligands together (Janowski et al., 1996).

Vertebrate RXRs are encoded by a multigene family and three RXR subtypes have been found to encode three distinct receptors: RXRα, RXRβ and RXRγ (Mangelsdorf et al., 1992). Furthermore, RXRβ and RXRγ RNAs both encode two isoforms (Liu and Linney, 1993; Fleishhauer et al., 1992; Nagata et al., 1994). The three RXR genes show both unique and overlapping patterns of expression corresponding to different stages of development and different tissues (Mangelsdorf et al., 1992; Mangelsdorf et al., 1990). Thus, the interaction of multiple RXRs with a wide variety of other nuclear receptors largely expands RXR regulated pathways.

Although it is a steroid receptor, EcR does not belong to the steroid receptor subfamily (iii). Instead, EcR belongs to the nuclear receptor subfamily i, in which most members function as RXR heterodimers (see Figure 2). Vertebrate steroid receptors, when activated by ligand, bind to DNA as homodimers to activate transcription of target genes (Beato et al., 1995). In contrast, the ecdysone receptor alone does not appear to bind 20-OH ecdysone or its target ecdysone response elements (EcREs) with high affinity. Instead, functional

ecdysone receptors are heterodimers of EcR and ultraspiracle (USP), the insect homologue of RXR (Thomas et al., 1993; Yao et al., 1993). Therefore, invertebrate EcRs are not typical steroid receptors, but more closely resemble vertebrate RXR heterodimeric receptors.

To regulate gene expression, the nuclear receptor-ligand complex has to bind specific DNA sequences in target genes, which are defined as hormone response elements (HREs). Typically, HREs for nuclear receptors are composed of one or two copies of a six nucleotide motif, termed a half-site (Evans, 1988). The binding specificity of HREs to receptors is determined not only by the half-site sequence, but also by the half site orientation and by the spacing between the two half-sites. The HREs for the members of steroid receptor subfamily, such as glucocorticoid response elements (GREs) and estrogen response elements (EREs), are oriented as inverted repeats spaced by 3 nucleotides (IR3) ((Martinez et al., 1987). The HREs for some members of the nonsteroid receptor subfamilies that pair with PXR, such as PPAR, VDR and LXR, are oriented as direct repeats (AGGTCA) separated by 1-5 nucleotides (designated as DR1, DR2, DR3, DR4 and DR5) (for reviews , see Giguere, 1994; Mangelsdorf et al., 1995; Willy et al., 1995). The HREs for RAR and TR are more divergent and can be composed of a single half-site, direct repeats and inverted repeats depending on target genes (for reviews, see Martinez et al., 1987; Giguere, 1994; Mangelsdorf et al., 1994; Mangelsdorf et al., 1995). The HREs for RXRs can be either direct repeats with a single nucleotide spacer (DR1) or inverted repeats without a space (IR0) (for review, see Mangelsdorf et al., 1995).

Similar to TR and RAR, ecdysone receptors are proposed to bind both classical steroid receptor elements (IR) and RXR heterodimeric-like response elements (DR). In gel shift assays, using fat body nuclear extracts from the third larval instar of *Drosophila* (EcR-EcRE complexes), Antoniewski, et al (1993) has

shown that ecdysone receptor could bind the inverted repeats with a 1 bp spacing (IR1): PuG(G/T)T(C/G)A(N)TG(C/A)(C/A)(C/T)Py (Antoniewski et al., 1993). In *in vitro* co-transfection assays of EcR-B1 and USP cDNAs, D'Avino, et al (1995) has also shown that EcR or USP alone or together could bind a subset of IR1s. In addition, they also showed that EcR/USP and USP can bind a DR3 as well. Therefore, like vertebrate RXR heterodimers, ecdysone receptors may bind a variety of DNA targets with varying affinities.

Ecdysone Action in Insects

Ecdysteroids, through corresponding ecdysone receptors, trigger many biological processes throughout arthropod life, including embryonic development (Bollenbacher et al., 1978; Bulliere et al., 1979), molting (Bollenbacher et al., 1981), metamorphosis (Nijhout, 1994) and ovarian development (Bollenbacher et al., 1978; Bulliere et al., 1979). In *Drosophila*, two significant pulses of ecdysteroids have been observed. One is the commitment peak that occurs at the end of third instar larval development and triggers puparium formation (Richards, 1981) and the other is the prepupal peak that triggers prepupae to pupae transition (Handler, 1982). Several small peaks have also been observed in the middle of first and second instars and in the early stages of the third instar (Riddiford, 1993). Accordingly, EcR mRNA expression in whole animals remains at a very low level during first and second instars, the early part of the third instar and early adult stages. Intermediate to high levels of EcR expression are observed during embryogenesis. Maximal levels of EcR mRNA are expressed at the time of pupal commitment and relatively high levels in early pupae (Koelle et al., 1991; Talbot et al., 1993). A similar temporal profile of EcR expression is observed in *M. sexta* epidermis, which is intermediate

during larval molts, low during early fifth instar and high at during larval-pupal transition (Riddiford, 1993).

The first ecdysone receptor (EcR-B1 isoform) was identified by Koelle et al., (1991) in *Drosophila*. Later, two additional isoforms encoded by the same EcR gene (EcR-A isoform and EcR-B2 isoform) were discovered (Talbot et al., 1993). The three isoforms share complete identity in DNA and ligand-binding domain but little similarity in the N-terminal region. The EcR-A and two EcR-B mRNAs are transcribed from two different promoters; EcR-B1 and EcR-B2 mRNAs are transcribed from the same promoter but are generated by alternative splicing.

The combination of EcR isoforms expressed in tissues can be grouped according to metamorphic class: tissues in the same metamorphic class exhibit similar isoform expression patterns; tissues in different metamorphic classes exhibit different isoform expression patterns. For example, at the onset of larval-adult metamorphosis of *Drosophila*, in response to ecdysone, the EcR-A isoform predominates in the imaginal discs that generate adult head and thoracic epithelium and, in imaginal rings that generate adult foregut, hindgut and salivary glands, and the prothoracic glands which still function at the late metamorphic stage. In contrast, the EcR-B1 isoform predominates in strictly larval tissues (except for prothoracic glands) that undergo apoptosis and in the imaginal cells of the midgut island and histoblast nests that generate adult abdominal epithelium and midgut (Talbot et al., 1993). The significance of this phenomenon lies in the proposition that different metamorphic responses of tissues to ecdysone may be achieved by expression of different combinations of EcR isoforms (Talbot et al., 1993). Functional analysis of *Drosophila* EcR-B1 mutants has confirmed that EcR isoforms are functionally distinct (Bender et al., 1997).

Additional EcR genes have now been cloned from several other insects, including three Dipterans: *Aedes aegypti* (AaEcR) (Cho et al., 1995), *Chironomus tentans* (CtEcR) (Imhof et al., 1993), *Lucilia cuprina* (LcEcR) (Hannan and Hill, 1997); three Lepidopterans: *Bombyx mori* (BmEcR) (Swevers et al., 1995), *Manduca sexta* (MsEcR) (Fujiwara et al., 1995), *Choristoneura fumiferana* (CfEcR) (Kothapalli et al., 1995); and one Coleopteran: *Tenebrio molitor* (TmEcR) (Mouillet et al., 1997). Most of the insect EcRs are homologues of the *Drosophila* EcR B1 isoform. However, homologues of the *Drosophila* EcR-A isoform have also been described in *M. sexta* and *T. molitor* (Jindra et al., 1996; Mouillet et al., 1997). When the predicted amino acid sequences of DmEcR, AaEcR, CtEcR, BmEcR and CfEcR were compared with the MsEcR (Table I) (Fujiwara et al., 1995), the DNA binding domains show the highest similarity as expected, from 95-100%. Slightly less similarity was found in the ligand binding domains (70-88%) and the least identity in A/B domains with <10 % similarity (Fujiwara et al., 1995).

Thus far, data from several groups suggests that the functional ecdysone receptor is a heterodimer of EcR and an RXR-like partner. In *Drosophila*, the partner of EcR is USP (Thomas et al., 1993; Yao et al., 1992; Yao et al., 1993) , the product of ultraspiracle locus (Oro et al., 1990). USP is the insect homologue of the vertebrate receptor RXR, because it shares 86% amino acid identity in the DNA binding domain and 49% in the ligand binding domain. The observation that the functional ecdysone receptor is the heterodimer of EcR and USP has also been confirmed in *B. mori* (Swevers et al., 1996).

USP homologues have been isolated from the fruit fly *Drosophila* (DmUSP), the mosquito *A. aegypti* (AaUSP), the silkmoth *B. mori* (BmCF1), and the tobacco hornworm, *M. sexta* (MsUSP), (Jindra et al., 1997; Kapitskaya et al., 1996; Tzertzinis et al., 1994). Although AaUSP, BmCF1 and MsUSP are more closely related to DmUSP than to any other vertebrate RXRs (α, β, γ), the

similarities among the ligand binding domains of insect USPs are lower than that found among vertebrate RXRs, suggesting high sequence divergence in the ligand binding domains of insect USPs (Tzertzinis et al., 1994).

While a single USP isoform has been described in *Drosophila* (Oro et al., 1992), two USP isoforms have been described in *A. aegypti* (Jindra et al., 1997) and *M. sexta* (Kapitskaya et al., 1996). The USP isoforms have unique N-termini but share common DNA and ligand binding domains. Each USP isoform possesses a unique tissue and temporal expression pattern, suggesting USP isoforms are also functionally distinct. When examining BmCF1 transcripts in *B. mori* using Northern blot analysis, two distinct mRNA fragments were detected in total RNA from larval, pupal and adult tissues (Tzertzinis et al., 1994). Whether they are derived from the same BmCF1, with different promoters or from alternative splicing, or if there is a second RXR-type gene, is not known. However, since these two transcripts are ubiquitously expressed in larval, pupal and adult, they may exert multiple functions during development.

Beyond the similarity between vertebrate RXRs and insect USPs, they are different in several ways. Unlike vertebrate RXRs (α, β, γ) which are encoded by a multigene family (for review, see Mangelsdorf and Evans, 1995), USP is encoded by a single gene that can be alternatively spliced to produce isoforms with different N-termini (Jindra et al., 1997). Because of the high sequence divergence in the ligand binding domains of insect USPs relative to vertebrate RXRs, it has been suggested that insect USPs do not bind a ligand and are true orphan receptors (Henrich et al., 1994; Thummel, 1995). Vertebrate RXRs, by contrast, bind 9-cis retinoic acid (9 cis-RA) as homodimers, in addition to their roles as silent partners in several ligand-driven responses (Mangelsdorf and Evans, 1995). While RXR can substitute for USP in *in vitro* assays, the RXR/EcR heterodimer does not bind 20-OH ecdysone with high affinity, suggesting that

RXR/EcR and USP/EcR heterodimers exhibit distinct properties (Thomas et al., 1993).

Ecdysone Action in Ticks

In ticks, ecdysteroids have been proposed to regulate molting, diapause termination, sex pheromone production, female and male reproduction, salivary gland degeneration and embryogenesis (Diehl et al., 1986; Sonenshine, 1991). Among these processes, the roles that ecdysteroids play in molting and salivary gland degeneration have been well demonstrated (Diehl et al., 1982; Germond et al., 1982; Kaufman, 1986).

The molting process is stimulated by an increase in the titer of ecdysone in both argasid and ixodid ticks. In the argasid tick *Ornithodoros moubata* (Germond et al., 1982) and the ixodid tick *A. hebraeum* (Diehl et al., 1982), higher titers of hemolymph ecdysone and 20-OH ecdysone parallel apolysis and epicuticle deposition, and declining titers of ecdysone trigger the ecdysis, the end of molting cycle. Exogenously applied ecdysteroids accelerate the molting of nymphal camel ticks (*Hyalomma dromedarii*) nymphs (Khalil et al., 1984).

Salivary gland degeneration is also controlled by ecdysteroids in ticks. The salivary glands of partially fed *A. americanum* and *A. herbraeum* lose secretory competence when incubated with 20-hydroxyecdysone (Kaufman, 1986; Lindsay and Kaufman, 1988). Kaufman (1991) further identified a direct correlation between hemolymph ecdysteroid titer and the degree of salivary gland degradation in *A. hebraeum*, suggesting that the degeneration of salivary glands after engorgement is triggered by an elevated concentration of hemolymph ecdysteroids. A 14-fold increase in hemolymph ecdysteroid titer by day 7 after engorgement has been correlated with complete loss of salivary gland fluid secretory competence (Kaufman, 1986; Kaufman, 1991).

High levels of ecdysteroids have also been observed in ovaries following engorgement and in newly laid eggs in female ixodid ticks (James et al., 1997; Kaufman, 1991; Magee et al., 1996). This has led to the proposal that ecdysteroids may provoke vitellogenesis, and play a role in embryogenesis and/or egg hatching.

Since ecdysteroids may exert similar physiological control over ticks and insects, a common biological pathway likely exists for ecdysteroid functions. In insects, ecdysteroid action is mediated by an ecdysone receptor complex which is comprised of two receptor subunits, EcR and USP (Thomas et al., 1993; Yao et al., 1992). Therefore, EcR and USP homologues are likely to exist in ticks and act in a manner similar to insects. Mao, et al. (1995) provided conclusive evidence for the existence of an ecdysteroid receptor in tick salivary glands. Using crude salivary gland extracts, they demonstrated that this receptor has a high affinity for ponasterone A (k_d=0.72 nM) and lower affinity for 20-OH Ecdysone (k_d=60 nM), similar to ecdysteroid receptors in insects. These data suggested that the ecdysteroid receptor in the tick salivary gland is a typical ecdysteroid receptor. These data, in combination with the previous work by Kaufman's group, in which they had demonstrated that ecdysteroids were responsible for triggering salivary gland degeneration following repletion (Kaufman, 1986; Kaufman, 1991; Kaufman, 1990), provided strong evidence that ecdysteroids regulate tick salivary gland degeneration via ecdysone receptors.

Using a combination of RT-PCR and cDNA screening, our laboratory has isolated cDNAs encoding at least three isoforms of the *A. americanum* EcR gene (Guo et al., 1997) (Figure 3). Like *Drosophila*, the three *A. americanum* EcR isoforms (AamEcRA1, AamEcRA2 and AamEcRA3) share common DNA and ligand binding domains. AamEcRA1 and AamEcRA2 share an additional 66 amino acid region that precedes the common DNA and ligand binding domain.

The N-termini of AamEcRA1, AamEcRA2 and AamEcRA3, which are 74 amino acids, 84 amino acids and 24 amino acids, respectively, share little identity. Unlike insect EcRs, there is no "B1" isoform equivalent in AamEcR. In addition, there is no C-terminal F domain in AamEcRs as in insect EcRs (Guo et al., 1997).

The translated sequences of the AamEcRs show a high degree of identity with insect EcR DNA binding domains (86-88%) and a relatively high degree of identity with insect EcR ligand binding domains (55-63%) (Table I). However, the DNA binding domain of the Coleopteran *Tenebrio moliter* EcR shows exceptionally high identity to AamEcR DNA-binding domain, revealing an unusual evolutionary pattern in insect and chelicerate EcRs. When the DNA binding domain sequences are compared, two evolutionary groups were found with Dipteran and Lepidopteran EcRs in one group (over 95% sequence identity) and AamEcR and TmEcR in the other group (98% sequence identity) (Guo et al., 1997). The division of two EcR groups is due mainly to the differences in the D box region, which forms a symmetrical dimerization interface in homodimeric steroid receptors that bind palindromic response elements (Umesono and Evans, 1989); and an asymmetrical dimerization interface in RXR heterodimers that bind direct repeat response elements (Mangelsdorf and Evans, 1995). While the proximal (P) box region, which is responsible for half-site recognition and DNA binding specificity, is conserved in all EcRs, the differences in the D box region suggest they may display functional differences with regard to EcRE binding.

Our laboratory has also isolated cDNAs encoding two distinct RXR genes from *A. americanum*, which encode full length proteins with unique N-termini and more conserved DNA and ligand binding domains (95% and 78% identity, respectively) (Figure 4) (Guo et al., 1998). Although the two RXR-like proteins share a higher degree of identity with insect USPs than with vertebrate RXR DNA binding domains (91-95% versus 82-87%), the ligand binding domains are

strikingly more similar to vertebrate RXRs than to insect USPs (70% versus 37-50%) and this is also true when both the DNA and ligand-binding domain are considered (Table II). Thus, we have chosen to use RXR nomenclature to describe the *A. americanum* homologues (Guo et al., 1998).

To confirm that AamEcR and AamRXRs can form functional ecdysteroid receptors, transient transfection assays were performed in monkey kidney cells (CV-1). When CV-1 cells were transfected with AamEcRA1, AamRXR1 or AamRXR2 alone, there was no significant transcription of the EcRE containing reporters in response to an ecdysone analogue, muristerone A (MurA). However, when cells were transfected with AamEcRA1 and AamRXR1 or AamRXR2 in combination, there was a significant increase in the transcription of reporter, suggesting AamEcRA1 and either AamRXR1 or AamRXR2 form heterodimeric ecdysteroid receptors that can activate transcription in response to ecdysteroid ligands (Guo et al., 1998).

Despite the similarity between AamRXRs and vertebrate RXRs, several unique features are observed in AamRXR1 and AamRXR2 as a result of several substitutions in the AamRXR LBDs. First, several substitutions occur in positions in the AamRXR ligand binding domain that are proposed to contact 9-cis retinoic acid (Figure 5, Panel A) (Wurtz et al., 1996). The transient transfection assays have shown that AamRXRs do not activate transcription in response to 9-cis retinoic acid (Guo et al., 1998). However, the replacement of the conserved glutamic acid in a C-terminal activation function domain (AF-2) to serine in AamRXR1 and aparagine in AamRXR2 AF-2 (Figure 5, Panel B), may affect AamRXR ligand-dependent transactivation ability and thus, AamRXRs may be obligate heterodimeric partners that lack functional AF-2s (Danielian et al., 1992; Durand et al., 1994). Last, numerous substitutions occur in helix 9 of AamRXR1, which are highly conserved in vertebrate RXRs and insect USPs (Figure 5, Panel

C). This may change the folding of the AamRXR1 LBD relative to other RXR proteins. Despite the differences between AamRXRs and vertebrate RXRs and insect USPs, AamRXRs retain their basic function: heterodimerizing with AamEcR to form functional ecdysteroid receptors in ecdysone response pathways (Guo et al., 1998).

Ecdysone Action in Tick Salivary Glands

In most bloodfeeding arthropods, the bloodmeal provides the necessary nutrients for growth and development. In ticks, bloodfeeding occurs over an interval of 3-14 days, depending on the life stage. Ticks feed in alternating cycles of sucking and salivation. Blood is taken in, concentrated in the gut and excess fluid is secreted into the host via salivary glands. To maintain the feeding site over a prolonged feeding period, the salivary glands secrete a number of biologically active agents, including anti-inflammatory compounds (Chinery and Ayitey-Smith, 1977), anticoagulants (Ribiero, 1987) and immunosuppressive agents (Wikel, 1996). These pharmacological molecules are injected into the host along with the excess fluid. Cement is also secreted to anchor the mouth parts (Sauer, 1977). As important, the salivary glands maintain water and ion balance both between and during bloodmeals (Needham and Teel, 1986). The salivary glands also serve as a reservoir for pathogens that are secreted into the host during salivation (Sonenshine, 1991).

The organization and morphology of ixodid tick salivary glands have been thoroughly studied by many investigators (Balashov, 1965; Binnington, 1978; Chinery, 1965; Megaw and Beadle, 1979; Meredith and Kaufman, 1973; Till, 1961). The salivary glands of female ticks consist of paired, grape-like clusters, called acini. There are three types of acini in the salivary glands of female ixodid ticks: Type I, Type II and Type III acini. Type I acini are agranular acini that

attach directly to the main salivary duct and lack large secretory granules. In contrast, both Type II and Type III acini contain granular secretory cells. Type II acini attach mainly to the secondary ducts, while Type III acini attach to the more terminal branches of the ducts at the periphery of the gland. Type III acini are also the most numerous.

Five to nine granular cell types have been reported within Type II and Type III acini of female ixodid ticks (Balashov, 1965; Binnington, 1978; Chinery, 1965; Fawcett et al.,1982; Megaw and Beadle, 1979; Meredith and Kaufman, 1973; Till, 1961). For example, in the study of *Boophilus microplus*, Binnington (1978) and Fawcett et al. (1982), described six granular cell types in Type II acini and three granular cell types in Type III acini (Table III). However, interpretation of the number and cell types differed considerably (Binnington, 1978; Megaw and Beadle, 1979). This may be due to differences in the preparation of tissues, method of analysis (light microscopy vs. electron microscopy) and stage at which the salivary glands were assayed.

In a study of type II and III acini on unfed *A. americanum* using both electron microscopy and light microscopy, Krolak et al. (1982) described three granular cell types in both type II and III acini that were based on morphology and staining properties: complex granular cells, which are densely stained and contain compact membrane bound granules; densely stained cells with simple granular cells, and lightly stained with simple granular (see Table III) (Krolak et al., 1982). The densely stained complex granular, and densely stained simple granular cells are located on either side of the valves and appear to be analogous to a, d and e cells described by Binnington (1978), which occupy similar positions. The f cells in *B. microplus* Type III acini are identical in number and description to the simple granular cells in *A. americanum* Type III acini (Krolak et al., 1982).

Although the number and kinds of cells in Type I, II and III acini of female ixodid ticks do not change during feeding (Barker et al., 1984; Binnington, 1978), significant changes in size and cytoplasmic organelle composition have been observed in all three acini at various feeding stages (Barker et al., 1984; Binnington, 1978; Fawcett et al., 1986; Krolak et al., 1982; Needham and Coons, 1984). No specific role has been associated with these changes in Type I acini during feeding. Type I acini are believed to actively absorb water from the atmosphere during off-host periods to prevent desiccation (McMullen et al., 1976; Rudolph and Knulle, 1974). The morphological changes in Type II and III acini during feeding are, in contrast, associated with subsequent functional transformations. For instance, in the process of enlarging and elongating of the interstitial cells between the granular cells during the early feeding stage, the interstitial cells acquire fluid and electrolyte transporting capacity that enable them to secrete copious saliva back to the host during the rapid feeding stage (Binnington, 1978; Fawcett et al., 1986). Granular cells also undergo morphological and cytoplasmic changes during feeding. The complex granular and densely staining simple granular cells described by Krolak, et al. (1982) in *A. americanum*, and analogous a, d and e cells described by Binnington (1978) in *B. microplus*, are filled with secretory granules in unfed glands and empty their contents early in feeding. They are likely the cells that secrete cement and other factors critical to establishing and maintaining host-vector interface during the early feeding stages (Jaworski et al., 1992). Cell type a in *B. microplus* and analogous complex granular cells in *A. americanum*, appear to become inactive in later stages of feeding (Binnington, 1978; Krolak et al., 1982). The f cells in *B. microplus* Type III acini and analogous simple granular cells in *A. americanum* Type III acini, become active following the onset of feeding and lose most of their granules by the fast feeding stages (Binnington, 1978; Krolak et al., 1982).

To date, no functional criteria have been definitively established for salivary gland cell types. Until products can be directly localized to specific cells, their roles remain speculative.

Besides obvious morphological and structural differentiation, the RNA and protein content of the salivary glands of female ixodid ticks increase drastically during feeding (Shelby et al., 1987). In *A. americanum*, the amount of total cytoplasmic RNA increases from 0.6 μg/gland pair in unfed to 5.2 μg / gland pair in replete ticks. The amount of Poly(A)$^+$ mRNA increases from 3.5 ng/gland pair to 15 ng/gland pair (5-fold) by the second day of feeding and reaches a peak of 370 ng/gland pair in rapidly feeding females (body wt>100 mg). The percentage of Poly(A)$^+$ mRNA to total cytoplasmic RNA content also increases, from 0.54% from unfed to 4.8% in the rapid-feeding phase (body wt > 120 mg). However, upon repletion, the amount of Poly(A)$^+$ mRNA declines from 370 ng/gland pair to 280 ng/gland, consistent with the decline in secretory competence and activity of the salivary glands. The increase of protein content parallels that of Poly(A)$^+$ mRNA (Shelby et al., 1987).

During feeding, the salivary glands of adult female ticks undergo tremendous growth and differentiation, which corresponds with changes in the complexity of the mRNA population, and in size and content of total cytoplasmic RNA and protein. Following feeding, the salivary glands undergo degeneration to provide nutrients for production of thousands of eggs. These changes require both temporal and cell-specific regulation of developmental programs. This regulation is likely to be induced, at least in part, by transcription factors such as the ecdysteroid receptors. In insects, EcR and USP isoforms are functionally distinct and the interaction with cell and tissue specific factors dictates the metamorphic response of the tissue (Talbot et al., 1993). Because the *A. americanum* EcR gene encodes three protein isoforms that can partner with two

distinct RXR proteins, it is our hypothesis that their differential expression result in temporal and cell-type regulation of salivary gland growth and differentiation. In addition, they are involved in the histolysis of the salivary glands that occurs in adult females following feeding. Although there is no direct evidence, by studying EcR and RXR gene expression in molting ticks and in the salivary glands and ovaries of adult females, we can also determine if the expression of EcR isoform and RXR subtype mRNAs display temporal, tissue-specific and/or cell-type specific patterns and if their expression patterns are associated with the different physiological response of tissues.

REFERENCES

Antoniewski, C., Laval, M., and Lepesant, J. (1993). Structural features critical to the activity of an ecdysone receptor binding site. Insect Biochem. Molec. Biol. 23, 105-114.

Ashburner, M., Chihara, C., Meltzer, P., and Richards, G. (1974). Temporal control of puffing activity in polytene chromosomes. Cold Spring Harbor Symp. Quant. Biol. 38, 655-662.

Balashov, Y. S. (1965). Mechanism of salivation and morphologic-histochemical peculiarities of salivary glands in ixodid ticks (Acarina, Ixodoidea). Entomologicheskoe Obozrenie 44, 785-802.

Baniahmad, A. (1993). Interaction of human thyroid hormone receptor beta with transcription factor TFIIB may mediate target gene derepression and activation by thyroid hormone. Proc. Natl. Acad. Sci. U.S.A. 90, 8832-8836.

Baniahmad, A. (1995). The tau 4 activation domain of the thyroid hormone receptor is required for a release of a putative corepressor(s) necessary for transcriptional silencing. Mol. Cell. Biol. 15, 76-86.

Barker, D. M., Ownby , C. L., Krolak, J. M., Claypool, P. L., and Sauer, J. R. (1984). The effects of attachment, feeding, and mating on the morphology of the type I alvelous of salivary glands of the lone star tick, *Amblyomma americanum* (L.). J. Parasitol. 70, 99-113.

Beato, M., Herrlich, P., and Schütz, G. (1995). Steroid hormone receptors: Many actors in search of a plot. Cell 83, 851-857.

Bender, M., Iman, F. B., Talbot, W. S., Ganetsky, B., and Hogness, D. S. (1997). *Drosophila* ecdysone receptor mutations reveal functional differences among receptor isoforms. Cell 91, 777-788.

Binnington, K. C. (1978). Sequential changes in salivary gland structure during attachment and feeding of the cattle tick, *Boophilus microplus*. Int. J. Parasitol. 8, 91-115.

Bollenbacher, W. E., Smith, S. L., Goodman, W., and Gilber, L. I. (1981). Ecdysteroid titer during larval-pupal-adult developement of the tobacco hormworm *Manduca sexta*. Gen. Comp. Endocrinol. 44, 302-306.

Bollenbacher, W. E., Zvenko, H., and Kumaran, A. K. (1978). Changes in ecdysone content during postembryonic development of the wax moth, *Galleria mellonella*: the role in the ovary. Gen. Comp. Endocrinol. 34, 169.

Bourguet, W., Ruff, M., Chambon, P., Gronemeyer, H., and Moras, D. (1995). Crystal structure of the ligand-binding domain of the human nuclear receptor RXR-α. Nature 375, 377-382.

Chinery, W. A. (1965). Studies on the various glands of the tick *Haemaphysalis spinigera* neumann 1897.3. The salivary glands. Acta Trop. 22, 321-349.

Chinery, W. A., and Ayitey-Smith, E. (1977). Histamine blocking agent in the salivary gland homogenate of the tick *Rhipicephalus sangineus sangineus*. Nature 265, 366-367.

Chino, H., Sakurai, S., and Ohtaki, T. (1974). Biosynthesis of a-ecdysone by prothoracic glands *in vitro*. Science 183, 529-530.

Cho, W.-L., Kapitskaya, M. Z., and Raikhel, A. S. (1995). Mosquito ecdysteroid receptor: analysis of cDNA and expression during vitellogenesis. Insect. Biochem. Molec. Biol. 25, 19-27.

D'Avino, P. P., Crispi, S., Cherbas, L., and Cherbas, P. (1995). The moulting hormone ecdysone is able to recognize target elements composed of direct repeats. Mol. and Cell. Endocrinol. 113, 1-9.

Dai, J.-D., and Gilbert, L. I. (1991). Metamorphosis of the corpus allatum and degeneration of the prothoracic glands during the larval-pupal-adult transformation of Drosphila melanogaster: a cytophysiological analysis of the ring gland. Dev. Biol. 144, 309-326.

Danielian, P. S., White, R., Lees, J. A., and Parker, M. G. (1992). Identification of a conserved region required for hormone dependent transcriptional activation by steroid hormone receptors. EMBO J 11, 1025-1033.

Delbecque, J.-P., Meister, M. F., and Quennedey, A. (1986). Conversion of radiolabelled 2,22,25-tri-deoxyecdysone in *Tenebrio* pupae. Insect Biochem. 16, 57-63.

Delbecque, J.-P., Weidner, K., and Hoffmann, K. H. (1990). Alternative sites for ecdysteroid production in insects. Invert. Reprod. Dev. 18, 29-42.

Diehl, P. A., Germond, J. E., and Morici, M. (1982). Correlation between ecdysteroid titers and integument structure in nymphs of the tick *Amblyomma hebraeum* koch (Acarina: Ixodidae). Rev. Suisse Zool. 89, 859-868.

Diehl, P. A., Connat, J.-L., and Dotson, E. (1986). Chemistry, function and metabolism of tick ecdysteroids. In Morphology, Pphysiology, and Behavioral Biology of Ticks, J. R. Sauer and J. A. Hair, eds. (New York: John Wiley and Sons), pp. 165-192.

Durand, B., Saunder, M., Gaudon, C., Roy, B., Losson, R., and Chambon, P. (1994). Activation function 2 (AF-2) of retinoic acid receptor and 9-cis retinoic acid receptor: presence of a conserved autonomous constitutive activation domain and influence of the nature of the response element of AF-2 activity. EMBO J 13, 5370-5382.

Evans, R. M. (1988). The steroid and thyroid hormone receptor superfamily. Science 240, 889-895.

Fawcett, D. W., Binnington, K., and Voight, W. P. (1986). The cell biology of the ixodid tick salivary gland. In Morphology, Physiology, and Behavioral Biology of Ticks, J. R. Sauer and J. A. Hair, eds. (New York: John Wiley and Sons), pp. 22-45.

Fleishhauer, K., Park, J. H., DiSanto, J. P., Marks, M., Ozato, K., and Yang, S. Y. (1992). Isolation of a full-length cDNA clone encoding a N-terminally variant form of the human retinoid X receptor B. Nucleic Acids Res. 20, 1801.

Fujiwara, H., Jindra, M., Newitt, R., Palli, S. R., Hiruma, K., and Riddiford, L. M. (1995). Cloning of an ecdysone receptor homolog from *Manduca sexta* and the developmental profile of its mRNA in wings. Insect Biochem. Molec. Biol. 25, 845-856.

Germond, J. E., Diehl, P. A., and Morici, M. (1982). Correlation between integument structure and ecdysteroid titers in fifth-stage nymphs of the tick, *Ornithodoros moubata*. Gen. Comp. Endocrinol. 46, 255-266.

Giguere, V. (1994). Retinoic acid receptors and cellular retinoid binding proteins complex interplay in retinoid signaling. Endocrinol. Rev. 15, 61-79.

Guo, X., Harmon, M.A., Lauder, V., Mangelsdorf, D. J., and Palmer, M. J. (1997). Isolation of a functional ecdysteroid receptor homologue from the ixodid tick, *Amblyomma americanum* (L.). Insect Biochem. Molec. Biol. 27, 945-962.

Guo, X., Xu, Q., Harmon, M., Jin, X., Laudet, V., Mangelsdorf, D.J., and Palmer, M.J. (1998). Isolation of two functional retinoid x receptor subtypes from the ixodid tick, *Amblyomma americanum* (L.). Mol. Cell. Endocrinol. 139, 45-60.

Hair, J. A., and Bowman, J. L. (1986). Behavioral ecology of *Amblyomma americanum* (L.). In Morphology, Physiology, and Behavioral Biology of Ticks, J. R. Sauer and J. A. Hair, eds. (New York: John Wiley and Sons), pp. 165-192.

Handler, A. M. (1982). Ecdysteroid Titers during Pupal and Adult Development in *Drosophila melanogaster*. Dev. Biol. 93, 73-82.

Hannan, G. N., and Hill, R. J. (1997). Cloning ans characterization of LcEcR1: a functional ecdysone receptor from the sheep blowfly *Lucilia cuprina*. Insect Biochem. Molec. Biol. 27, 479-488.

Henrich, V., Szekely, A. A., Kim, S. J., Brown, N. E., Antoniewski, C., Hayden, M. A., Lepesant, J.-A., and Gilbert, L. I. (1994). Expression and function of the *ultraspiracle* (usp) gene during development of *Drosophila melanogaster*. Dev. Biol. 165, 38-52.

Hoskins, J. D. (1991). Tick-Transmitted Diseases: W. B. Saunders Company).

Imhof, M. O., Rusconi, S., and Lezzi, M. (1993). Cloning of a *Chironomus tentans* cDNA encoding a protein (cEcRH) homologous to the *Drosophila melanogaster* ecdysteroid receptor (dEcR). Insect Biochem. Molec. Biol. 23, 115-124.

Ioffe, I. D. (1964). Seasonal changes of the contents of neurosecretory material in neurosecretory cells of *dermacentor pictus*. Med. Parazitol. (Mosk) 34, 57-63.

James, A. M., Zhu, X. X., and Oliver, J. H., Jr. (1997). Vitellogenin and ecdysteroid titers in *Ixodes scapularis* during vitellogenesis. J. Parasitol. 83, 559-563.

Janowski, B. A., Willy, P. J., Devi, T. R., Falck, J. R., and Mangelsdorf, D. J. (1996). An oxysterol signalling pathway mediated by the nuclear receptor LXRα. Nature 383, 728-731.

Jaworski, D. C., Rosell, R., Coons, L. B., and Needham, G. R. (1992). Tick (Acari: Ixodidae) attachment cement and salivary gland cells contain similar immunoreactive polypeptides. J. Med. Entomol. 29, 305-309.

Jiang, C., Baehrecke, E. H., and Thummel, C. S. (1997). Steroid regulated programmed cell death during *Drosophila* metamorphosis. Development 124, 4673-4683.

Jindra, M., Huang, J.-Y., Malone, F., Asahina, M., and Riddiford, L. M. (1997). Identification and mRNA developmental profiles of two ultraspiracle isoforms in the epidermis and wings of *Manduca sexta*. Insect Mol. Biol. 6, 41-53.

Jindra, M., Malone, F., Hiruma, K., and Riddiford, L. M. (1996). Developmental profiles and ecdysteroid regulation of the mRNAs for two ecdysone receptor isoforms in the epidermis and wings of the tobacco hornworm, *Manduca sexta*. Dev. Biol. 180, 258-272.

Kapitskaya, M., Wang, S., Cress, D. E., Dhadialla, T., and Raikhel, A. S. (1996). The mosquito *ultraspiracle* homologue, a partner of ecdysteroid receptor heterodimer: cloning and characterization of isoforms expressed during vitellogenesis. Mol. Cell. Endocrinol. 121, 119-132.

Kaufman, R. (1986). Salivary gland degeneration in female tick *Amblyomma hebraeum* koch (Acarina: Ixodidae). In Morphology, Physiology, and Behavioral Biology of Ticks, J. R. Sauer and J. A. Hair, eds. (New York: John Wiley and Sons), pp. 46-54.

Kaufman, W. R. (1991). Correlation between haemolymph ecdysteroid titre, salivary gland degeneration and ovarian development in the ixodid tick, *Amblyomma herbraem* KOCH. Insect Physiol. 37, 95-99.

Kaufman, W. R. (1990). Effect of 20-hydroxyecdysone on the salivary glands of the male tick *Amblyomma hebraeum*. Exp. Appl. Acarol. 9, 87-95.

Khalil, G. M. (1976). Hormaonal control of diapause in the tick, *Argas arboreus*. J. Insect Physiol. 22, 1659-1663.

Khalil, G. M., Sharawy, A. A. A., Soneshine, D. E., and Gad, S. M. (1984). β-ecdysone effects on the camel tick, *Hyalomma dromedarri* (Acari: Ixodidae). J. Med. Entomol. 21, 188-193.

King, D. S., Bollenbacher, W. E., and Borst, W. Y. (1974). The secretion of a-ecdysone by the prothoracic glands of *Manduce sexta* in vitro. Proc. Natl. Acad. Sci. U.S.A. 71, 793-796.

Koelle, M. R., Talbot, W. S., Seagraves, W. A., Bender, M. T., Cherbas, P., and Hogness, D. A. (1991). The Drosophila EcR gene encodes an ecdysone receptor, a new member of the steroid receptor superfamily. Cell 67, 59-77.

Koolman, J. (1990). Ecdysteroids. Zool. Sci. 7, 563-580.

Kothapalli, R., Palli, S. R., Ladd, T. R., Sohi, S. S., Cress, D., Dhadialla, T. S., Tzertzinis, G., and Retnakaran, A. (1995). Cloning and developmental expression of the ecdysone receptor gene from the Spruce Budworm *Choristoneura fumiferana*. Dev. Genet. 17, 319-330.

Krolak, J. M., Ownby, C. L., and Sauer, J. R. (1982). Alveolar structure of salivary glands of the lone star tick, *Amblyomma Americanum* (L.): unfed females. J. Parasitol. 68, 61-82.

Laudet, V. (1997). Viewpoint: Evolution of the nuclear receptor superfamily: early diversification from an ancestral orphan receptor. J. Mol. Endocrinol. 19, 207-226.

Lehninger, A. L., Nelson, D. L., and Cox, M. M. (1993). Principles of Biochemistry (New York: Worth Publishers).

Lindsay, P. J., and Kaufman, W. R. (1988). Action of some steroids on salivary gland degeneration in the ixodid tick *A. americanum* L. J. Insect Physiol. 34, 351-359.

Liu, Q., and Linney, E. (1993). The mouse retinoid-x receptor-gamma gene: genomic organization and evidence for functional isoforms. Mol. Endocrinol. 7, 651-658.

Lomas, L. O., Turner, P. C., and Rees, H. H. (1997). A novel neuropeptide-endocrine interaction controlling ecdysteroid production in ixodid ticks. Proc. R. Soc. Lond. B 264, 589-596.

Magee, R. M., Jones, L. D., and Rees, H. H. (1996). Ecdysteroids in relation to Adult development and reproduction in female *Rhipicephalus appendiculatus* (Acari; Ixodidae). Arch. Insect Biochem. Physiol. 31, 197-206.

Mangelsdorf, D. J., Borgmeryer, U., Heyman, R. A., Zhou, J. Y., Ong, E. S., Oro, A. E., Kakizuka, A., and Evans, R. M. (1992). Characterization of three RXR genes that mediate the action of 9-cis retinoic acid. Genes Dev. 6, 329-344.

Mangelsdorf, D. J., and Evans, R. M. (1995). The RXR heterodimers and orphan receptors. Cell 83, 841-850.

Mangelsdorf, D. J., Ong, E. S., and Dyck, J. A. (1990). Nuclear receptor that identifies a novel retinoic acid response pathway. Nature 345, 224-229.

Mangelsdorf, D. J., Umesono, K., and Evans, R., M. (1994). The retinoid receptors. The Retinoids 2nd edition, pp. 319-349.

Mangelsdorf, D. J., Thummel, C., Beato, M., Herrlich, P., Schütz, G., Umesono, K., Blumberg, B., Kastner, P., Mark, M., Chambon, P., and Evans, R. M. (1995). The nuclear receptor superfamily: The second decade. Cell 83, 835-839.

Mao, H., McBlain, W. A., and Kaufamn, W. R. (1995). Some properties of the ecdysteroid receptor in the salivary gland of the ixodid tick, *Amblyomma hebraeum*. Gen. Comp. Endocrinol. 99, 340-348.

Martinez, E., Givel, F., and Wahli, W. (1987). The estrogen-responsive element as an inducible enhancer: DNA sequence requirements and conversion to a glucocorticoid-reponsive element. EMBO J. 6, 3719-3727.

McMullen, H. L., Sauer, J. R., and Burton, R. L. (1976). Possible role in uptake of water vapor by ixodid tick salivary glands. J. Insect Physiol. 22, 1281-1286.

Megaw, M. W., and Beadle, D. J. (1979). Structure and function of the salivary glands of the tick, *Boophilus Microplus Canestrini* (Acarina: Ixodidae). Int. J. Insect Morphol. Embryol. 8, 67-83.

Meredith, J., and Kaufman, W. R. (1973). A proposed site of fluid secretion in the salivary gland of the ixodid tick *Dermacentor andersoni*. Parasitol. 67, 205-217.

Mouillet, J.-F., Delbecque, J.-P., Quennedey, B., and Delachambre, J. (1997). Cloning of two putative ecdysteroid receptor isoforms from *Tenebrio molitor* and their developmental expression in the epidermis during metamorphosis. Eur. J. Biochem. 248, 856-863.

Nagata, T., Kanno, Y., Ozato, K., and Taketo, M. (1994). The mouse *Rxrb* gene encoding RXRβ: genomic organization and two mRNA isoforms generated by alternative splicing of transcripts initiated from CpG island pomoters. Gene 142, 183-189.

Needham, G. R., and Coons, L. B. (1984). Ultrastructural changes in type I alveoli of the salivary glands from hydrating and desiccating lone star ticks. In *Acarology*, D. A. Griffiths and C. E. Bowman, eds.: Ellis Horwood Ltd.), pp. 366-373.

Needham, G. R., and Teel, P. D. (1986). Water balance by ticks between bloodmeals. In Morphology, Physiology, and Behavioral Biology of Ticks, J. R. Sauer and J. A. Hair, eds.: Ellis Horwood Ltd.), pp. 100-140.

Nijhout, H. F. (1994). Insect Hormones (Princeton: Princeton University Press).

Oliver, J. H. Jr, Pound, J. M., and Andrews, R. H. (1984). Induction of egg malturation and oviposition in the tick *Ornithodoros parker*i (Acari: Argasidae). J. Parasitol. 70, 337-342.

Oro, A. E., McKeown, M., and Evans, R. M. (1992). The Drosophila retinoid X r eceptor homologue ultraspiracle functions in both female reproduction and eye morphogenesis. Development 115, 440-462.

Oro, A. E., MeKeown, M., and Evans, R. M. (1990). Relationship between the product of the *Drosophila ultraspiracle* locus and the vertebrate retinoid X receptor. Nature 347, 298-301.

Rees, H. H. (1985). Biosynthesis of ecdysone. In Comprehensive Insect Physiology, Biochemistry, and Phamacology, K. G.A. and L. I. Gilbert, eds. (Oxford: Pergamon Press), pp. 249-293.

Renaud, J.-P., Rochel, N., Ruff, M., Vivat, V., Chambon, P., Gronemeyer, H., and Moras, D. (1995). Crystal structure of the RAR-γ ligand-binding domain bound to all-trans retinoic acid. Nature 378, 681-689.

Ribiero, J. M. C. (1987). Role of saliva in blood feeding by arthropods. Annual. Rev. Entomol. 32, 463-478.

Richards, G. (1981). The radioimmune assay of ecdysteroid titres in *Drosophila melanogaster*. Mol. Cell. Endocrinol. 21, 181-197.

Riddiford, L. M. (1993). Hormones and *Drodophila* development. In The Development of *Drosophila melanogaster*, M. Bate and A. M. Arias, eds. (Cold Spring Harbor, New York: Cold Spring Harbor Laboratory), pp. 899-939.

Rudolph, D., and Knulle, W. (1974). Site and mechanism of water vapor uptake from the atmosphere in ixodid ticks. Nature 249, 84-85.

Sakurai, S., Warren, J. T., and Gilbert, L. I. (1991). Ecdysteroid synthesis and molting by the tobacco hornworm, *Manduca sexta*, in the absence of prothoracic glands. Arch. Insect Biochem. Physiol. 18, 31-36.

Sauer, J. R. (1977). Acarine salivary glands-physiological relationships. J. Med. Entomol. 14, 1-9.

Schriefer, M. E. (1991). Vitellogenesis in Hyalomma dromedarii (Acari: Ixodidae): A model for analysis of endocrine regulation in ixodid ticks. Ph. D. Dissertation (Norfolk, Virginia, USA: Old Dominion University).

Shelby, K. S., Bantle, J. A., and Sauer, J. R. (1987). Biochemical differentiation of lone star tick, *Amblyomma americanum* (L), salivary glands: effects of attachment, feeding and mating. Insect Biochem. 17, 883-890.

Sonnenshine, D. E. (1991). Biology of Ticks, Volume 1 (Oxford: Oxford University Press).

Swevers, L., Cherbas, L., Cherbas, P., and Iatrou, K. (1996). *Bombyx* EcR (BmEcR) and *Bombyx* USP (BMCF1) combine to form a functional ecdysone receptor. Insect Biochem. Mol. Biol. 26, 217-221.

Swevers, L., Drevet, J. R., Lunke, M. D., and Iatrou, K. (1995). The silkmoth homolog of the *Drosophila* ecdysone receptor (B1 isoform): Cloning and analysis of expression during follicular cell differentiation. Insect Biochem. Molec. Biol. 25, 857-866.

Talbot, W. S., Swyryd, E. A., and Hogness, D. S. (1993). *Drosophila* tissues with different metamorphic responses to ecdysone express different ecdysone receptor isoforms. Cell 73, 1323-1337.

Thomas, H. E., Stunnenberg, H. G., and Stewart, A. F. (1993). Heterodimerization of the *Drosophila* ecdysone receptor with retinoid X receptor and *ultraspiracle*. Nature 362, 471-475.

Thummel, C. S. (1995). From embryogenesis to metamorphosis: The regulation and function of *Drosophila* nuclear receptor superfamily members. Cell 83, 871-877.

Till, W. M. (1961). A contribution to the anatomy and histology of the brown ear tick *Rhipicephalus Appendiculatus Neumann*. Mem. Ent. Soc. S. Afr. 6, 3-124.

Tzertzinis, G., Malecki, A., and Kafatos, F. C. (1994). BmCF1, a *Bombyx mori* RXR-type Receptor Related to the *Drosophila ultraspiracle*. J. Mol. Biol. 238, 479-486.

Umesono, K., and Evans, R. M. (1989). Determinants of target gene specificity for steroid/thyroid hormone receptors. Cell 57, 1139-1146.

Voet, D., and Voet, J. G. (1990). Biochemistry (New York: John Wiley and Sons), pp. 779-783.

Wagner, R. L., Apriletti, J. W., McGrath, M. E., West, B. L., Baxter, J. D., and Fletterick, R. J. (1995). A structural role for hormone in the thyroid hormone receptor. Nature 378, 690-697.

Wikel, S. K. (1996). Host immunity to ticks. Annual. Rev. Entomol. 41, 1-22.

Willy, P. J., Umesono, K., Ong, E. S., Evans, R. M., Heyman, R. A., and Mangelsdorf, D. J. (1995). LXR, a nuclear receptor that defines a distinct retinoid response pathway. Genes Dev. 9, 1033-1045.

Wurtz, J. M., Bourguet, W., Renaud, J. P., Vivat, V., Chambon, P., Moras, D., and Grenemeyer, H. (1996). A canonical structure for the ligand-binding domain of nuclear receptors. Nat. Struct. Biol. 3, 87-94.

Yao, T., Segraves, W. A., Oro, A. E., Mckeown, M., and Evans, R. M. (1992). Drosophila *ultraspiracle* modulates ecdysone receptor function via heterodimer formation. Cell 71, 63-72.

Yao, T.-P., Forman, B. M., Jiang, Z., Cherbas, L., Chen, J.-D., Mckeown, M., Cherbas, P., and Evans, R. M. (1993). Functional ecdysone receptor is the product of EcR and *Ultraspiracle* genes. Nature 366, 476-479.

Zhu, X. X., Oliver, J. H., and Dotson, E. M. (1991). Epidermis as the source of ecdysone in an argasid tick. Proc. Natl. Acad. Sci. USA 88, 3744-3747.

CHAPTER II

DEVELOPING AN RT-PCR ASSAY

Introduction

Northern blot analysis (White and Bancroft, 1982), RNase protection assays (Lynn et al., 1983; Zinn et al., 1983), *in situ* hybridization, and the Reverse Transcription-Polymerase Chain Reaction (RT-PCR) (Veres et al., 1987), are techniques that are commonly used to detect and quantitate the expression levels of specific RNAs. In northern blot analysis, the total or Poly(A)$^+$ fraction of RNA is electrophoresed on a denaturing agarose gel and then transferred to a solid membrane, which is hybridized with an isotopic or non-isotopic probe complementary to the sequence of the gene of interest. For rare messenger RNAs (mRNAs), northern blot analysis requires enrichment of the Poly(A)$^+$ fraction, and even then rare messages are difficult to detect. Northern blot analysis is commonly used to provide information about the number, size and relative abundance of transcripts. However, it cannot discriminate between products of highly related genes. It is also the least sensitive RNA detection technique and is most vulnerable to the effects of RNA degradation (Lader, 1997).

The RNase protection assay uses an antisense RNA probe to hybridize to complimentary regions of target RNAs. Because hybridization occurs in solution, it is more efficient than northern blot analysis. Following hybridization, RNase is used to degrade single stranded regions of RNA that are not protected. This method allows researchers to discriminate between products of related genes or between alternatively spliced products of the same gene. The RNase

protection assay is 10-100 fold more sensitive than northern blot analysis and is more tolerant of partial RNA degradation (Lader, 1997).

RT-PCR is a method in which the mRNA is first reverse transcribed into complementary DNA (cDNA), and then is amplified exponentially by PCR using gene-specific primers. This is the most sensitive RNA detection technique, and can often detect transcripts present at extremely low levels in tissue or transcripts from very little starting material (Byrne et al., 1988; Wang et al., 1989). RT-PCR is often the method of choice when assaying expression of multiple targets simultaneously and/or when the amount of RNA is limiting.

Regardless of the method, quantitating RNA expression levels requires the use of internal controls to serve as standards to compare the expression levels of target transcripts. Optimally, the internal standard should be constitutively expressed and remain at constant level in all tissues. A number of "housekeeping" genes from vertebrates have been used as endogenous internal standards, including the β-actin mRNA, which encodes a ubiquitous cytoskeleton protein (Horikoshi et al., 1992; Kinoshita et al., 1992), and the GAPDH mRNA, which encodes glyceraldehyde-3-phosphate-dehydrogenase, a key enzyme in glycolysis (Diffenbach et al., 1988; Inghirami et al., 1990). However, in actuality, these genes are not always expressed at a constant level in all tissues (Bhatia et al., 1994; Elder et al., 1988; Mansur et al., 1993; Siebert and Fukuda, 1984). Therefore, the researcher must first examine the expression of the internal standard to determine if a particular standard is suitable for his/her particular system.

An alternative endogenous internal standard is 28S or 18S ribosomal RNAs, which are abundant in all cell types and are generally expressed at a constant level (deLeeuw et al., 1989; Khan et al., 1992). However, because of their

abundance (80% of the total RNA), they are not practical to use for most targets, whose expression levels are much lower.

Exogenous RNA and DNA standards are another option for normalizing sample-to-sample variations. When using exogenous RNA, a known amount is added prior to reverse transcription, and serves as a control both for reverse transcription and PCR. Regardless of the tube-to-tube variation, the target and standard amplify with the same efficiency. Thus, exogenous RNA and DNA can serve as internal standards. The advantage of exogenous standards over endogenous standards is that the amount of standard used in quantitation assays can be manipulated to match the abundance of the transcript being assayed.

In ticks, as in insects, ecdysteroids regulate development, molting, and salivary gland degeneration (Diehl et al., 1986; Sonnenshine, 1991). In insects, there is evidence for differential expression of both EcR and USP isoform mRNAs during different periods of development (Jindra et al., 1997; Jindra et al., 1996; Talbot et al., 1993). Isoform-specific expression of EcR mRNAs correlates with differential responses of tissues to hormone (i.e. differentiative versus degenerative). Therefore, we wanted to test the hypothesis that EcR and RXR-like mRNAs are also differentially expressed in tick tissues.

Northern blot analysis of mRNA isolated from mixed populations of embryos, larvae and nymphs, as well as salivary glands and ovaries during adult feeding, has confirmed that there is complex regulation of both AamEcR and AamRXR expression (Guo et al., 1997; Guo et al., 1998). However, AamEcRA1 and A3 transcripts are difficult to discriminate by size, and AamEcRA2 is difficult to detect both in whole animals and in isolated salivary glands. AamRXR1 and RXR2-specific probes both detect multiple transcripts, which suggests that each gene encodes multiple RNA isoforms, or that the probes detect

transcripts from related genes (Guo et al., 1998). For these reasons, we wished to use another method to assay their expression. RT-PCR was chosen because small numbers of ticks and tick tissues can be staged and assayed simultaneously for AamEcR isoform and AamRXR mRNA expression.

Although RT-PCR is an extremely sensitive method to detect RNA expression, inconsistencies in procedures used to isolate RNA, to synthesize first strand cDNA and to amplify cDNAs makes it difficult to obtain quantitative information with RT-PCR. The purity, quality and integrity of RNA are major sources of variation in RT-PCR because they can affect the efficiency of reverse transcription. If total RNA is used, contamination with genomic DNA can make it difficult to assess the amount of initial target. If Poly(A)$^+$ mRNA is used, contamination of the Poly(A)$^+$ fraction with cytoplasmic RNAs can introduce another source of variation. In addition, RNA produced using different RNA extraction procedures can also vary greatly in quality and affect the yield of cDNA from reverse transcription. Furthermore, RNA degradation is a source of variation that can not be detected by spectrophotometry.

Another variable is tube to tube variation in PCR amplification. For instance, small differences in temperature during the first few cycles of PCR, which are due to temperature variances across the thermal cycler block and variances in the thickness of tube walls, can lead significant differences in PCR product yield (Gilliland et al., 1990).

Another major factor is the plateau effect that usually occurs at the later thermal cycles. This phenomenon is caused by depletion of the reaction components, degradation of nucleotides or primers, and accumulation of inhibitors over time. At later stages, these effects cause the amplification efficiency to fall and the rate of product accumulation to plateau. Thus, the product yield will no longer be proportional to the amount of starting transcript.

Therefore, to provide a more accurate estimate of initial target levels, several different approaches have been developed that involve using internal controls, which serve as standards to monitor the variability in RNA quality and quantity, and in amplification.

The use of an exogenous RNA competitor in competitive RT-PCR (cRT-PCR) is currently the most sensitive and accurate way to quantitate specific gene expression since RNA competitors can be used to monitor variability in both reverse transcription and PCR reactions (Wang et al., 1989). The construction of a synthetic RNA standard usually involves *in vitro* transcription of cloned DNA templates and quantitation of the RNA standard (Chang et al., 1993; Wang et al., 1989). Because the synthetic RNA must be engineered to contain the flanking sequences of a specific target gene, these procedures are very labor-intensive and time-consuming. In addition, RNA standards are also susceptible to degradation.

Exogenous DNA standards are a popular alternative in quantitation of gene expression. Exogenous DNA can function as an internal control because it competes for the same primer set as the target cDNA in the PCR reaction, and thus, the amplification efficiencies of both remain the same in both exponential and plateau phases of the PCR reaction. Another advantage of using an exogenous DNA in competitive PCR is that it is easy to synthesize and handle (Siebert and Larrick, 1992). The synthesis of a DNA standard requires a two-round PCR reaction to add specific flanking sequences to the neutral DNA and quantitation of the PCR product.

As mentioned previously, endogenous standards, such as β-actin and GAPDH genes, are most commonly used for RT-PCR (Diffenbach et al., 1988; Horikoshi et al., 1992; Inghirami et al., 1990; Kinoshita et al., 1992). In contrast to mammalian systems, in which a wide variety of internal standards are

commercially available, few internal controls exist for arthropods. At the time we initiated this work, no house-keeping genes had been cloned from ixodid ticks. To test its efficacy as an internal control, our laboratory isolated a cytoplasmic actin gene from *A. americanum* (Palmer et al., unpublished data). However, like analogous vertebrate standards, there is stage and tissue-specific variation in the number and level of transcripts produced from the actin gene (Guo et al., 1998).

The goal of this study was to examine the expression patterns of AamEcR and AamRXR mRNAs in processes that are likely to be regulated by ecdysteroids. To accomplish this, we designed gene-specific primers to amplify AamEcR and AamRXR mRNAs. We also designed exogenous DNA standards with AamEcR and AamRXR-specific primer sites for competitive PCR as well as actin-specific primers, which served as an endogenous internal standard.

Materials and Methods

Animals and tissues

Adult ticks *A. americanum*, were reared on sheep according to the methods of Patrick and Hair (1975) at the Oklahoma State University Centralized Ticking Rearing Facility. Unfed, partially fed and replete adult female ticks were collected, placed in groups according to body weight or to days following repletion, as is shown in Table IV. Salivary glands and ovaries were dissected in 4°C tick saline with 20 mM MOPS (TS/$MOPS_{20}$, pH 7.0) (Needham and Sauer, 1979) and quick frozen in liquid nitrogen. Dissected tissues were stored at -70°C until needed.

RNA extraction

RNA was prepared from staged salivary glands and ovaries by a hot phenol/chloroform RNA extraction procedure, adapted from the procedure described by Joett, 1986. RNA was extracted from approximately 30 ovaries or 30 pairs of salivary glands from each feeding stage. The tissue was ground to a fine powder in liquid nitrogen using a mortar and pestle and collected in a 50 ml polypropylene tube. Ten ml of hot phenol (65°C) saturated with 0.2 M sodium acetate (pH 5.0) was added to the tube and the tissue was further disrupted with Brinkman homogenizer. Seven and one-half ml of 0.2 M sodium acetate (pH 5.0) and 1 ml of 20% SDS were added and the mixture was incubated at 65°C for 5 minutes. After vortexing the solution and cooling it to room temperature, 10 ml of chloroform was added and the solution was mixed by vortexing and centrifuged at 14,000 x g for 5 minutes to separate the phases. The lower organic phase was removed with a pipetter. The chloroform extraction was repeated 2-3 times until the aqueous phase was clear and the interface between the aqueous and organic phases was minimal. The aqueous phase was then transferred to a RNase-free centrifuge tube, and precipitated with 2.5 volumes of 100% ethanol at -20°C overnight. To recover RNA, the precipitated RNA was centrifuged at 10,000 x g for 10 minutes, washed with 70% ethanol, dried in a vacuum desiccater, and resuspended in DEPC-treated water. RNA concentrations were estimated by measuring the absorbance at 260 nm and 280 nm using Beckman DU-65 Spectrophotometer. Aliquots of 1 μg of total RNA, were re-precipitated with 0.1 volume of 3.0 M sodium acetate (pH 5.2) and 2.5 volumes of 100% ethanol and stored at -70°C for subsequent RT-PCR reactions.

Oligonucleotide primer set design

To detect AamEcR and AamRXR mRNAs, gene and isoform-specific primers were designed based on the sequences of AamEcRA1, AamEcRA2, AamEcRA3, AamRXR1 and AamRXR2 (Guo et al., 1997; Guo et al., 1998). A total of eighteen oligonucleotide primers were selected using MacVector™ 6.0, (Oxford Molecular Ltd's Sequence Analysis Software for Macintosh) and OLIGO 4.1 (Molecular Biology Insights). Oligonucleotide primers were synthesized on an ABI 392 DNA/RNA synthesizer at the Oklahoma State University Recombinant DNA/Protein Resource Facility. The positions of primers are shown in Figures 6 and 7, and the primer sequences are listed in Table V.

PCR Mimic construction

Primary Mimic DNAs were amplified in a SingleBlock™ thermal cycler system (ERICOMP, inc.), in a 50 µl volume with 10 mM Tris-HCl (pH 9.0 at 25°C), 50 mM KCl, 0.1% Triton ®X-100, 1.5 mM $MgCl_2$, 200 mM of dNTP mix, 2.5 units Promega Taq DNA polymerase, 200 pmol of forward and reverse Mimic primers, and 2 ng neutral DNA (Clontech's PCR MIMIC™ Construction Kit). The PCR reactions were performed for five minutes at 94°C, followed by 16 cycles of 94°C for 45 seconds, 60°C for 45 seconds, and 72°C for one and a half minutes, followed by five minutes at 70°C and two minutes at 30°C.

The products of the first-round PCR reactions were diluted 100-fold, and 2 µl of this diluted DNA was then amplified in a second PCR reaction in a 100 µl volume with 10 mM Tris-HCl (pH 9.0 at 25°C), 50 mM KCl, 0.1% Triton ®X-100, 1.5 mM $MgCl_2$, 200 mM of dNTP mix, 200 pmol of forward and reverse of AamEcR-common or AamRXR1 specific primers, and 5 units Promega Taq DNA polymerase. The second-round PCR reactions were performed for five minutes

at 94°C, followed by 18 cycles of 94°C for 45 seconds, 60°C for 45 seconds, and 72°C for one and a half minutes, followed by five minutes at 70°C and two minutes at 30°C.

The yield of PCR Mimic was estimated by visual comparison of electrophoretic bands produced in the PCR reaction to a standard provided in the PCR MIMIC™ Construction Kit (Clontech). Five µl of the PCR Mimic was diluted in 5 µl of H_2O, 1.5 µl of 10 x PCR buffer (100 mM Tris-HCl (pH 9.0 at 25°C), 500 mM KCl, 1% Triton ®X-100) (Promega) and 2 µl of 6 x DNA gel dye. The diluted PCR Mimic DNA was electrophoresed on a 1% agarose gel along with three dilutions of a ϕX174/*Hae* III digested DNA (100 ng/µl). Following staining with ethidium bromide (10 µg/ml), band intensities of PCR Mimic and the DNA size marker were visually compared, and the concentration of the PCR Mimic was calculated based on the amount of the DNA size marker and the volume of Mimic loaded.

Amplification of genomic DNA with PCR

Four primer sets that span the AamEcR DNA and ligand binding domains were used to amplify genomic DNA (Figure 8). PCR reactions were performed in a 50 µl volume with 10 mM Tris-HCl (pH 9.0 at 25°C), 50 mM KCl, 0.1% Triton ®X-100, 1.5 mM $MgCl_2$, 200 mM of dNTP mix, 200 pmol of forward and reverse primers, 2.5 units Promega Taq DNA polymerase, and 150 ng genomic DNA. The PCR reactions were performed for three minutes at 94°C, five minutes at 80°C, followed by 30 cycles of 94°C for one minutes, 55°C for one and a half minute, and 72°C for two minutes, followed by five minutes at 70°C and two minutes at 30°C. Primer sets that were designed to amplify AamEcR isoform-specific RNAs (Figure 8), and AamRXR1 and AamRXR2 RNA (Figure 7) were also used to amplify genomic DNA . PCR conditions for AamRXR1 and

AamRXR2 were the same as the preceding conditions except the annealing temperature was 60°C.

To amplify AamEcRA1 and AamEcRA2, the Advantage-GC™ cDNA PCR Kit (Clontech) was used. One hundred fifty ng of genomic DNAs were amplified in a 50 µl volume with 40 mM Tricine-KOH (pH 9.2 at 25C), 15 mM KOAc, 3.5 mM $Mg(OAc)_2$, 5% Dimethyl Sulfoxide (DMSO), 3.75 mg/ml Bovine Serum Albumin (BSA), 0.5 M GC-Melt, 400 pM of dNTP mix, 1 µl/20 µl RT product, 1 ml of 50 x Advantage KlenTaq Polymerase Mix (Clontech's Advantage-GC™ cDNA PCR Kit). The PCR reactions were performed for five minutes at 94°C, followed by 30 cycles of 94°C for one minutes, and 68°C for three minutes, followed by five minutes at 68°C and two minutes at 20°C.

RT-PCR assays

Prior to reverse transcription, total RNA was treated with DNase I to eliminate DNA contamination. One µg of total RNA was incubated at room temperature for 15 minutes, with 20 mM Tris-HCl (pH 8.4), 50 mM KCl, 2 mM $MgCl_2$, and 10 units of GIBCO-BRL DNase I in DEPC-treated water. One µl of 25 mM EDTA was added and the reaction is incubated at 65°C for 15 minutes to heat inactivate the residual DNase I. The treated RNA was then subjected to reverse transcription.

Reverse Transcription reactions were performed using SuperScript™ Preamplification System for first Strand cDNA Synthesis (GIBCO-BRL). The first strand cDNAs were synthesized from 1 µg total RNA isolated from staged salivary glands or ovaries. One µg of DNase I-treated RNA, 50 ng of random hexamers, and DEPC-treated water in a total volume of 12 µl, was incubated at 70°C for 10 minutes, and cooled on ice for 1 minute. The mixture was then incubated at 25°C for 5 minutes in 20 mM Tris-HCl (pH 8.4), 50 mM KCl, 2.5 mM

$MgCl_2$, 1 mM dNTP mix and 0.01 M DTT. Reverse transcriptase reactions were performed with 200 units of SuperScript II reverse transcriptase and incubated at 25°C for 10 minutes, followed by incubation at 42°C for 50 minutes. The reaction was terminated at 70°C for 15 minutes and then chilled on ice. The RNA templates were destroyed by adding 2 units of RNase H and incubating at 37°C for 20 minutes.

Competitive PCR reactions were performed using either AamEcR-common or AamRXR1 primers. One µl of 2×10^{-1} attomoles/µl (amol/µl, amol = 10^{-18} moles) AamEcR-PCR Mimic DNA or one µl of 10^{-1} amol/µl AamRXR1-PCR Mimic DNA was added prior to the reaction. PCR reactions were performed in a 100 µl volume with 10 mM Tris-HCl (pH 9.0 at 25°C), 50 mM KCl, 0.1% Triton ®X-100, 2.5 mM $MgCl_2$, 200 mM of dNTP mix, 200 pmol of forward and reverse AamEcR-common or AamRXR1 primers, 5 units Promega Taq DNA polymerase, and 1 µl/20 µl of cDNA produced from reverse transcription of salivary glands or ovarian RNA. The PCR reactions were performed for three minutes at 94°C, five minutes at 80°C, followed by 30 cycles of 94°C for one minutes, 60°C for one and a half minute, and 72°C for one minutes, followed by five minutes at 70°C and two minutes at 30°C.

Amplification of GC -rich regions of AamEcR mRNAs

The first strand cDNA from GC-rich RNAs were amplified using the following modified PCR conditions:

(1) PCR with 7-deaza-dGTP. PCR reactions were modified to include a mix of nucleotides containing both 7-deaza-dGTP and dGTP in a ratio of 3:1. The PCR reactions were performed in a volume of 100 µl with 10 mM Tris-HCl (pH 9.0 at 25°C), 50 mM KCl, 0.1% Triton®X-100, 2.5 mM $MgCl_2$, 50mM of dATP, dTTP and dCTP mix, 12.5 mM dGTP, 37.5 mM 7-deaza-dGTP (Pharmacia

Biotech), 100 pmol of forward and reverse gene-specific primer, 5 units Promega Taq DNA polymerase, and 2 µl/20 µl first strand cDNA from reverse transcription.

(2) PCR with "GC-Melt". The optimal concentration of GC-Melt (Clontech's Advantage-GC™ cDNA PCR Kit) was titrated using from 0 to 1.5 M in each PCR reaction. AamEcRA1 and AamEcRA2 cDNAs were amplified in a 50 µl volume with 40 mM Tricine-KOH (pH 9.2 at 25°C), 15 mM KOAc, 3.5 mM $Mg(OAc)_2$, 5% Dimethyl Sulfoxide (DMSO), 3.75 mg/ml Bovine Serum Albumin (BSA), 0.5 M GC-Melt, 400 pM of dNTP mix, 1 µl/20 µl RT product, 1 ml of 50 x Advantage KlenTaq Polymerase Mix (Clontech's Advantage-GC™ cDNA PCR Kit). The PCR reactions were performed for five minutes at 94°C, followed by 30 cycles of 94°C for one minutes, and 68°C for two minutes, followed by five minutes at 68°C and two minutes at 20°C.

Results and Discussion

Primer set design

Total RNA is often contaminated with small amounts of genomic DNA that can act as a template in RT-PCR. Therefore, oligonucleotide primers are usually designed to span at least one intron so that products amplified from genomic DNA can be easily distinguished from those amplified from cDNA. In cases where the genomic structure is unknown or primers do not span an intron, samples are either treated with DNase I prior to reverse transcription to remove DNA or controls lacking reverse transcriptase are included. We designed oligonucleotide primers (Figure 8) that spanned conserved introns in *Drosophila* and *Manduca* EcR and RXR/USP genes where possible (Fujiwara et al., 1995; Jindra et al., 1997; Koelle et al., 1991; Oro et al., 1990; Talbot et al., 1993).

To standardize PCR conditions for all primer sets, we initially designed primers 20 nucleotides in length with GC contents close to 50%. Primers were designed to span 300-1000 bp regions to assure that fragments would amplify efficiently and that different products could be discriminated by size.

Initially, oligonucleotide primers were designed to span portions of the AamEcR and AamRXR1 LBDs because we lacked cDNA sequences containing 5' sequences. These primer sets amplified 623 bp (AamEcR) and 665 bp (AamRXR1) products of the expected sizes from total RNA. When we tried to extend the sequences using 5' RACE, we repeatedly failed to amplify portions of the cDNAs encoding the DBD and amino termini, suggesting that secondary structure in the mRNAs were terminating reverse transcription. To isolate full length cDNAs, cDNA libraries were constructed using methyl mercuric hydroxide, a strong inhibitor of RNA secondary structure. Our laboratory subsequently isolated AamEcR cDNAs encoding three unique N-termini (Guo et al., 1997) as well as RXR cDNAs encoding the N-terminus of AamRXR1, and a second RXR gene, AamRXR2 (Guo et al., 1998). Because of the difficulty amplifying products spanning the DBD of the AamRXRs, we chose RXR primer sets spanning the LBDs, which contained multiple introns in most vertebrate RXR genes (Laudet et al., 1992).

The 5' regions containing sequences unique to each of the three AamEcR isoforms are GC rich. The GC content spanning the 5' UT and DBD of AamEcRA1, AamEcRA2, and AamEcRA3 are 72%, 66%, and 62% respectively. Therefore, we had difficulty finding primer sets that met our criteria. When the AamEcRA1 cDNA was amplified using our standard PCR conditions, we obtained a product that was 1 kb larger than predicted size (561 bp) (Figure 9, lane 2). Further, we detected no product when we amplified the AamEcRA2 cloned cDNA with primer sets for AamEcRA2 (Figure 15, lane 1). The most

likely reason for the failure to amplify products of the predicted size is the high GC content in these regions of the AamEcR mRNAs.

To try to overcome the secondary structure, we adopted PCR conditions using 7-deaza-dGTP (Innis, 1990). 7-deaza-dGTP is a dGTP analog that can be incorporated into the DNA sequence but pairs with conventional bases only weakly. This feature of 7-deaza-dGTP enables it to overcome the secondary structure problem so that the full length PCR product can be produced. Using 7-deaza-dGTP, we were able to amplify a PCR product of the correct size using the cloned AamEcRA2 cDNA but no product was amplified using the cloned AamEcRA1 cDNA (data not shown). Using these conditions, however, we were still unable to detect AamEcRA2 mRNA with RT-PCR. Because AamEcRA1 and AamEcRA2 mRNAs can be detected using Northern blot analysis (Guo et al., 1997), we suspected that the 7-deaza-dGTP was not able to completely disrupt secondary structure in the 5' regions of AamEcRA1 and AamEcRA2.

As an alternative, we tried a Advantage-GC^{TM} cDNA PCR kit (Clontech), which contains a novel reagent "GC-Melt" for amplifying GC-rich RNAs. We designed longer primers (~30 nucleotides) with annealing temperatures over 70°C to achieve better amplification at the higher temperatures required to resolve secondary structure, and used a two step PCR program with a 68°C annealing/extension step (Figure 6 and Table V). Using this kit, we have been able to reproducibly amplify AamEcRA1 and AamEcRA2 mRNAs, although we still observe some additional product with AamEcRA1 primers (for example, see Figures 17, 20 and 23).

Genomic structure of AamEcR and AamRXR

Shown in Figure 8 is the putative genomic structure of the AamEcR gene. Intron positions were indicated by arrows 1-1 (AamEcRA1), 1-2 (AamEcRA2), 1-3

(AamEcRA3), and 2, 3, 4 were inferred from the AamEcR cDNA structures, which presumably arise from alternative RNA splicing at these positions. Putative splice sites 5-8 are based on those detected in *D. melanogaster* (6, 7, 8) (Koelle et al., 1991; Talbot et al., 1993) or *M. sexta* (5, 6, 7) (Fujiwara et al., 1995; Jindra et al., 1997). To determine if splice sites 5-8 were conserved in *A. americanum*, we amplified various portions of the AamEcR gene from genomic DNA using the primer sets indicated in Figure 8. A primer set spanning exon 8 (1421/1791) detected a ~900 bp product (Figure 10, panel A, lane 4), while another primer set spanning exons 7 and 8 detected a ~3.2 kb product (Figure 10, panel A, lane 3). The predicted sizes of products lacking introns at these positions are 229 bp and 331 bp, respectively. We were unable to detect a product in genomic DNA when a primer set spanning exons 7, 8 and 9 (1792/1791) was used (Figure 10, panel A, lane 2), suggesting that an additional intron exists at position 6. But the product was too large to be efficiently amplified. The primer set 1792/1791 amplified a 623 bp product of the predicted size from RNA by RT-PCR (Figure 10, panel A, lane 1). This primer set was subsequently chosen to amplify all AamEcR isoforms and is designated AamEcR-common.

Our results indicate that the AamEcR gene also contains introns at position 6-8, similar to *D. melanogaster* and *M. sexta*. However, a primer set spanning the DBD (2024/1878) detected a 217 bp product, identical in size to the cDNA (Figure 10, panel B). Therefore, the intron at position 5 in the DBD, present in most members of the nuclear receptor superfamily (Laudet et al., 1992) is absent in *A. americanum*. This is similar to *D. melanogaster*, which also lacks an intron at that position.

We failed to detect amplification products in genomic DNA with a primer set (3201/3200) spanning splice site (1-1 + 2) (Figure 10, panel C, lane 2) and a

primer set (2285/1878) spanning splice site (1-3 + 4 + 5) (Figure 10, panel C, lane 6), confirming that there are introns spanning the priming sites of AamEcRA1 and AamEcRA2. Using standard PCR conditions and AamEcRA2-specific primers, which encompass a 428 bp region of the 5' untranslated region and first exon, we amplified identical products from genomic DNA and reversed transcribed mRNA (Figure 10, panel C, lane 3 and 4). Therefore, there is no intron between the primer sites for AamEcRA2.

The genomic organization for murine RXR genes (RXRβ and RXRγ) indicates from 3-5 introns in the LBDs (Liu and Linney, 1993). In contrast, the *Drosophila* homologue, USP is intronless (Oro et al., 1990). When genomic DNA was amplified with AamRXR1 or RXR2 primers spanning portions of the ligand binding domain (see Figure 7), we detected products identical in size to the cDNAs (Figure 10, panel C, lane 8-10), indicating that the *A. americanum* RXR LBD apparently also lack introns.

To assure that amplification products were derived from an mRNA template rather than contaminating genomic DNA, we performed RT-PCR on (1) samples without DNase I and reverse transcriptase to test for genomic contamination, (2) samples treated with DNase I but without reverse transcriptase to test the effectiveness of DNase I treatment, and (3) samples treated with both DNase I and reverse transcriptase. We used actin primers (1333/1334) to perform RT-PCR on ovarian RNA isolated from vitellogenic ovaries (250-500 mg) or ovaries nearing oviposition (>5 days). The 660 bp actin product was detectable only in samples with reverse transcriptase (Figure 11), confirming that there is little or no genomic DNA contamination and that PCR products are produced from cDNA.

Developing internal standards

We initially isolated a cytoplasmic actin gene to use as an internal standard in RT-PCR and Northern blot analysis (Palmer et al., unpublished results). Northern blot analysis and RT-PCR results, however, suggested that the number and abundance of actin transcripts was not constant. Therefore, actin would not be a suitable internal standard to measure relative mRNA levels of AamEcR and AamRXR1 targets.

As an alternative, exogenous DNA standards were constructed from a 574 bp BamHI/EcoRI fragment of v-erbB, provided in the PCR MIMIC™ Construction Kit (Clontech), by a two-round PCR reaction, as is shown in Figure 12. In the first PCR reaction, composite primers were used to attach AamEcR or AamRXR1-specific sequences to the PCR Mimic DNA. The composite primers for AamEcR common region were hybrid primers that contain EcR-common primer sequences (1792-1791) (sequences shown in Table VI) that flanked a stretch of 20-nucleotide sequence of the neutral DNA fragment (sequences shown in Table V). The 20-nucleotide sequences of the neutral DNA were selected so that the Mimic DNAs differed in size by approximately 100 bp from target gene transcripts. The hybrid primers contain the EcR-common primer sequences at their 5' end. The same principle was applied to design the composite primers for AamRXR1 (sequences shown in Table V). In the second PCR reaction, the AamEcR-common or AamRXR1-specific primers were used to amplify the primary PCR reaction products.

We constructed a 426 bp mimic DNA as a competitor for amplifying an AamEcR-common region (DBD-LBD) product and a 321 bp mimic for amplifying RXR1-specific ligand binding domain region product. Both Mimics differ in size

by 200 bp with their target cDNAs so that Mimic and target can be well separated on agarose gel.

The yield of PCR Mimics were estimated by visual comparison of electrophoretic bands produced in the PCR reaction to a standard, ϕX174/*Hae* III-digest DNA, provided in the PCR MIMIC™ Construction Kit (Clontech). The yield of Mimic for AamEcR-common region was 5.4×10^6 amol/100 µl and 4.2×10^6 amol/100 µl.

The proper concentration of PCR Mimic for competitive PCR was tested by co-amplifying a series of ten-fold dilutions of the PCR Mimic DNA ($100\text{-}10^{-5}$ amol/µl) with cDNA from salivary glands mRNAs in a competitive PCR reaction using either AamEcR-common or AamRXR1 primers. The intensity of the amplification products electrophoresed on 1% agarose gel was visually compared to find a concentration of Mimic, where the amplification of Mimic DNA and target cDNA were comparable, if not identical. After titration of the Mimic DNA, the optimal concentrations of Mimic for AamEcR-common region and for AamRXR1 were determined to be 2×10^{-1} (Figure 13) and 10^{-1} amol/µl (data not shown), respectively.

Examining AamEcR and AamRXR1 mRNA expression with RT-PCR

To determine AamEcR-common and AamRXR1 mRNA levels, one µg of total RNA isolated from staged salivary glands was treated with DNase I, and reverse transcribed into first strand cDNA with random hexamers. Products were subsequently co-amplified with 1 µl of 2×10^{-1} amol/µl EcR Mimic using EcR-common primer set (1792-1791), or 1 µl of 10^{-1} amol/µl RXR Mimic using AamRXR1 primer set (1511-1595). One-fifth of the competitive PCR reactions were electrophoresed on an agarose gel and the intensity of the target gene product and PCR Mimic product were visually compared.

As shown in Figure 14, when AamEcR and AamRXR1 mRNAs were amplified in competitive PCR using the Mimic DNAs, the levels of EcR Mimic and RXR Mimic remained relatively constant in all samples, suggesting that PCR conditions were uniform. However, the intensity of AamEcR and AamRXR1-specific bands varied. For example, the expression of AamEcR-common mRNAs was fairly constant throughout feeding, but was more robust in 50-500 mg stages of salivary glands. The expression of AamRXR1 mRNAs was notably lower in 20-50 mg and >500 mg stages. However, when competitive PCR was repeated using different aliquots of the same total RNA samples, slight differences in the temporal levels of AamEcR mRNAs were observed. The major differences were in the unfed and replete stages, where in some experiments the mRNA levels were very low (data not shown). These data suggested that the variability was due to either the amount of total RNA in each aliquot and/or in the reverse transcription reactions.

When ovarian cDNAs were amplified (Figure 15), both EcR and RXR1 Mimics were relatively constant, while AamEcR and AamRXR1 mRNAs both showed stage-specific variation. Both mRNAs appeared to decrease in abundance during slow feeding (20-50 mg) and again during rapid engorgement (>250 mg). The level of both mRNAs increased again following repletion in preparation for oviposition. However, as shown in Figure 15, we obtained an additional product of approximately 500 bp, when AamEcR-common primers were used. This, and other products, were also seen when ovarian RNA was amplified with AamEcRA3 and AamRXR1-specific primers (data not shown). Because additional bands were not detected in RT-PCR products of salivary gland RNAs, we suggest that they might represent incompletely processed RNAs present in the germline. Alternatively, some may represent products of alternatively spliced RNAs that do not encode full-length products, such as those

detected in AamEcR and AamRXR screen (Guo et al., 1997; Guo et al., 1998). Nevertheless, their presence makes it impossible to provide a quantitative estimation of target mRNA levels.

Developing a quantitative RT-PCR approach to measure AamEcR and AamRXR transcripts levels hinged on the ability to develop both gene-specific primers and internal standards that can be used in concert. Because of the number of transcripts we wished to assay and technical problems we encountered, this objective was not met. However, the primary objective of this study was to use RT-PCR to develop a profile of the relative level and temporal expression patterns of AamEcR and AamRXR mRNAs. Although actin mRNAs levels are not constant in all the tissues and stages tested, we decided to include it as a control for RNA input and to judge the quality of reverse transcription reactions. For example, if AamEcR and/or AamRXR levels are low in some stages but actin is not, this likely reflects a true difference in their target levels, not simply a difference in RNA input or quality. As shown in chapter III Figures 22-24, when actin was amplified from the same cDNA template as AamEcR, it amplified robustly in all feeding stages except unfed glands. In addition, its level continued to increase during feeding, consistent with previous Northern blot analysis results (Guo et al., 1997). When the levels of actin and other targets from the same stage were compared, we noted that differences in the levels between actin and AamEcR and AamRXR likely reflect true differences in the abundance of mRNAs.

As illustrated in chapter three, cDNA from single RT reactions can be used to simultaneously analyze the expression of AamEcR isoform, AamRXR subtype, and actin mRNAs. Further, these data can be used in concert to develop an overall picture of temporal and tissue-specific expression patterns of these genes during different life stages of *A. americanum*.

REFERENCES

Bhatia, P., Taylor, W., Greenberg, A., and Wright, J. (1994). Comparison of glyceraldehyde-3-phosphate dehygrogenase and 28S-ribosomal RNA gene expression as RNA loading controls for Northern blot analysis of cell lines of varying malignant potenial. Analyt. Biochem. 216, 223-226.

Byrne, B. C., Li, J. J., Sninsky, J., and Poiesz, B. J. (1988). Detection of HIV-1 RNA sequences by *in vitro* DNA amplification. Nucleic Acids Res. 16, 4165-4170.

Chang, P.-F., Narasimhan, M. L., Hasegawa, P. M., and Bressan, R. A. (1993). Quantitative mRNA-PCR for expression analysis of low-abundance transcripts. Plant Molec. Biol. Reporter 11, 237-248.

deLeeuw, W., Slagboom, P., and Vijg, J. (1989). Quantitative comparison of mRNA levels in mammalian tissues: 28S ribosomal RNA level as an acurate internal control. NAR 17, 10137-10138.

Diehl, P. A., Connat, J.-L., and Dotson, E. (1986). Chemistry, function and metabolism of tick ecdysteroids. In Morphology, Physiology, and Behavioral Biology of Ticks, J. R. Sauer and J. A. Hair, eds. (New York: John Wiley and Sons), pp. 165-192.

Diffenbach, C., SenGupta, D., Krause, D., Sawzak, D., and Silverman, R. (1988). Cloning of murine gelsolin and its regulation during differentiation of embryonal carcinoma cells. J. Biol. Chem. 264, 13281-13288.

Elder, P., French, C., Subramaniam, M., Schmidt, L., and Getz, M. (1988). Evidence that the functional β-actin gene is single copy in most mice and is associated with 5' sequences capable of conferring serum- and cycloheximide-dependent regulation. Mol. Cell. Biol. 8, 480-485.

Fujiwara, H., Jindra, M., Newitt, R., Palli, S. R., Hiruma, K., and Riddiford, L. M. (1995). Cloning of an ecdysone receptor homolog from *Manduca sexta* and the developmental profile of its mRNA in wings. Insect Biochem. Molec. Biol. 25, 845-856.

Gilliland, G., Perrin, S., and Bunn, H. F. (1990). Competitive PCR for quantitation of mRNA. In PCR protocols: A Guide to Methods and Applicaitons, M. A.

Innis, D. H. Gelfand, J. J. Sninsky and T. J. White, eds. (San Diego, CA: Academic Press, Inc.), pp. 60-69.

Guo, X., Harmon, M. A., Laudet, V., Mangelsdorf, D. J., and Palmer, M. J. (1997). Isolation of a functional ecdysteroid receptor homologue from the ixodid tick, *Amblyomma americanum* (L.). Insect Biochem. Molec. Biol. 27, 945-962.

Guo, X., Xu, Q., Harmon, M., Jin, X., Laudet, V., Mangelsdorf, D. J., and Palmer, M. J. (1998). Isolation of two functional retinoid x receptor subtypes from the ixodid tick, *Amblyomma americanum* (L.). Mol. Cell. Endocrinol. 139, 45-60.

Horikoshi, T., Danenberg, K. D., Stadlbauer, T. H. W., Volkenandt, M., Shea, L. C. C., Aigner, K., Gustavsson, B., Leichman, L., Frosing, R., Ray, M., Gibson, N. W., Spears, C. P., and Danenberg, P. V. (1992). Quantitation of thymidylate synthase, dihydrofolate reductase, and DT-diaphoroase gene expression in human tumors using the polymerase chain reaction. Cancer Res. 52, 108-116.

Inghirami, G., Grignani, F., Sternas, L., Lombardi, L., Knowles, D., and Dalla-Favera, R. (1990). Down-regulation of LFA-I adhesion receptors by c-myc oncogene in human B lumphoblastoid cells. Science 250, 682-685.

Innis, M. A. (1990). PCR with 7-deaza-2'-deoxyguanosine triphosphate. In PCR protocols: A Guide to Methods and Applications, M. A. Innis, D. H. Gelfand, J. J. Sninsky and T. J. White, eds. (San Diego, CA: Academic Press, Inc.), pp. 54-59.

Jindra, M., Huang, J.-Y., Malone, F., Asahina, M., and Riddiford, L. M. (1997). Identification and mRNA developmental profiles of two ultraspiracle isoforms in the epidermis and wings of *Manduca sexta*. Insect Mol. Biol. 6, 41-53.

Jindra, M., Malone, F., Hiruma, K., and Riddiford, L. M. (1996). Developmental profiles and ecdysteroid regulation of the mRNAs for two ecdysone receptor isoforms in the epidermis and wings of the tobacco hornworm, *Manduca sexta*. Dev. Biol. 180, 258-272.

Joett, T. (1986). Preparation of nucleic acids. In *Drosophila*, a Practical Approach, D. B. Roberts, ed. (Oxford: Oxford Press), pp. 89-97.

Khan, I., Tabb, T., Garfield, R. E., and Grover, A. K. (1992). Polymerase chain reaction assay of mRNA using 28S rRNA as internal standard. Neuroscience Letters 136, T18.

Kinoshita, T., Imamura, J., Nagai, H., and Shimotohno, K. (1992). Quantification of gene expression over a wide range by the polymerase chain reaction. Anal. Biochem. 206, 231-235.

Koelle, M. R., Talbot, W. S., Seagraves, W. A., Bender, M. T., Cherbas, P., and Hogness, D. A. (1991). The Drosophila EcR gene encodes an ecdysone receptor, a new member of the steroid receptor superfamily. Cell 67, 59-77.

Lader, E. (1997). Strategies for quantitation of mRNA: Northern blotting, RPA, and RT-PCR Analysis. Ambion TechNotes 4, 1-12.

Laudet, V., Hanni, C., Coll, J., Catzeflis, F., and Stehelin, D. (1992). Evolution of the nuclear receptor gene superfamily. EMBO J. 11, 1003-1013.

Liu, Q., and Linney, E. (1993). The mouse retinoid-x receptor-gamma gene: genomic organization and evidence for functional isoforms. Mol. Endrocrinol. 7, 651-658.

Lynn, D. A., Angerer, L. M., Bruskin, A. M., Klein, W. H., and Angerer, R. C. (1983). Localization of a family of mRNAs in a single cell type and its precursors in sea urchin embryos. Proc. Natl. Acad. Sci. 80, 2656-2660.

Mansur, N., Meyer-Siegler, K., Wurzer, J., and Sirover, M. (1993). Cell cycle regulation of the glyceraldehyde-3-phosphate dehygrogenase/uracil DNA glycosylase gene in normal human cells. NAR 4, 993-998.

Needham, G. R., and Sauer, J. R. (1979). Involvement of calcium and cyclic AMP in controlling ixodid tick salivary fluid secretion. J. Parasitol. 65, 531-542.

Oro, A. E., MeKeown, M., and Evans, R. M. (1990). Relationship between the product of the *Drosophila ultraspiracle* locus and the vertebrate retinoid X receptor. Nature 347, 298-301.

Patrick, C. D., and Hair, J. A. (1975). Laboratory rearing procedures and equipment for multi-host ticks (*Acarina:Ixodidae*). J. Med. Entomol. 12, 389-390.

Siebert, P., and Fukuda, M. (1984). Induction of cytoskeletal vimentin and actin gene expression by a tumor-promoting phorbol easter in human leukemic cell line. J. Biol. Chem. 260, 3868-3874.

Siebert, P. D., and Larrick, J. W. (1992). Competitive PCR. Nature 359, 557-558.

Sonnenshine, D. E. (1991). Biology of Ticks, Volume 1 (Oxford: Oxford University Press).

Talbot, W. S., Swyryd, E. A., and Hogness, D. S. (1993). *Drosophila* tissues with different metamorphic responses to ecdysone express different ecdysone receptor isoforms. Cell 73, 1323-1337.

Veres, G., Gibbs, R. A., Scherer, S. E., and Caskey, C. T. (1987). The molecular basis of the sparse fur mouse mutation. Science, 415-417.

Wang, A. M., Doyle, M. V., and Mark, D. F. (1989). Quantification of mRNA by the polymerase chain reaction. Proc. Natl. Acad. Sci. USA 86, 9717-9721.

White, B. A., and Bancroft, F. C. (1982). Cytoplasmic dot hybridization: Simple analysis of relative mRNA levels in multiple small cell or tissue samples. J. Biol. Chem. 257, 8569-8572.

Zinn, K., DiMaio, D., and Maniatis, T. (1983). Identification of two distinct regulatory regions adjacent to the human β-interferon gene. Cell 34, 865-879.

CHAPTER III

ANALYSIS OF

AamEcR AND AamRXR mRNA EXPRESSION USING RT-PCR

Introduction

The tick life cycle consists of four distinct stages: embryonic, larval, nymphal, and adult. Bloodfeeding occurs in all but the embryonic stage. For the ixodid tick, *A. americanum*, embryogenesis proceeds over approximately 30 days. In immature stages, the bloodmeal is required to molt to the next stage. Following the embryonic molt, unfed larvae seek a suitable vertebrate host, feed for 3-5 days and then drop from the host upon repletion. The replete larvae take approximately 12-14 days to molt to nymphs. Nymphs also feed for 3-5 days, but the nymphal to adult molt requires about 30 days to complete (Palmer, unpublished results).

The molting process is a programmed sequence of events in which a new cuticle is generated underneath the old one (Nijhout, 1994). The molting process starts with apolysis: the separation of old cuticle from the epidermis and the secretion of a molting gel in the space between. Molting gel contains a number of enzymes that digest the old cuticle and aid in resorption of nutrients used to build the new cuticle. Apolysis is generally the time where mitosis resumes in epidermal cells in preparation for depositing a new cuticle.

After a new cuticulin layer is secreted to protect the epidermis from digestion, the molting gel is activated to digest old endocuticle and the new

exocuticle is secreted on the epidermis. The time at which the molting gel is activated varies in arthropods. However, in all arthropods the molting gel is resorbed shortly before ecdysis and replaced with air, which acts to split the old cuticle along ecdysial sutures. Ecdysis is the actual shedding of the old cuticle. After ecdysis, the new exocuticle is tanned and a new endocuticle is deposited.

Ecdysteroids are best known for their roles in the molting process. In insect models, there is a direct correlation between the profile of ecdysteroid titers and various physiological and morphological events in the molting process (Nijhout, 1994). The early rising phase of the ecdysteroid titer corresponds to the preparatory phase of the molting cycle, which is characterized by DNA and RNA synthesis in the epidermal cells. The latter rising phase of ecdysteroid peak corresponds to apolysis. The decline of the ecdysteroid titer to its basal level initiates ecdysis.

Ecdysteroid titers have also been studied in several ixodid ticks, *A. hebraeum* (Diehl et al., 1982), *Amblyomma variegatum* (Ellis and Obenchain, 1984) and *Dermacentor variabilis* (Dees et al., 1984) during their development. In *D. variabilis*, ecdysteroids occur in every life stage, and their levels are low in unfed larvae and nymphs. During the larval stage, the ecdysteroid content increases sharply during feeding, and continues to increase until the early stages of molting, where the ecdysteroid titer reaches its peak. The ecdysteroid titer then declines sharply during the later stages of molting, as in insects. In the nymphal molt, the ecdysteroid content also increases rapidly during feeding, and peaks during the early stages of molting. However, the ecdysteroid titer declines only slightly during the later stages of molting, remaining fairly high until the end of nymphal molting. The ecdysteroid content is also high in unfed females. This clearly differs from the insect models where a sharp decline in ecdysteroid titer is necessary for ecdysis. Because this decline does occur in larval molting, it

suggests a fundamental difference in the way larval and nymphal molts are regulated in *D. variabilis*. A similar 20-OH ecdysone profile is found in *A. variegatum* molting nymphs (Ellis and Obenchain, 1984), where the ecdysone titer increases at the time of apolysis, peaks after the completion of apolysis, declines slightly but still remains high until ecdysis.

A. hebraeum shows a slightly different ecdysteroid profile during nymphal molting. 20-OH ecdysone is barely detectable until 16 days after nymphal feeding, which is half way through molting, but increases rapidly from then on to a peak on day 23, which is about the time of apolysis, and then declines at the time of ecdysis as in insects.

The feeding behavior of adult ixodid male and female ticks is very different. For example, while male *A. americanum* feed intermittently, taking small blood meals and mating, females feed for up to 14 days. They feed slowly up to 7 days increasing in weight from approximately 5 mg to 20-50 mg. After the slow feeding phase, there is a transitional phase, where mating presumably occurs and then there is a shift to fast feeding. During fast feeding or rapid engorgement, the weight of female ticks increase significantly from approximately 50-100 mg to over 500-1,000 mg at repletion. Depending on the environment and conditions, the total feeding time ranges from 9-14 days (Barker et al., 1984).

A. americanum adult females have a single gonotrophic cycle in which mating is a pre-requisite for fast feeding and oogenesis (Balashov, 1972; Oliver et al., 1984). Oviposition generally begins 7-9 days following repletion. Because of the large mass of eggs produced (up to 20,000), oogenesis and oviposition proceed asynchronously. Oviposition occurs over ~16 days. During this process, much of the body mass is resorbed and nutrients are utilized for egg production. The female dies after completing oviposition.

Ecdysteroid profiles have also been measured in the adult stage of several tick species. In *B. microplus*, the ecdysteroid titer peaks following repletion (Wigglesworth et al., 1985). In *A. hebraeum*, there is no peak in the ecdysteroid titer but there is a consistant increase throughout feeding and oviposition (Kaufman, 1991). In *Rhipicephalus appendiculatus*, the ecdysteroid titer peaks at day 3 post engorgement and decreases gradually thereafter, but is still high at the beginning of oviposition (Magee et al., 1996). There is currently no published information about ecdysteroid titers in any life stage of *A. americanum*.

The role of ecdysteroids in salivary gland degeneration has been studied in female *A. americanum* and *A. hebraeum* (Kaufman, 1986; Kaufman, 1991; Lindsay and Kaufman, 1988). Kaufman's group (1991) demonstrated a direct correlation between the hemolymph ecdysteroid titer and the degree of salivary gland degradation in *A. hebraeum*. These data suggest that the degeneration of salivary glands following engorgement is triggered by an elevated concentration of hemolymph ecdysteroid. A 14-fold increase in hemolymph ecdysteroid titer by day 7 after engorgement has been correlated with complete loss of salivary gland fluid secretory competence (Kaufman, 1986; Kaufman, 1991). Mao, et al. (1995) confirmed the existence of an ecdysteroid receptor in *A. hebraeum* salivary glands, which has a high affinity for ponasterone A (k_d=0.72 nM) and lower affinity for 20-OH ecdysone (k_d=60 nM), similar to ecdysteroid receptors in insects. These data provided strong evidence that ecdysteroids regulate tick salivary gland degeneration via ecdysteroid receptors.

Vitellogenesis and oogenesis are also events that may be regulated by ecdysteroids in ticks (for review see Sonenshine, 1991; Oliver and Dotson, 1993). In ticks oocyte development is divided into five stages (Balashov, 1972). In stage I, which usually occurs in the immature ticks, primary oocytes undergo a small amount of cytoplasmic growth. Stage II involves a great amount of cytoplasmic

growth and is associated with the initiation of adult feeding. Stage III is characterized by vitellogenin uptake by oocytes and yolk-body formation, the initiation of vitellogenesis. This process continues in stage IV. In stage V, mature oocytes are produced.

In adult females, the bloodmeal provides essential nutrients for vitellogenin synthesis. In many species, mating is a prerequisite for oogenesis and oviposition (for reviews see Oliver, 1974; Diehl et al., 1982). The major site of vitellogenin synthesis is believed to be fat body (Chinzei and Yano, 1985), but there is also evidence for a vitellogenic cell in the midgut that also produces vitellogenin (Coons, 1989). Thus, the process of digestion may be linked to the process of vitellogenesis.

In *Drosophila*, pulses of ecdysteroids are associated with the major developmental events in the life cycle (Riddiford, 1993; Thummel, 1995). A peak of 20-OH ecdysone occurs during embryogenesis and several small peaks occur during the three larval instars. A high titer pulse of ecdysteroids at the end of third instar initiates the larval-pupal transition. The highest titer of ecdysteroids occurs during pupariation, and is associated with initiation of metamorphosis.

The expression of *Drosophila* EcRA and EcRB1 mRNA isoforms and their corresponding proteins parallel the profile of ecdysteroid titers (Talbot et al., 1993), but each shows a different temporal and tissue-specific expression pattern. The level of EcRA mRNA is high during embryogenesis and the pupal developmental stage, whereas the level of EcRB1 mRNA is high during embryogensis and at the larval-pupal transition. During the larval-to-adult metamorphosis, the EcRB1 isoform predominates in strictly larval tissues (except for prothoracic glands), that undergo apoptosis, whereas the EcRA isoform predominates in the imaginal rings and imaginal discs. There is no information about the expression of the EcRB2 isoform, which has a short 17 amino acids

terminus. However, these data suggest that the ratio of EcR isoforms is important in determining the fate of particular cells or tissues.

Although we lack information about ecdysteroid titers in *A. americanum*, we wanted to examine the expression of AamEcR and AamRXR mRNAs in processes that are likely to be regulated by ecdysteroids in immature ticks, salivary gland differentiation during feeding and degeneration following feeding, and in ovarian development.

Materials and Methods

Animals and tissues

Lone star ticks, *Amblyomma americanum*, were reared on rabbits (larvae) or sheep (nymphs and adults) according to the methods of Patrick and Hair (1975) at the Oklahoma State University Centralized Ticking rearing Facility. Heterogeneous populations of larvae and nymphs were collected within 24 hours following repletion (D0) and transferred to an incubator (Percival Scientific Inc.), where they were maintained at 24°C, 60% relative humidity (RH) and a photo period of 16 hours light/8 hours darkness. One half gram of larvae were removed from the incubator every other day and quick frozen until day 15 (D15) when molting was completed in all larvae. One gram of nymphs were collected every three days and quick frozen until day 33 (D33) when molting was completed in all nymphs. To assess AamEcR and AamRXR expression in early feeding stages, whole animals of adult female ticks were collected from sheep and separated according to weight (<10 mg, 10-20 mg, 25-50 mg, 50-75 mg, 75-100 mg, and 100-125 mg). Salivary glands and ovaries were dissected from adult ticks, which were separated according to weight and days post-feeding as shown in Table IV, and quickly frozen and stored at -70°C until needed.

RNA extraction

RNA was prepared from molting *A. americanum* larvae and nymphs, staged salivary glands and ovaries, and from whole adult females by the hot phenol/chloroform RNA extraction procedure adapted from the procedure described by (Joett, 1986). RNA was extracted from 0.5 g of larvae, 1 g of nymphs, or 100 mg of whole adult females, using the RAPID Total RNA Isolation Kit (5' Prime → 3' Prime, INC. ®). The tissue was ground in liquid nitrogen to a fine powder using a mortar and pestle and collected into a 50 ml polypropylene tube. Nine ml of 4 M guanidium isothiocyanate was added to the tube and the tissue was further disrupted with a high speed homogenizer. The homogenized tissue was transferred to a pre-spun Phase Lock Gel (PLG) tube and 1.0 ml of 2.0 M sodium acetate (pH 4.0), 9.0 ml of H_2O-saturated phenol, and 3.6 ml of chloroform-isoamyl alcohol (49:1) were added and thoroughly mixed with the tissue. Samples were chilled on ice for 10 minutes and the mixture was centrifuged at 4500 x g for 5 minutes to separate the phases. The upper aqueous phase was then transferred to a fresh pre-spun PLG tube and 5.0 ml of phenol-chloroform-isoamyl alcohol (50:49:1) added and mixed by inversion. The mixture was centrifuged again at 4500 x g for 5 minutes to separate the phases. Five ml of phenol-chloroform-isoamyl alcohol was added and mixed with the upper aqueous phase. The mixture was centrifuged for a third time at 4500 x g for 5 minutes to separate the phases. The resultant aqueous phase was equally dispensed in two RNase-free centrifuge tubes and an equal volume of 100% isopropanol was added to each tube. After incubation at room temperature for 20-30 minutes, the mixture was centrifuged at 16,000 x g for 30 minutes. The pellet was washed with 5 ml of 70% ethanol and re-pelleted at 16,000 x g for 5 minutes. The pellet was further washed with 100% ethanol and dried at room

temperature. RNA was resuspended in a suitable volume of DEPC-treated water. RNA concentrations were estimated by measuring the absorbance at 260 nm and 280 nm using Beckman DU-65 Spectrophotometer. Aliquots of 1 μg of total RNA were precipitated with 0.1 volume of 3.0 M sodium acetate (pH 5.2) and 2.5 volumes of 100% ethanol and stored at -70°C.

RNA was prepared from staged salivary glands and ovaries by a hot phenol/chloroform RNA extraction procedure, adapted from the procedure described by (Joett, 1986). RNA was extracted from approximately 30 ovaries or 30 pairs of salivary glands from each feeding stage. The tissue was ground to a fine powder in liquid nitrogen using a mortar and pestle and collected in a 50 ml polypropylene tube. Ten ml of hot phenol (65°C) saturated with 0.2 M sodium acetate (pH 5.0) was added to the tube and the tissue was further disrupted with Brinkman homogenizer. Seven and one-half ml of 0.2 M sodium acetate (pH 5.0) and 1 ml of 20% SDS were added and the mixture was incubated at 65°C for 5 minutes. After vortexing the solution and cooling it to room temperature, 10 ml of chloroform was added and the solution was mixed by vortexing and centrifuged at 14,000 x g for 5 minutes to separate the phases. The lower organic phase was removed with a pipetter. The chloroform extraction was repeated 2-3 times until the aqueous phase was clear and the interface between the aqueous and organic phases was minimal. The aqueous phase was then transferred to a RNase-free centrifuge tube, and precipitated with 2.5 volumes of 100% ethanol at -20°C overnight. To recover RNA, the precipitated RNA was centrifuged at 10,000 x g for 10 minutes, washed with 70% ethanol, dried in a vacuum desiccater, and resuspended in DEPC-treated water. RNA concentrations were estimated by measuring the absorbance at 260 nm and 280 nm using Beckman DU-65 Spectrophotometer. Aliquots of 1 μg of total RNA, were re-precipitated

with 0.1 volume of 3.0 M sodium acetate (pH 5.2) and 2.5 volumes of 100% ethanol and stored at -70°C for subsequent RT-PCR reactions.

Primer set design

To detect the AamEcR, AamRXR and actin mRNAs, gene and isoform-specific primers were designed based on the sequences of actin (Palmer et al., unpublished results), AamEcRA1, AamEcRA2, AamEcRA3, AamRXR1 and AamRXR2 (Guo et al., 1997; Guo et al., 1998). Using MacVector™ 6.0, (Oxford Molecular Ltd's Sequence Analysis Software for Macintosh) and OLIGO 4.1 (Molecular Biology Insights), a total of eighteen oligonucleotide primers were selected. Primers were synthesized on an ABI 392 DNA/RNA synthesizer at the Oklahoma State University Recombinant DNA/Protein Resource Facility. The oligonucleotide primer sequences are listed in Table V. A primer set that is corresponded to the conserved amino acids in cytoplasmic actins were designed to amplify all actin transcripts that are encoded by members of multigene families (Hightower and Meagher, 1986). A primer set that amplifies the EcR common region spanning the DBD and LBD was used to detect all EcR isoforms (Figure 6). EcR isoform-specific primers were designed to amplify the unique sequences from the 5' regions of AamEcRA1, AamEcRA2, and AamEcRA3 mRNAs (Figure 6). Because of their extensive DNA sequence identity, gene-specific primers were synthesized from unique sequences in the ligand binding domains of AamRXR1 and AamRXR2 (Figure 7) (Guo et al., 1998).

RT-PCR assays

Prior to reverse transcription, total RNA was treated with DNase I to eliminate DNA contamination. One μg of total RNA were incubated at room temperature for 15 minutes, with 20 mM Tris-HCl (pH 8.4), 50 mM KCl, 2 mM

$MgCl_2$, and 10 units of GIBCO-BRL DNase I in DEPC-treated water. One µl of 25 mM EDTA was added and the reaction is incubated at 65°C for 15 minutes to heat inactivate the residual DNase I. The treated RNA was then subjected to reverse transcription.

Reverse Transcription reactions were performed using SuperScript™ Preamplification System for first Strand cDNA Synthesis (GIBCO-BRL). The first strand cDNAs were synthesized from 1 µg total RNA isolated from staged salivary glands or ovaries. One µg of DNase I-treated RNA, 50 ng of random hexamers, and DEPC-treated water in a total volume of 12 µl, was incubated at 70°C for 10 minutes, and cooled on ice for 1 minute. The mixture was then incubated at 25°C for 5 minutes in 20 mM Tris-HCl (pH 8.4), 50 mM KCl, 2.5 mM $MgCl_2$, 1 mM dNTP mix and 0.01 M DTT. Reverse transcriptase reactions were performed with 200 units of SuperScript II reverse transcriptase and incubated at 25°C for 10 minutes, followed by incubation at 42°C for 50 minutes. The reaction was terminated at 70°C for 15 minutes and then chilled on ice. The RNA templates were destroyed by adding 2 units of RNase H and incubating at 37°C for 20 minutes.

AamEcR-common, AamEcRA3, AamRXR1 and AamRXR2 RT products were amplified using regular PCR conditions. PCR reactions were performed in a 50 µl volume with 10 mM Tris-HCl (pH 9.0 at 25°C), 50 mM KCl, 0.1% Triton ®X-100, 2.5 mM $MgCl_2$, 200 mM of dNTP mix, 100 pmol of forward and reverse AamEcR-common, AamEcRA3, AamRXR1 or AamRXR2 primers, 2.5 units Promega Taq DNA polymerase, and 1 µl/20 µl of cDNA produced from reverse transcription. The PCR reactions were performed for three minutes at 94°C, five minutes at 80°C, followed by 30 cycles of 94°C for one minutes, 60°C for one and a half minute, and 72°C for one minutes, followed by five minutes at 70°C and two minutes at 30°C.

Because the high GC contents in the 5' untranslated regions of AamEcRA1 and A2 mRNA, PCR conditons with "GC-Melt" (Clontech's Advantage-GC™ cDNA PCR Kit) were adopted. The optimal concentration of GC-Melt was titrated using from 0 to 1.5 M in each PCR reaction. AamEcRA1 and AamEcRA2 cDNAs were amplified in a 50 µl volume with 40 mM Tricine-KOH (pH 9.2 at 25C), 15 mM KOAc, 3.5 mM $Mg(OAc)_2$, 5% Dimethyl Sulfoxide (DMSO), 3.75 mg/ml Bovine Serum Albumin (BSA), 0.5 M GC-Melt, 400 pM of dNTP mix, 200 pmol of forward and reverse AamEcRA1 or A2 primers, 1 µl/20 µl RT product and 1 µl of 50 x Advantage KlenTaq Polymerase Mix (Clontech's Advantage-GC™ cDNA PCR Kit). The PCR reactions were performed for three minutes at 94°C, followed by 30 cycles of 94°C for one minutes, and 68°C for two minutes, followed by five minutes at 68°C and two minutes at 20°C.

Blot hybridizations

Following RT-PCR, 20% of the PCR products were electrophoresed on 1.2% agarose gels and visualized by ethidium bromide staining. The agarose gels were denatured in two volumes of denaturation buffer (0.5 M NaOH, 1.5 M NaCl) twice for 30 minutes and neutralized in two volumes of neutralization buffer (1M NH_4OAc) twice for 30 minutes (Smith and Summers, 1980). The amplification products were then transferred to nitrocellulose membrane and fixed by UV-crosslinking.

Internal oligonucleotides specific for each RT-PCR product (see Table V) were end-labeled with γATP^{32} (New England Nuclear) (Sambrook et al., 1989). Two hundred pmol of internal oligonucleotides were incubated at 37°C for 5 minutes in a 50 µl volume with 1 X Kinase buffer (70 mM Tris-HCl (pH 7.6), 10 mM $MgCl_2$ and 5 mM DTT), 150 µCi γATP^{32} and 8 units of T4 polymerase Kinase (Promega). The samples were incubated at 68°C for 10 minutes. The γATP^{32}-

labeled oligonucleotides were loaded on Bio-Spin® 6 Chromatography Columns(BIO-RAD) and centrifuged for 4 minutes at 1,000 x g to separate labeled oligonucletides from uncorporated γATP^{32}. The blots were prehybridized overnight at 42°C in hybridization buffer (6 X SSC, 1 mM EDTA, 0.5% SDS, 0.1 mg/ml ssDNA, 1 X Denhardts). The γATP^{32}-labeled oligonucleotides were then added to hybridization buffer and incubated at 42°C for 6 hours. After hybridization, blots were washed with 2 X SSC, 0.1% SDS twice at room temperature for 30 minutes, followed by exposure to Kodak X-ray film (Sambrook et al., 1989).

Results and Discussion

We previously isolated a cytoplasmic actin cDNA (Palmer, unpublished results) and designed actin specific primers to assess its utility as an internal standard in Northern blot analysis and RT-PCR. Our results indicated that while actin mRNAs were generally abundant, there were both temporal and tissue specific variation in the number and abundance of transcripts (Guo et al., 1998). Despite these limitations, we chose to use actin primers to compare the relative levels of actin mRNAs amplified from different stages to those amplified with AamEcR and AamRXR primer sets. Using actin, we could assess both relative RNA input and quality. This was particularly important when AamEcR and/or AamRXR mRNA levels were low or absent. Because actin amplification was usually robust, and we could determine that RNA input or quality was not a factor in reduced levels of AamEcR and AamRXR mRNA.

Molting larvae

To assess AamEcR and AamRXR expression during larval molting, we collected larvae within 24 hours after repletion and stored them in an incubator

maintained at 24°C, 60% RH with a photo period of 16 hours light/8 hours darkness. Ticks were frozen at 2-day intervals throughout molting. To assess their molting progress, larvae were placed under a dissecting microscope and scored for the separation of the cuticle (apolysis), appearance of molting gel, resorption of molting gel and the occurrence of ecdysis (Table VII).

We began to see separation of the old cuticle from epidermis in some ticks around D4, followed by accumulation of molting gel in most by D6-8. Apolysis was completed in most larvae by D8. Because molting gel obscures the underlying epidermis, we did not observe changes until D12 when the extra cuticular space cleared and the old cuticle began to separate. Ecdysis was completed in most larvae between D12-15.

To assess AamEcR and AamRXR mRNA expression, total RNA was prepared from molting larvae, and stored in one μg aliquots. RNA samples were treated with DNase I to remove any contaminating genomic DNA, and mRNA was reverse transcribed to cDNA with SUPERSCRIPT II reverse transcriptase (GIBCO BRL). One-twentieth of each RT reaction was amplified with actin, AamEcR isoform-specific (Figure 6) and AamRXR primer sets (Figure 7).

The data collected from molting larvae are summarized in Table VIII and presented in Figures 16-18 and represent two day intervals. As seen in Figure 16, when EcR-common and Actin primers were used to amplify cDNA from molting larvae, the levels of both mRNAs were low in replete larvae (D0) but rapidly increased during molting. In contrast to actin mRNA, which remained fairly constant after D6, EcR-common levels peaked on D6-8, around apolysis, declined slightly by D10, and peaked again on D12. EcR-common levels decreased sharply by D15 at ecdysis, similar to insect EcRs.

When the levels of the individual AamEcR isoform mRNAs were assessed, a more complicated pattern emerged (Figure 17). While all three AamEcR

isoform mRNAs were low at D0 and D15, only AamEcRA1 paralleled the pattern seen with AamEcR-common primers, with high levels persisting through D12. AamEcRA2 mRNA expression overlapped AamEcRA1, but its expression lagged behind AamEcRA1, peaking around apolysis, declining on D10 and increasing slightly on D12. AamEcRA2 mRNA was undetectable at ecdysis. AamEcRA3 mRNA showed the tightest regulation, with only a brief period of expression around apolysis from D4 to D8.

Like AamEcR, AamRXR1 and AamRXR2 mRNAs were also very low in replete larvae, and both appeared to peak during apolysis. AamRXR1 levels were more tightly regulated, and like AamEcRA2, declined on D10, peaked again on D12 and were undetectable at ecdysis. AamRXR2 expression was most similar to AamEcRA1, being broadly expressed throughout molting. AamRXR2 was the predominant AamRXR expressed at ecdysis (Figure 18).

As shown in Table VIII, there was a general pattern in both AamEcR and AamRXR expression that correlated with the molting cycle. All mRNAs peaked at apolysis, paralleling the high titer of ecdysteroid seen in *D. variabilis* molting larvae (Dees et al., 1984). Interestingly there was a decline at D10, which was followed by another peak at D12 when the molting gel was resorbed. Ecdysis paralleled the declining level of ecdysteroid seen in *D. variabilis* molting larvae (Dees et al., 1984). By the time ecdysis was complete on D15, the levels of all mRNAs, except AamRXR2, were low or undetectable. This suggests that AamRXR2 may play a role in ecdysis independent of AamEcR. The most tightly regulated transcript was AamEcRA2, which was expressed only briefly during apolysis, suggesting that its role is limited to events initiated at that time.

Molting Nymphs

To assess AamEcR and AamRXR expression during nymphal molting, we collected nymphs within 24 hours after repletion and stored them in an incubator maintained at 24°C, 60% RH with a photo period of 16 hours light/8 hours darkness. Aliquots were frozen at 3-day intervals throughout molting. To assess their molting progress, nymphs were placed under a dissecting microscope and scored for the separation of the cuticle, appearance of molting gel, resorption of molting gel and the occurrence of ecdysis (Table VII). We began to see separation of the old cuticle from epidermis in some ticks around D8, followed by accumulation of molting gel by D9-16. Apolysis was completed in all nymphs by D18. The molting gel was resorbed starting around D24 and ecdysis occurred between D27-33.

Total RNA was prepared from molting nymphs, and stored in one µg aliquots. As with larval samples, RNA was treated with DNase I and then reverse transcribed as described in Materials and Methods. One-twentieth of each RT reaction was amplified with actin, AamEcR isoform-specific and AamRXR primer sets.

The data collected from molting nymphs are summarized in Table IX and presented in Figure 19-21. As seen in Figure 19, actin mRNA amplified robustly from D0-D33, while EcR-common mRNA was low or undetectable until D6. As with larvae, there were two peaks of AamEcR mRNA during the molting cycle. The first occurred from D6-18 during apolysis and the second around D24-27, when molting gel was resorbed. Like larvae, when individual AamEcR isoforms were amplified (Figure 20), AamEcRA1 appeared to have the broadest expression pattern. Unlike larvae, there was not a lag between the expression of AamEcRA1 and AamEcRA2 mRNAs, and the expression pattern of AamEcRA2

paralleled AamEcRA1. The only exception was in the D21 sample, where AamEcRA2 expression was significantly lower than AamEcRA1. Again, as with larvae, AamEcRA3 was tightly regulated, with a distinct peak occurring at D9-D12, around apolysis. Very low levels, however, were detected at other times, using a ^{32}P-labeled oligonucleotide internal to AamEcRA3 (Figure 20, panel B).

When the AamRXR mRNAs were amplified (Figure 21), the expression pattern of AamRXR1 closely paralleled that of the composite AamEcR expression pattern. AamRXR2 expression overlapped AamRXR1, but there were significant differences on D0 and D21. AamRXR1 expression was undetectable on D0 and D21, while AamRXR2 was expressed, suggesting it is the sole AamRXR expressed on D0 and D21.

When AamEcR and AamRXR expression profiles are considered together, there were three notable dips in AamEcR and AamRXR expression that occurred around D3, D21 and D30 (see Table IX).

In our study, larval and nymphal molt of *A. americanum* took up to 15 and 33 days, respectively. While there is no information about ecdysteroid titers during molting in *A. americanum*, similar studies performed in other ixodid ticks, *A. herbraeum* (Diehl et al., 1982) and *D. variabilis* (Dees et al., 1984) suggest that ecdysteroid titers are low in unfed larvae, increase sharply during feeding, peak at the early molting stage and slowly decline until the end of molting. However, there is a notable difference in ecdysteroid levels in nymphal molting among different species. In *D. variabilis* and *A. variegatum* (Ellis and Obenchain, 1984) molting nymphs, ecdysteroid titers rise during feeding and remain high throughout molting, while in *A. hebraeum* molting nymphs, ecdysteroid titers rise just before apolysis and peak at apolysis but decline to basal levels at the end of molting. The high ecdysteroid titer in *D. variabilis* and *A. variegatum* molting nymphs contrasts with insect models, where the increased ecdysteroid titers

trigger apolysis and low titers trigger ecdysis (Thummel, 1995), while *A. hebraeum* ecdysteroid titer conforms to insect models.

Our results of AamEcR and AamRXR mRNA profiles in molting nymphs seem to parallel the ecdysteroid profiles seen in *D. variabilis* and *A. variegatum*, where low ecdysteroids titers may correspond to low or absent AamEcR and AamRXR mRNA expression and relatively high titers of ecdysteroids may correspond to relatively high levels of AamEcR and AamRXR mRNA expression.

An other interesting result is the restricted expression pattern of AamEcRA3 mRNA, which is expressed only during apolysis in both molting larvae and nymphs. These data suggest AamEcRA3 expression is tightly regulated during molting and may be associated with initiating events such as the synthesis and secretion of the molting gel or the mitosis and cell division of the underlying epidermis (Nijhout, 1994). There is a notable dip in AamEcRA2 mRNA expression and to a lesser extent in AamEcRA1 around D10 in molting larvae and D21 in molting nymphs. This dip is also evident in AamRXR1 and to a lesser extent in AamRXR2. In some insect species, activation of molting gel and subsequent digestion of old cuticle does not occur until late in molting cycle (Nijhout, 1994). It is possible that this process is also linked to changing ecdysteroid titers.

Another interesting observation is the expression of AamRXR2 mRNA when AamRXR1 and AamEcR mRNA levels are low. These data suggest that AamRXR2 may play a role independent of AamEcR.

Salivary Glands

Salivary glands are crucial to maintaining a viable host-tick interface and are the major organ for osmoregulation during feeding (Sauer et al., 1986). During slow feeding, salivary glands produce and secrete a number of products

designed to evade host immune responses (Wikel, 1996), and prevent blood coagulation and platelet aggregation (Ribiero, 1987). During fast feeding, salivary gland morphology changes dramatically (Binnington, 1978; Krolak et al., 1982; Megaw and Beadle, 1979) and the salivary gland clearly resembles a secretory organ, providing the major route for pumping excess fluid and ions into the host. Cells become smaller, no longer contain secretory granules, and the lumen enlarges considerably at repletion. Following repletion, salivary glands undergo degeneration, ecdysteroid mediated programmed cell death (Kaufman, 1986; Kaufman, 1991).

In insect models, apoptosis of obsolete larval tissues and their subsequent replacement is initiated by ecdysone. Selective expression of EcR isoforms are associated with differentiative versus apoptotic response. In some tissues, the ratio of EcR isoforms dictates the response (Jiang et al., 1997; Talbot et al., 1993; Truman, 1996; Truman et al., 1994). To test the hypothesis that differential expression of AamEcR and AamRXR may regulate differentiation and degeneration programs in tick salivary glands, we performed RT-PCR of salivary gland RNA isolated throughout feeding. As shown in Table IV, we collected glands from ticks weighing 20-50 mg (D5-7), 50-100 mg (D7-9), 100-250 mg (D10-12), 250-500 mg (D12-14), >500 mg (>D14) and replete ticks.

Similar to Northern blot analysis results (Guo et al., 1998), actin mRNA levels were low in unfed salivary glands and the levels steadily increased throughout feeding (Figure 22). AamEcR-common RNA was also very low in unfed glands but increased dramatically in 20-50 mg tick salivary glands. However, its level remained relatively constant thereafter (Figure 22). As shown in Figure 23, AamEcRA1 mRNA expression steadily increased throughout feeding as did AamEcRA3 and both mRNAs were most abundant in the fast feeding stages. In contrast, AamEcRA2 had a reciprocal expression pattern,

where the highest levels of expression occurred in the unfed and slow feeding stages and steadily declined during fast feeding. AamEcRA2 mRNA was absent in replete salivary glands. This result is consistent with those obtained from Northern blot analysis where AamEcRA1 and AamEcRA3 levels appeared to increase during feeding, whereas AamEcRA2 was difficult to detect (Guo et al., 1998).

AamRXR1 mRNA was present at fairly constant levels in both unfed and feeding glands, with the possible exception of slow feeding, where it appeared to decline slightly. Therefore, AamRXR1 was expressed constitutively throughout feeding (Figure 24). In striking contrast, AamRXR2 mRNA was not detectable during slow feeding but appeared in 50-100 mg ticks, when mating and the transition from slow to fast feeding presumably occur. AamRXR2 mRNA levels peaked during the fast feeding stages and remained high in salivary glands from replete females.

These data show that AamEcRA2 and AamRXR1 may be the predominant mRNA isoforms expressed in the salivary glands during the early feeding stages. This suggests that the AamEcRA2/AamRXR1 heterodimer may predominate during the early feeding stages, at least in some cell types. Because AamEcRA1 and A3 are also expressed, they may play a role in controlling regulatory circuits important in production and secretion of products important in establishing the host-vector interface.

Equally as striking is the appearance of AamRXR2 mRNA during the transition from slow to fast feeding. The appearance of AamRXR2 may signal a major switch in salivary gland physiology from a tissue that is producing and secreting products to one that now is transporting fluid generated during fast feeding back to the host. Both AamEcRA1 and AamEcRA3 (but not AamEcRA2)

mRNA levels also increase dramatically in fast feeding salivary glands, suggesting they too may play a role in fast feeding.

Because AamRXR2 is absent in salivary glands in the early feeding stages, we wanted to determine if AamRXR2 is also absent in other tissues during slow feeding. Therefore, we examined the expression of AamEcR/AamRXR mRNA in adults females weighing <10 mg, 10-20 mg, 25-50 mg, 50-75 mg, 75-100 mg and 100-125 mg.

The data collected from RT-PCR of mRNA isolated from whole animals are summarized in Table XI and presented in Figure 25-27. The expression of actin and AamEcR-common was fairly constant in all stages tested (Figure 25). When isoform specific expression of AamEcR was examined (Figure 26), AamEcRA1 was constant while AamEcRA2 appeared to decline near the transition phrase from slow to fast feeding. AamEcRA3 levels fluctuated and were lower in 25-75 mg animals. However, expression of both AamRXR1 and AamRXR2 were fairly constant throughout slow feeding (Figure 27), demonstrating that AamRXR2 is expressed in other tissues during slow feeding. Therefore, the absence of AamRXR2 mRNA expression in salivary glands during the slow feeding stages is tissue-specific.

Ovaries

In many insects, adult reproduction is controlled by juvenile hormone (JH) (for review, see Wyatt, 1997). However, in some insects ecdysteroids also play a role in adult reproduction (for review see Hagedorn, 1985). In ticks, there has been no definitive evidence that JH is synthesized, although they may utilize a molecule with a similar mechanism of action (Pound and Oliver, 1979). Recent evidence, however, suggests a positive correlation between vitellogenesis and ecdysteroid titers in *Ixodes scapularis* (James et al., 1997), *B. microplus*

(Wigglesworth et al., 1985) and *Rhipicephalus appendiculatus* (Magee et al., 1996). In *I. scapularis* and *B. microplus* , ecdysteroid levels rise and peak at the end of feeding , while in *R. appendiculatus* ecdysteroid titers peak 3 days post-engorgement, 1 day preceding oviposition. In *A. hebraeum*, ecdysteroid levels rise during feeding and remain high until oviposition (Kaufman, 1991). Since ecdysteroids do play an important role in ticks, we wanted to examine AamEcR an AamRXR mRNA expression in ovaries of adult female *A. americaumm*.

To assess AamEcR/AamRXR expression in ovarian development throughout feeding and following repletion, we examined AamEcR and AamRXR expression. As shown in Table IV, we collected ovaries from unfed ticks and feeding ticks weighing 20-50 mg (D5-7), 50-100 mg (D7-9), 100-250 mg (D10-12), 250-500 mg (D12-14), >500 mg (>D14) and from replete ticks from 1-2 days, 3-4 days, 4-6 days, 5-6 days to >6 days post-feeding, where oviposition begins.

When actin primers were used to assess actin mRNA abundance in ovaries in unfed females, feeding females, and up to 6 days post repletion, there was little variation except in fast feeding and newly replete ovaries, where there was a slight down regulation (Figure 28).

In contrast, AamEcR-common mRNA expression fluctuated through feeding (Figure 28). For example, while AamEcR-common was present in ovaries dissected from unfed females, its level was low in 20-50 mg ticks and then increased during the transitional feeding phase when vitellogenin synthesis begins (Balashov, 1972; Coons, 1989). AamEcR-common levels again declined during fast feeding, a period when blood digestion is reduced while the tick imbibes a large volume of blood. AamEcR mRNA level increased again 1-2 days post repletion when digestion and presumably vitellogenesis resume (Coons, 1989). This pattern was mirrored with all three AamEcR isoforms (Figure 29) and

both AamRXR mRNAs (Figure 30), suggesting that there is coordinate regulation of AamEcR isoforms and the AamRXRs.

SDS-PAGE analysis of ovarian AamEcR proteins isolated from post-feeding ticks (D1-6) show a dramatic change in protein profiles on D4 post-repletion that is consistent with active uptake of vitellogenin (Guo, unpublished results). Therefore, the increase in AamEcR and AamRXR mRNA expression on D3-4 post-repletion is positively correlated with vitellogenin uptake and oocyte maturation in preparation for oviposition.

Conclusions

Our results show that the changes in AamEcR and AamRXR mRNA expression parallel events in the tick that are likely to be regulated by ecdysteroids. As in insects, the regulation of different reponses to ecysteroids in different tissues at different stages is likely to be achieved by changes in AamEcR and AamRXR partner and/or by changes of relative ratios within AamEcR isoforms and two AamRXRs.

In molting larvae, the increase of three AamEcR isoforms and two AamRXRs parallels apolysis, and the decline of three AamEcR isoforms and AamRXR1 occurs at ecdysis. AamRXR2, which level remains high at ecdysis, may play a specific role in ecdysis that is independent of AamEcR. In molting nymphs, the increase of three AamEcR isoforms and two AamRXRs also parallels apolysis. However, there is no decline of AamEcR and AamRXR mRNAs at ecdysis, suggesting there is a fundamental difference between larval and nymphal ecdysis as seen in *D. variabilis* (Dees et al., 1984) and *A. variegatum* (Ellis and Obenchain, 1984). The tightly regulated expression of AamEcRA3 only during apolysis in both molting larvae and nymphs suggests that its roles is limited to events that occur during apolysis.

In the salivary glands, AamEcRA2 and AamEcRA1 and A3 have reciprocal expression patterns with high levels of AamEcRA2 in the unfed and slow feeding stages. Another striking feature is the onset of AamRXR2 expression during the transitional phase from slow to fast feeding, while AamRXR1 is expressed constitutively throughout feeding. These suggest that salivary gland differentiation and degeneration may be regulated by changes in the ratios of the three AamEcR isoforms at different feeding stages and the change from AamRXR1 to AamRXR2 partner, in some cell types during fast feeding.

In ovaries, AamEcR and AamRXR have similar expression patterns, in which the declining expression levels correlate with reduced digestion and perhaps with the onset of vitellogenesis at the fast feeding stages and increasing expression levels correlate with active vitellogenin uptake post-engorgement in preparation for ovipostion.

REFERENCE S

Balashov, Y. S. (1972). Bloodsucking ticks (Ixodoidea) vectors of disease of man a and animals. Misc. Pub. Entomol. Soc. Am. 8, 161-376.

Barker, D. M., Ownby , C. L., Krolak, J. M., Claypool, P. L., and Sauer, J. R. (1984). The effects of attachment, feeding, and mating on the morphology of the type I avelous of salivary glands of the lone star tick, *Amblyomma americanum* (L.). J. Parasitol. 70, 99-113.

Binnington, K. C. (1978). Sequential changes in salivary gland structure during attachment and feeding of the cattle tick, *Boophilus microplus*. Int. J. Parasitol. 8, 91-115.

Chinzei, Y., and Yano, I. (1985). Fat body is the site of vitellogenin synthesis in the soft tick, *Ornithodoros moubata*. J. Comp. Physiol. 155, 671-678.

Coons, L. B., Lamoreaux, W. J., Rosell-Davis, R., Tarnowski, B. I. (1989). Onset of vitellogenin production and vitellogenesis, and their relationship to changes in the midgut epithelium and oocytes in the tick *Dermacentor variabilis*. Exp. and App. Acarol. 6, 291-305.

Dees, W. H., Sonnenshine, D. E., and Breidling, E. (1984). Ecdysteroids in the american dog tick, *Dermacentor variabilis* (Acari: Ixodidae), during different periods of tick development. J. Med. Entomol. 21, 514-523.

Diehl, P. A., Aeschlimann, A., and Obenchain, F. D. (1982). Tick reproduction: oogenesis and oviposition. In Physiology of Ticks, F. D. Obenchain and R. Galun, eds. (Oxford: Pergamon Press), pp. 277-350.

Diehl, P. A., Germond, J. E., and Morici, M. (1982). Correlation between ecdysteroid (Acarina: Ixodidae). Rev. Suisse Zool. 89, 859-868.

Ellis, B., and Obenchain, F. D. (1984). *In vitro* and *in vivo* production of ecdysteroids by nymphal *Amblyomma variegatum* ticks. In Acarology VI, D. A. Griffiths and C. E. Bowman, eds. (Chichester: Ellis Horwood), pp. 400-404.

Guo, X., Harmon, M. A., Laudet, V., Mangelsdorf, D. J., and Palmer, M. J. (1997). Isolation of a functional ecdysteroid receptor homologue from the ixodid tick, *Amblyomma americanum* (L.). Insect Biochem Molec. Biol. 27, 945-962.

Guo, X., Xu, Q., Harmon, M., Jin, X., Laudet, V., Mangelsdorf, D. J., and Palmer, M. J. (1998). Isolation of two functional retinoid x receptor subtypes from the ixodid tick, *Amblyomma americanum* (L.). Mol. Cell. Endocrinol. 139, 45-60.

Hagedorn, H. H. (1985). The role of ecdysteroids in reproduction. Comp. Insect Physiol. Biochem. Pharm. 8, 205-261.

Hightower, R. C., and Meagher, R. B. (1986). The molecular evolution of actin. Genetics 114, 315-332.

James, A. M., Zhu, X. X., and Oliver, J. H., Jr. (1997). Vitellogenin and ecdysteroid titers in ixodes scapularis during vitellogenesis. J. Parasitol. 83, 559-563.

Jiang, C., Baehrecke, E. H., and Thummel, C. S. (1997). Steroid regulated programmed cell death during *Drosophila* metamorphosis. Development 124, 4673-4683.

Joett, T. (1986). Preparation of nucleic acids. In *Drosophila*, a Practical Approach, D. B. Roberts, ed. (Oxford: Oxford Press), pp. 89-97.

Kaufman, R. (1986). Salivary gland degeneration in female tick *Amblyomma hebraeum* koch (Acarina: Ixodidae). In Morphology, Physiology, and Behavioral Biology of Ticks, J. R. Sauer and J. A. Hair, eds. (New York: John Wiley and Sons), pp. 46-54.

Kaufman, W. R. (1991). Correlation between haemolymph ecdysteroid titre, salivary gland degeneration and ovarian development in the ixodid tick, *Amblyomma herbraem* KOCH. Insect Physiol. 37, 95-99.

Krolak, J. M., Ownby, C. L., and Sauer, J. R. (1982). Alveolar structure of salivary glands of the lone star tick, *Amblyomma Americanum* (L.): unfed females. J. Parasitol. 68, 61-82.

Lindsay, P. J., and Kaufman, W. R. (1988). Action of some steroids on salivary gland degeneration in the ixodid tick *A. americanum* L. J. Insect Physiol. 34, 351-359.

Magee, R. M., Jones, L. D., and Rees, H. H. (1996). Ecdysteroids in relation to Adult development and reproduction in female *Rhipicephalus appendiculatus* (Acari: Ixodidae). Arch. Insect Biochem. Physiol. 31, 197-206.

Mao, H., McBlain, W. A., and Kaufamn, W. R. (1995). Some properties of the ecdysteroid receptor in the salivary gland of the ixodid tick, *Amblyomma hebraeum*. Gen. Comp. Endocrinol. 99, 340-348.

Megaw, M. W., and Beadle, D. J. (1979). Structure and function of the salivary glands of the tick, *Boophilus Microplus Canestrini* (Acarina: Ixodidae). Int. J. Insect Morphol. Embryol. 8, 67-83.

Nijhout, H. F. (1994). Insect Hormones (Princeton: Princeton University Press).

Oliver, J. H., and M., D. E. (1993). Hormonal control of molting and reproduction in ticks. Am. Zool. 33, 384-396.

Oliver, J. H. J. (1974). Symposium on reproduction of arthropods of medical and veterinary importance. IV. Reproduction in ticks (Ixodoidea). J. Med. Entomol. 11, 26-34.

Oliver, J. H. Jr., Pound, J. M., and Andrews, R. H. (1984). Induction of egg malturation and oviposition in the tick *Ornithodoros parker*i (Acari: Argasidae). J. Parasitol. 70, 337-342.

Patrick, C. D., and Hair, J. A. (1975). Laboratory rearing procedures and equipment for multi-host ticks (*Acarina:Ixodidae*). J. Med. Entomol. 12, 389-390.

Pound, J. M., and Oliver, J. H. Jr. (1979). Juvenile hormone: Evidence of its role in the reproduction of ticks. Science 206, 355-357.

Ribiero, J. M. C. (1987). Role of saliva in blood feeding by arthropods. Annual. Rev. Entomol. 32, 463-478.

Riddiford, L. M. (1993). Hormones and *Drosophila* development. In The Development of *Drosophila melanogaster*, M. Bate and A. M. Arias, eds. (Cold Spring Harbor, New York: Cold Spring Harbor Laboratory), pp. 899-939.

Sambrook, J., Fritsch, E. F., and Maniatis, T. (1989). Molecular Cloning: A Laboratory Manual, Second Edition (Planview: Cold Spring Harbor Press).

Sauer, J. R., Mane, S. S., Schmidt, S. P., and Essenburg, R. C. (1986). Molecular basis for salivary fluid secretion in ixodid ticks. In Morphology, Physiology, and Behavioral Biology of Ticks, J. R. Sauer and J. A. Hair, eds. (New York: John Wiley and Sons), pp. 55-74.

Smith, G. E., and Summers, M. D. (1980). The bidirectional transfer of DNA and RNA to nitrocellulose or diazobenzyloxymethy-paper. Anal. Biochem. 109, 123-129.

Sonenshine, D. E. (1991). Biology of Ticks, Volume 1 (Oxford: Oxford University Press).

Talbot, W. S., Swyryd, E. A., and Hogness, D. S. (1993). *Drosophila* tissues with different metamorphic responses to ecdysone express different ecdysone receptor isoforms. Cell 73, 1323-1337.

Thummel, C. S. (1995). From embryogenesis to metamorphosis: The regulation and function of *Drosophila* nuclear receptor superfamily members. Cell 83, 871-877.

Truman, J. W. (1996). Steroid receptors and nervous system metamorphosis in insects. Dev. Neurosci. 18, 87-101.

Truman, J. W., Talbot, W. S., Fahrbach, S. E., and Hogness, D. S. (1994). Ecdysone receptor expression in the CNS correlates with stage-specific responses to ecdysteroids during *Drosophila* and *Manduca* development. Development 120, 219-234.

Wigglesworth, K. P., Lewis, D., and Rees, H. H. (1985). Ecdysteroid titre and metabolism to novel apolar derivatives in adult female *Boophilus microplus* (Ixodidae). Arch. Insect Biochem. Physiol. 2, 39-54.

Wikel, S. K. (1996). Host immunity to ticks. Annual. Rev. Entomol. 41, 1-22.

Wyatt, G. R. (1997). Juvenile hormone in insect reproduction - a paradox? Eur. J. Entomol. 94, 323-333.

APPENDIX: TABLES AND FIGURES

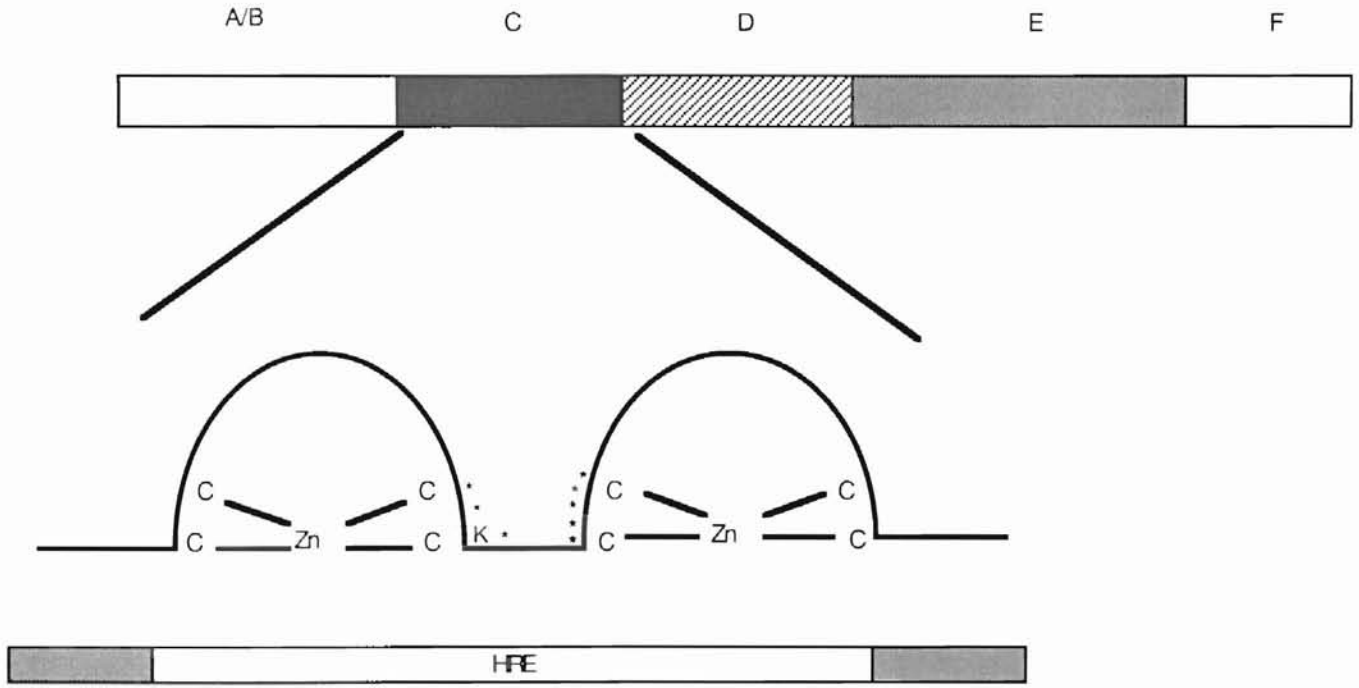

Figure 1. Structural organization of nuclear hormone receptors.

The receptors can be divided into six domains. The amino- terminal domain A/B is involved in transcriptional activation. The DNA-binding domain (C) is comprise of two zinc-fingers, each of which is coordinated with a zinc atom and four cysteine residues. The asterisks (*) at the C-terminus of the first zinc-finger denote for P box and asterisks at the N-terminus of the second zinc-finger denote the D box. The DNA-binding domain binds to sequences in target genes called hormone response elements (HREs). The Ligand-binding domain (E) binds ligand and participates in dimerization, nuclear translocation, and ligand-dependent transcriptional activation. The D domain provides a hinge between the DNA and ligand binding domains. The function of the C-terminal F domain, found in some nuclear receptors, is unknown.

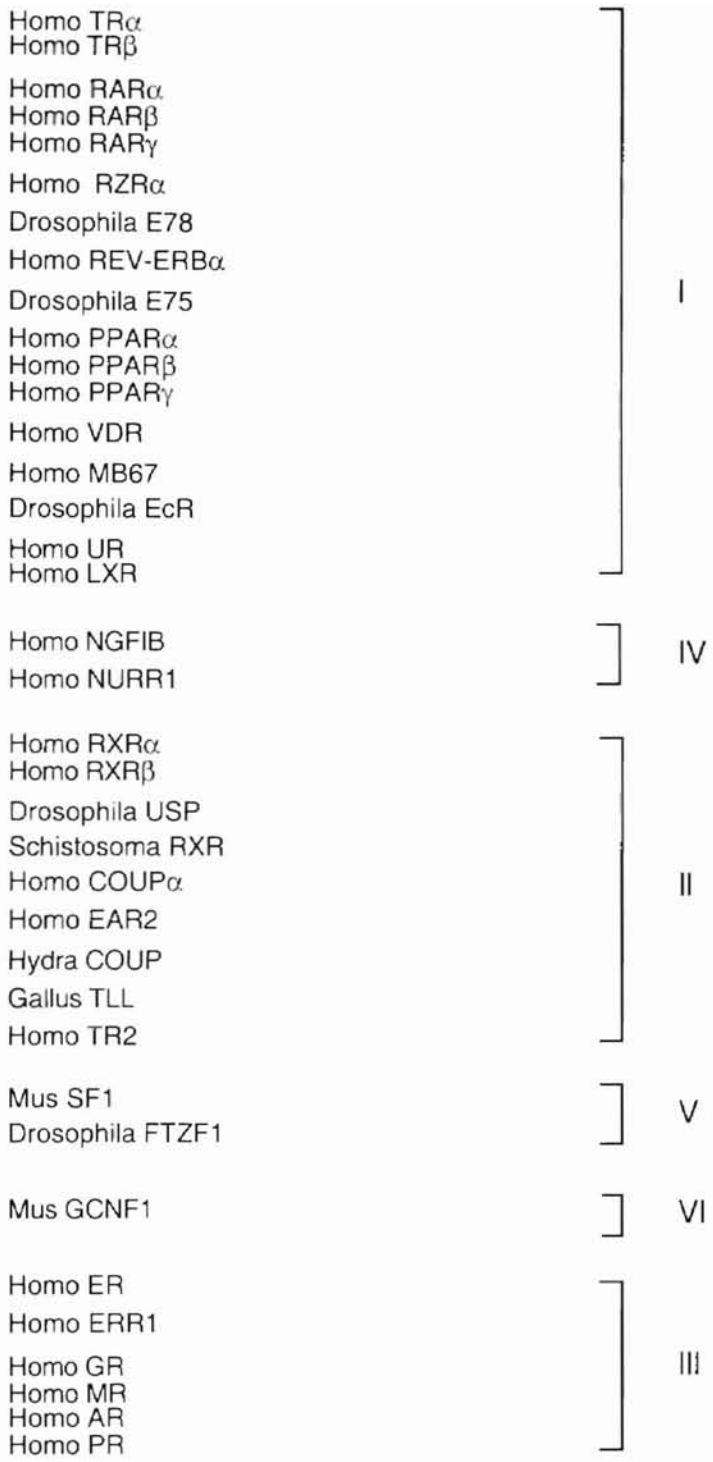

Figure 2. Classification of the six subfamilies comprising the nuclear receptor superfamily (Laudet,1997).

Homo = human, Mus = mouse, Gallus = chicken, Drosophila = fruit fly, Schistosoma = flatworm, hydra = cnidarian.

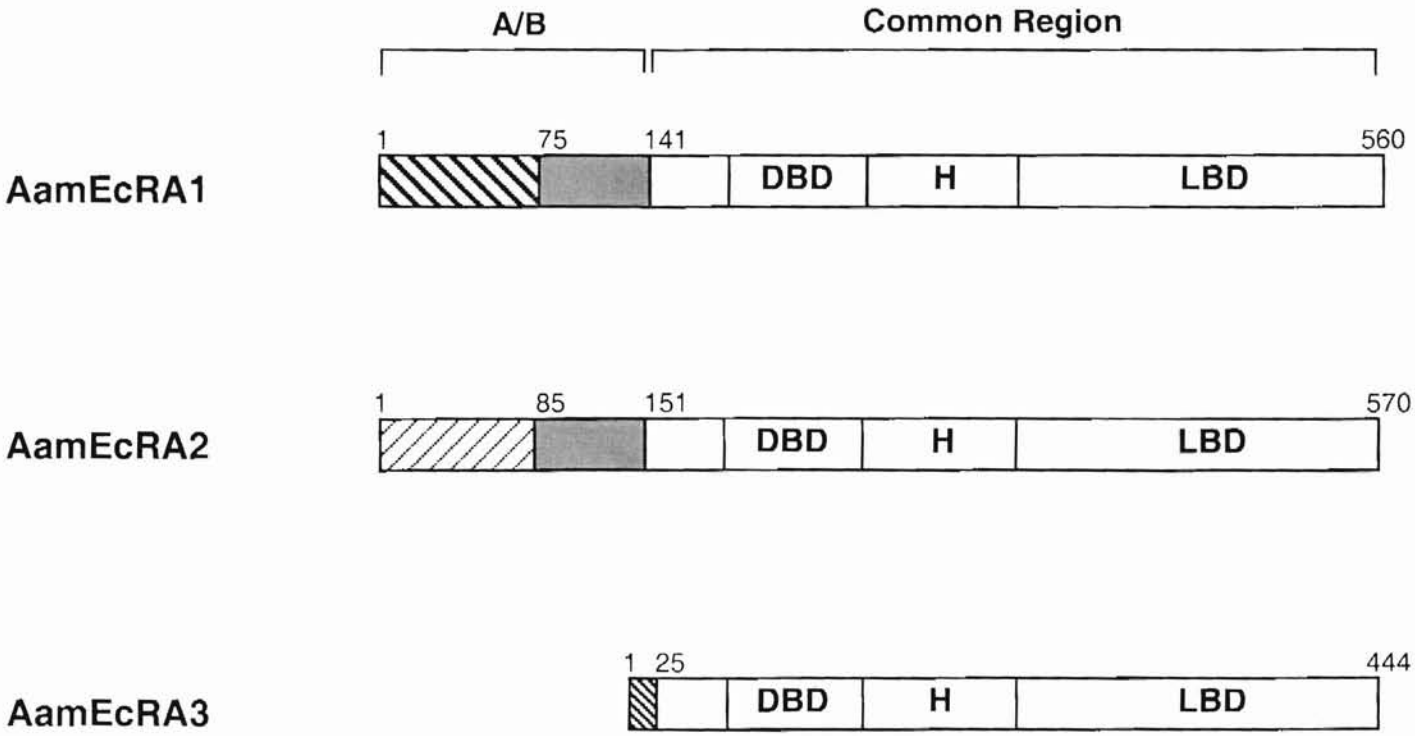

Figure 3. Schematic representation of the cDNAs of the three *A. americanum* EcR isoforms (AamEcR). Regions of the isoforms containing regions corresponding to the unique N-termini (A/B) or the common regions are bracketed. Striped boxes indicate unique regions of the N-termini, shaded boxes indicate the shared regions in the N-termini of AamEcRA1 and AamEcRA2, and unshaded boxs indicate the common region containing the DNA (DBD), ligand (LBD) binding domain and hinge region (H).

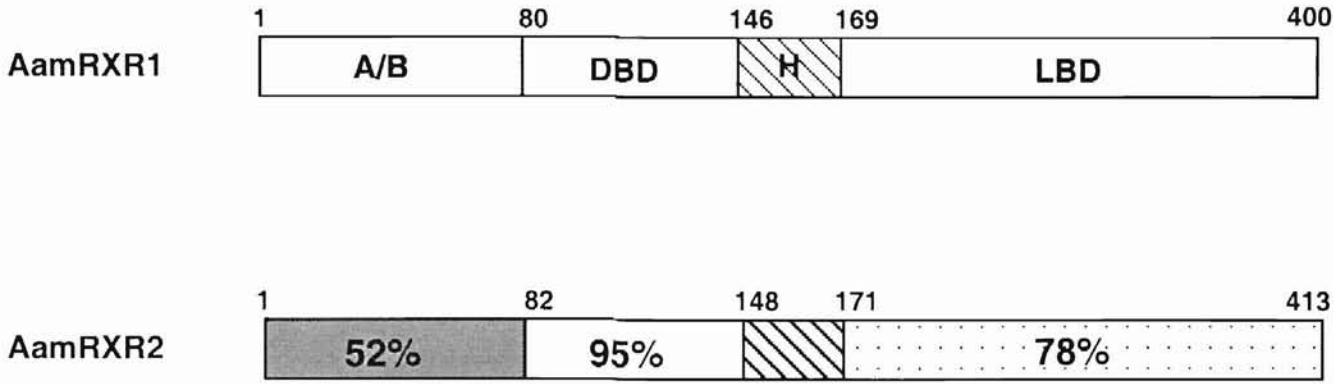

Figure 4. Schematic representation of *A. americanum* RXR1 and RXR2 cDNAs (AamRXR1 and AamRXR2). A/B = amino-terminal domain; DBD = DNA-binding domain; H = hinge domain; LBD = ligand binding domain. Numbers within the AamRXR2 domains indicate the percent identity between Aam RXR1 and AamRXR2.

Figure 5. Unusual Features of the AamRXR Ligand Binding Domains.
Panel A: several amino acid substitutions in the AamRXR LBDs compared to murine RXRa (mRXRa) that are proposed to contact 9-cis retinoic acid. The small numbers indicate amino acid positions in the mRXRa sequence.
Panel B: alignment of the nine amino acids comprising the AF-2 domain of AamRXR1, AamRXR2, mRXRa, Drosophila USP (DmUSP).
Panel C: Cluster W alignment (Higgins and Sharp, 1989) of the amino acids comprising helix 9 of AamRXR1, AamRXR2, murine RXRa, and Drosophila USP LBDs. Identical amino acids are boxed.

SUBPHYLLUM ORDER	SPECIES	ACCESSION NUMBER	% IDENTITY	
			DBD	LBD
Chelicerate	AamEcR	AFO20186 AFO20187 AFO20188	100	100
Dipteran	AaEcR	U02021	86	61
	CtEcR	S60739	88	55
	DmEcR	M74078	86	61
Lepidopteran	BmEcR	L35266	88	57
	MsEcR	U19826	88	57
Coleopteran	TmEcR	Y11533	98	63

Table I. Percentage of identity of the predicted amino acid sequences of *A. americanum* EcR to insect USPs.

AaEcR = *Aedes aegypti* EcR; AamEcR = *Amblyomma americanum* EcR; BmEcR = *Bombyx mori* EcR; CtEcR = *Chironomus tentans* EcR; DmEcR = *Drosophila melanogaster* EcR; MsEcR = *Manduca sexta* EcR; TmEcR = *Tenebrio molitor* EcR. DBD = DNA-binding domain; LBD = Ligand-binding domain.

USP/RXR	% IDENTITY			
	DBD		LBD	
	AamRXR1	AamRXR2	AamRXR1	AamRXR2
DmUSP	95	92	50	46
BmUSP	91	94	43	37
mRXRa	86	82	70	70

Table II. Percentage of identity of the predicted amino acid sequences of *A. americanum* RXR1 (AamRXR1, AFO35537) and RXR2 (AamRXR2, AFO35578) to *Drosophila melanogaster* USP (DmUSP, X52591), *Bombyx mori* USP (BmUSP, U06073), and murine RXRα (mRXRα, X66223). DBD = DNA-binding domain; LBD = Ligand-binding domain.

Table III. Nomenclature for ixodid salivary gland cell types*

Author	Binnington (1978)	Krolak et al. (1982)
species	*Boophilus microplus*	*Amblyomma americanum*
method	Light microscopy	Electron microscopy and Light microscopy
Acinus I	Acinus I	Acinus I
Acinus II	a	densely stained cells with complex granules
	b	densely stained cells with simple granules
	c1	lightly stained granular cells
	c2	
	c3	
	c4	
	epithelial cells	epithelial cells
Acinus III	d	densely stained cells with complex granules
	e	densely stained cells with simple granules
	f	lightly stained granular cells

* Please note that interpretations of the number of granular cell types in type II and III acini differ considerably between Binnington (1978) and Krolak et al. (1982). Studies performed by Megaw and Beadle (1979) in *B. microplus* using EM concur with Krolak et al. (1982).

Table IV. Classification of stages of salivary glands and ovaries according to the weight of partially fed ticks and days following repletion of fed ticks

	Weight (mg)	Day of Feeding*
unfed ticks		0
partially fed ticks	20-50	5-7
	50-100	7-9
	100-250	10-12
	250-500	12-14
	>500	>12
		Day following repletion **
replete ticks		1-2
		3-4
		4-6
		5-6
		>6

* Ovaries and salivary glands

** Ovaries only

Table V. Gene-specific primers for amplification of *A. americanum* EcR, RXR and actin mRNAs

Gene	Forward Primers	Reverse Primers
AamEcR-common	CGTCTCAAGAAGTGCCTCAGC	GCGGTAGTTGTCCCTCGTGTA
AamEcRA1	GGATAGCGTGCTGTGTTGTGCGTTTGC	ATCTGGGACGACGGCGACGAGATCCAC
AamEcRA2	TGGGATTAGCGAAGGCAGGCTTTGCGTC	CGTTCATCACGTTTGGCAGCGACGAAGATG
AamEcRA3	ACCACCCCGGATACGAGGAC	CGGCACTCCTGGCACTTG
AamRXR1	CAGTGAGGTGGAAAGCACTAG	TGTCCCCGATGAGCTTGAAG
AamRXR2	CTGCTTATTGCCGCCTTTTC	TGTCCCCGATGAGCTTGAAG
Actin	CGCAGATGATGTTTGAGACC	GGGCGGTGATTTCCTTCTGC
EcR-Mimic	CGTCTCAAGAAGTGCCTCAGC CAAGTTTCGTGAGCTGATTG	GCGGTAGTTGTCCCTCGTGTA ATTTGATTCTGGACCATGGC
RXR1-Mimic	CAGTGAGGTGGAAAGCACTAG CAAGTTTCGTGAGCTGATTG	TGTCCCCGATGAGCTTGAAG TCTGTCAATGCAGTTTGTAG

Table VI. Data for primer sets for PCR amplification of actin, AamEcR and AamRXR

Gene	Primer Set	Primer Size	GC content (%)	Tm (°C)	Size of Product	Internal Primer
AamEcR-common (DBD-LBD)	1792 (F)*	21	57.1	66.0	623	2045
	1791 (R)**	21	57.1	66.0		
AamEcRA1	3201 (F)	27	55.6	79.3	530	2831
	3200 (R)	27	59.3	83.0		
AamEcRA2	3132 (F)	28	57.1	81.0	428	2021
	3133 (R)	30	53.3	81.0		
AamEcRA3	2285 (F)	20	65.0	69.9	348	1907
	1878 (R)	18	66.7	67.0		
AamRXR1	1511 (F)	20	55.0	62.0	665	2336
	1595 (R)	21	52.4	64.0		
AamRXR2	2830 (F)	20	50.0	60.0	412	3487
	1595 (R)	21	52.4	64.0		
Actin	1333 (F)	20	50.0	60.0	660	1408
	1334 (R)	20	60.0	64.0		

* F = Forward primer

** R = Reverse primer

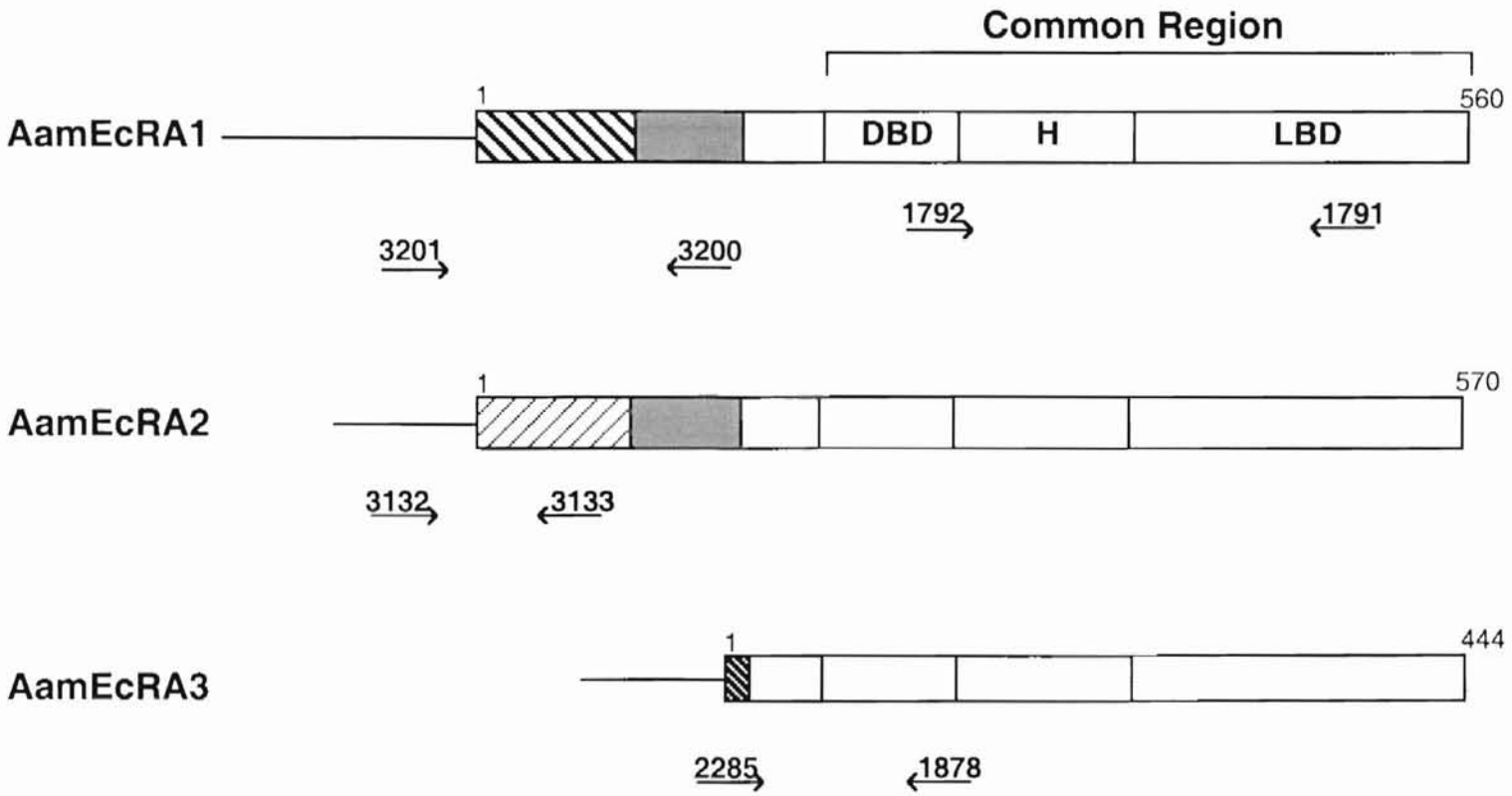

Figure 6. Schematic representation of the cDNAs of the three AamEcR isoforms and locations of the corresponding primer sets. Blocks represent the open reading frames. Striped boxes indicate unique N-termini, dark shaded boxes indicate the shared regions between AamEcRA1 and AamEcRA2, and unshaded boxes indicate the common region containing the DNA binding domain (DBD), hinge region (H) and ligand binding domain (LBD) binding domain. Arrows denote the locations of common region (1792-1791), AamEcRA1-specific (3201-3200), AamEcRA2-specific (3132-3133) and AamEcRA3-specific (2285-1878) primers.

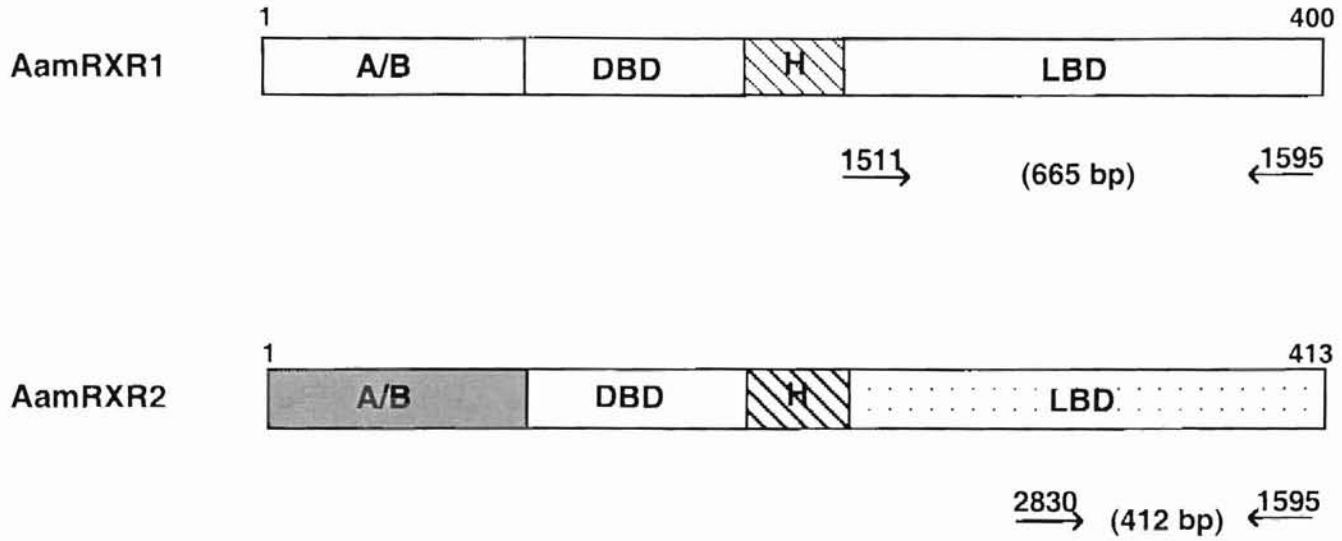

Figure 7. Schematic representation of AamRXR1 and AamRXR2 cDNAs and the locations of the corresponding primer sets. A/B = amino-terminal domain; DBD = DNA binding domain; H = hinge domain; LBD = ligand binding domain. Arrows denote the locations of AamRXR1-specific (1511-1595) and AamRXR2-specific (2830-1595) primers.

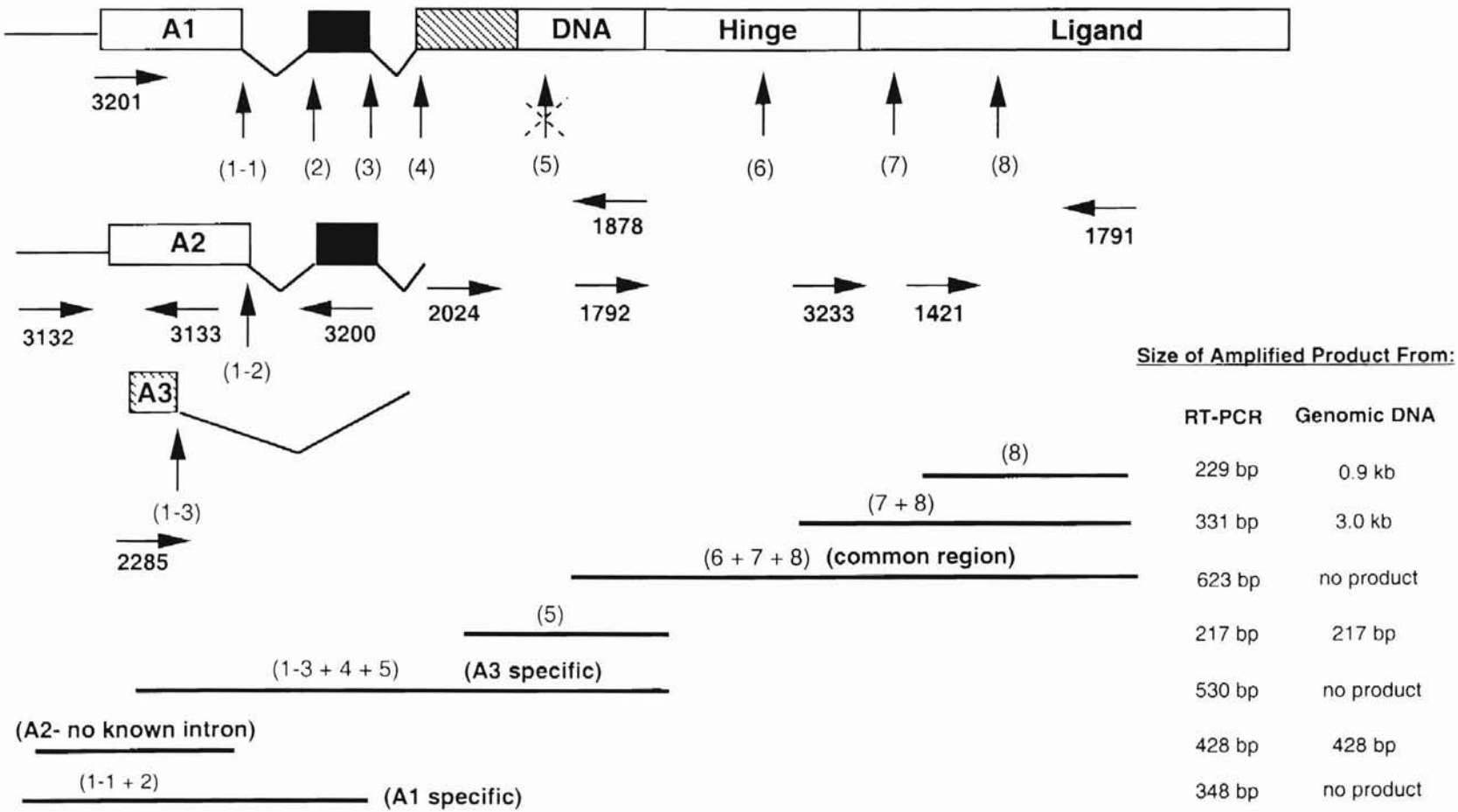

Figure 8. Deduced AamEcR intron/exon structure from genomic DNA amplification.

Putative intron positions (1-1, 1-2, 1-3, 2, 3, and 4) were deduced from AamEcR cDNA sequences where cDNAs clearly diverged. Putative introns (5, 6, 7, 8) were inferred from known intron positions in *D. melanogaster* (6, 7, and 8) or *M. Sexta* (5, 6, 7) EcR genes. Dashed X over arrow for intron 5 indicates that we did not find evidence for that intron. The sizes of the amplified products from the cDNA (RT-PCR) or genomic DNA are indicated.

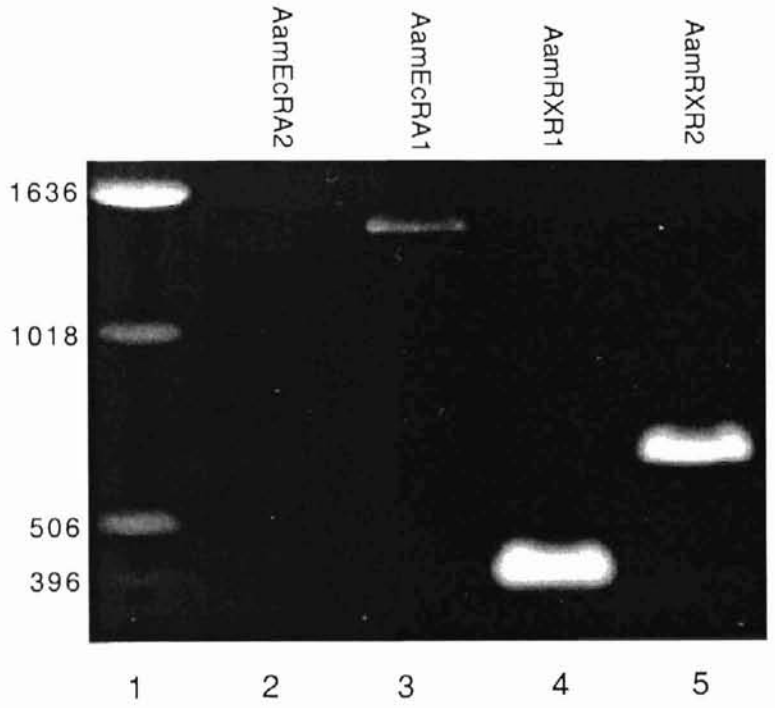

Figure 9. Amplification products of AamEcRA1 and AamEcRA2 cDNAs using standard PCR conditions. 100ng of AamEcRA1, AamEcRA2, AamRXR1 and AamRXR2 cloned cDNAs were amplified using standard PCR conditions. Amplification of AamRXR1 (lane 3, 412 bp) and AamRXR2 (lane 4, 665 bp) cDNAs produced products of the expected size. The AamEcRA1 cDNA product was approximately 1 kb larger than predicted (lane 2, 561 bp), while there was no product amplified with the AamEcRA2 cDNA (lane 1).

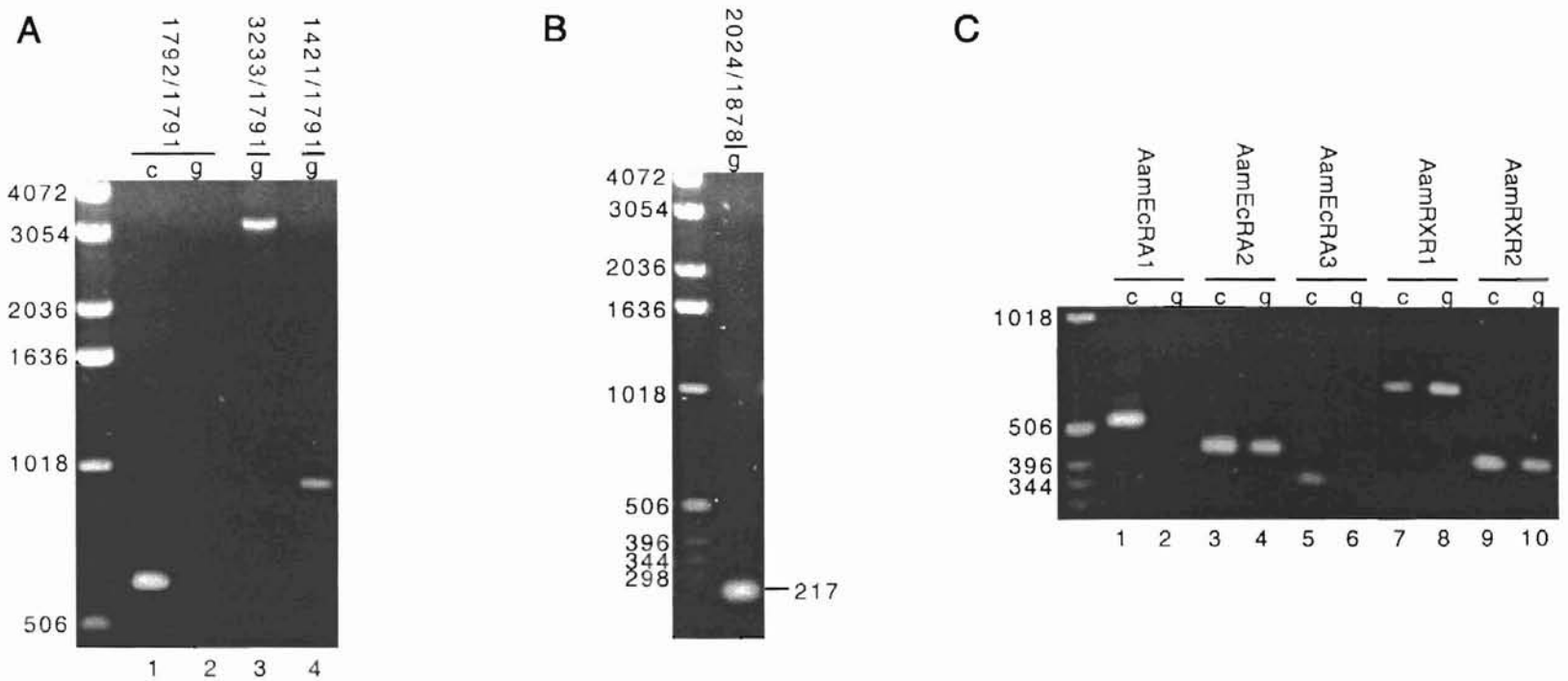

Figure 10. Comparision of AamEcR and AamRXR amplication products from genomic DNAs and cDNAs.

c = cDNA, g = genomic DNA.

Panel A: Three primers were used to test for the presence of putative introns (6,7,8,) in the AamEcR LBD. Lane 1, 2 (1792/1791), introns 6, 7, 8; lane 3 (3233/1791), introns 7, 8 and lane 4 (1421/1791), intron 8.

Panel B: The primer set (2024/1878) was used to test genomic DNA for the presence of a putative intron in the AamEcR DBD. The product size was same as the predicted size from cDNA sequence (217 bp).

Panel C: cDNAs and genomic DNAs were amplified in parallel with AamEcR isoform and AamRXR-specific-primer set to test for introns. Lane 1, 2, AamEcRA1 (3201-3200); lane 3, 4, AamEcRA2 (3132-3133): lane 5, 6, AamEcRA3 (2285-1878), lane 7, 8, AamRXR1 (1511-1595) and lane 9, 10, AamRXR2 (2830-1595).

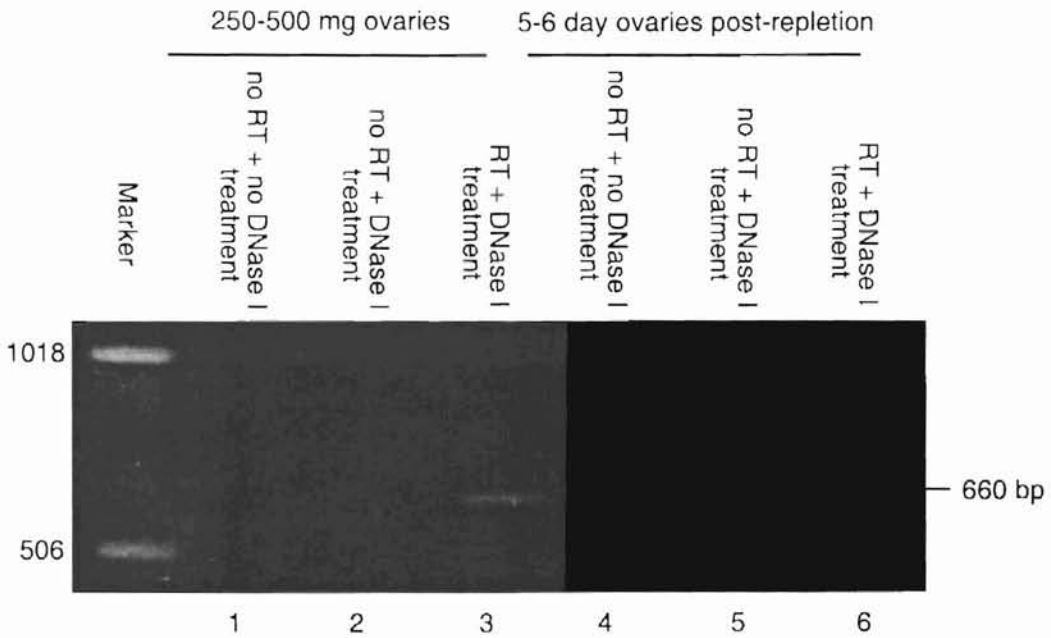

Figure 11. No reverse transcriptase and DNase I controls for RT-PCR.
One μg of total RNA from ovaries (250-500 mg and 5-6 day post-repletion) was reverse transcribed under the following conditions: no DNase I treatment and no reverse transcriptase (lane 1, 4); DNase I treatment and no reverse transcriptase (lane 2, 5); DNase I treatment and reverse transcriptase (lane 3, 6). Only samples containing reverse transcriptase produced an actin-specific band of the predicted size, demonstrating the products were derived from RNA and not from genomic DNA contaminants.

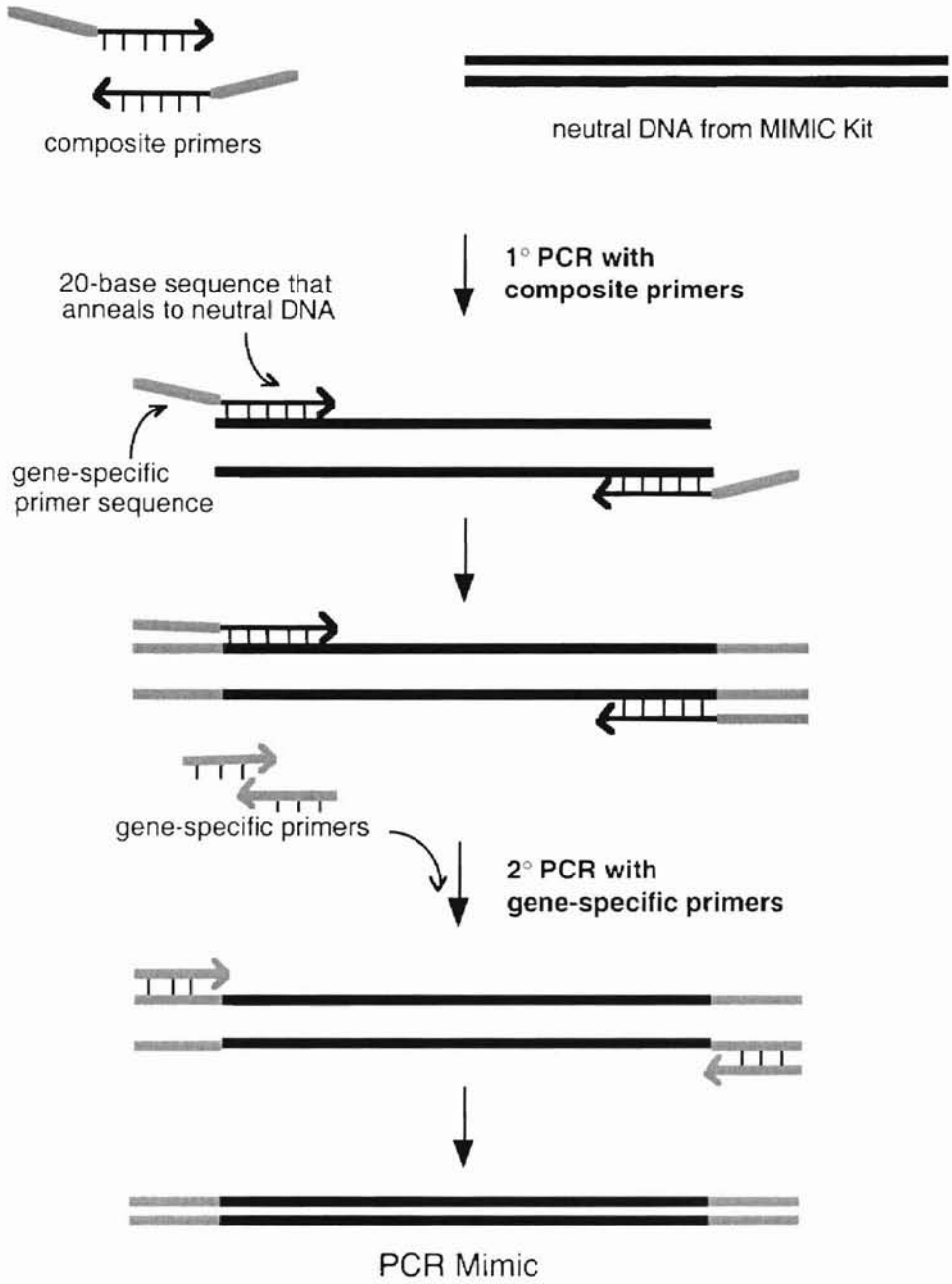

Figure 12. Construction of PCR Mimics. The PCR Mimics were constructed in a two-round PCR reaction. In the first round, two composite primers were used, which contained the target gene primer sequence attached to a 20-nucleotide sequence of the neutral DNA fragment (BamHI/EcoR I fragment of v-erbB) provided in the PCR MIMIC^{TM} Construction Kit (Clontech). In the second round, a dilution of the first PCR reaction product was amplified directly using the target gene primer sets. The resulting PCR Mimics were neutral DNA fragments with target gene-specific primer sequences attached to both ends.

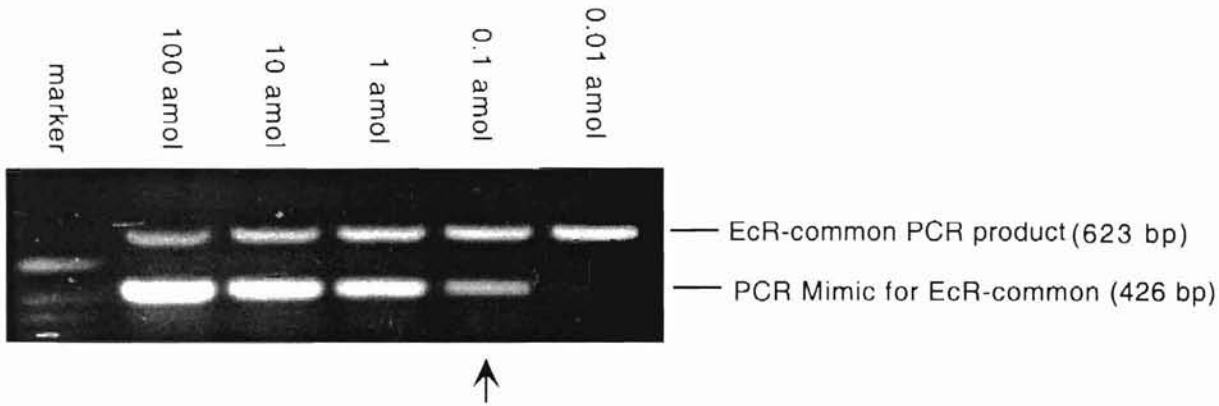

Figure 13. Titration of the PCR Mimic for competitive amplification of the AamEcR common region. One μl of a series of ten-fold dilutions of PCR Mimic for AamEcR-common region were co-amplified with 1/20 μl of AamEcR cDNAs produced from reverse transcription of 1μg total RNA from salivary gland (250-500 mg). The amount of PCR Mimic fhat is equivalent to the EcR-common specific product is approximately 0.1 amol (indicated by arrow).

Salivary Glands

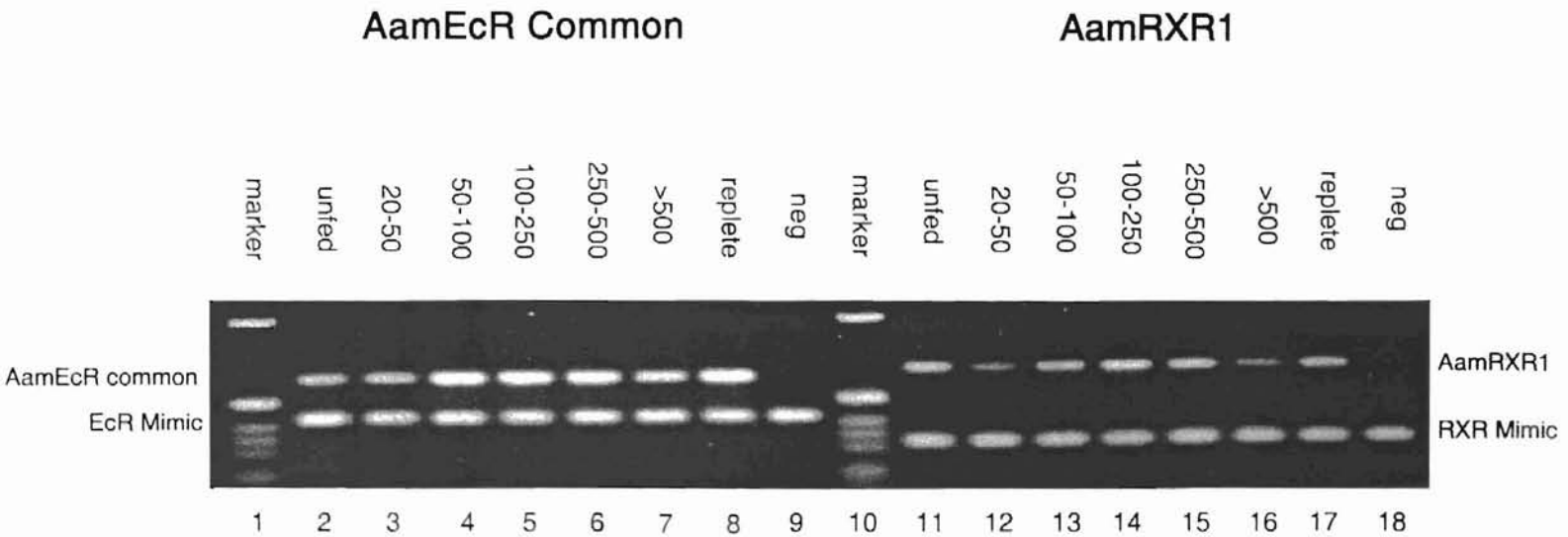

Figure 14. Competitive RT-PCR of *A. americanum* nuclear receptors using Mimic DNAs. The expression of AamEcR-common and AamRXR1 mRNA in salivary glands of different weights during feeding were examined. The concentration of Mimic DNA was 0.2 amol for AamEcR-common and 0.1 amol for AamRXR1. Following PCR, the products were electrophoresed on a 1.2% agarose gel and visualized by ethidium bromide staining. AamEcR-common (623 bp); AamEcR-Mimic (426 bp); of AamRXR1 (665 bp); AamRXR1-Mimic (321 bp).

Ovaries

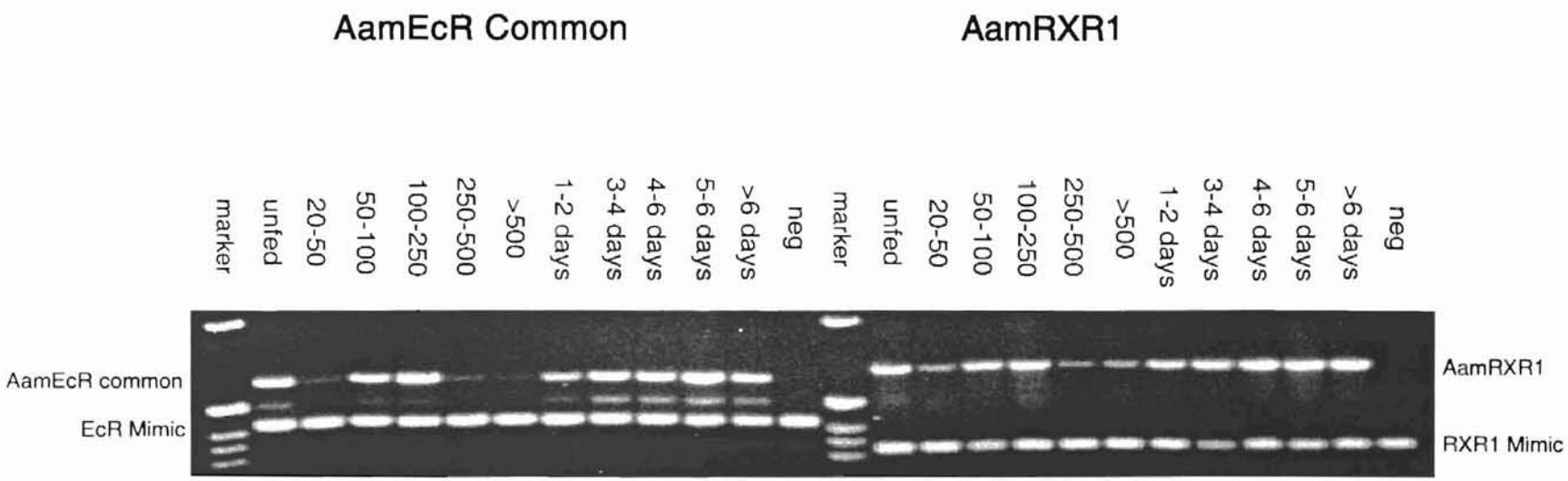

Figure 15. Competitive RT-PCR of *A. americanum* nuclear receptors using Mimic DNAs. The expression of AamEcR-common and AamRXR1 mRNA in ovaries during feeding and post repletion were examined. The concentration of Mimic DNA was 0.2 atmol for AamEcR-common and 0.1 amol for AamRXR1. Following PCR, the products were electrophoresed on 1.2% agarose gel and visualized by ethidium bromide staining. AamEcR-common (623 bp); AamEcR-Mimic (426 bp); AamRXR1 (665 bp); AamRXR1-Mimic (321 bp).

Table VII. The events associated with the molting process in larvae and nymphs

Events		Larvae	Nymphs
Repletion		D0	D0
Apolysis:	Separation of cuticle	D4	D8
	The appearance of molting gel	D6	D9
Molting gel resorption		D10*	D24*
Ecdysis		D12-15	D27-33

* The process of molting gel accumulation is asynchronous in tick population.

Molting Larvae

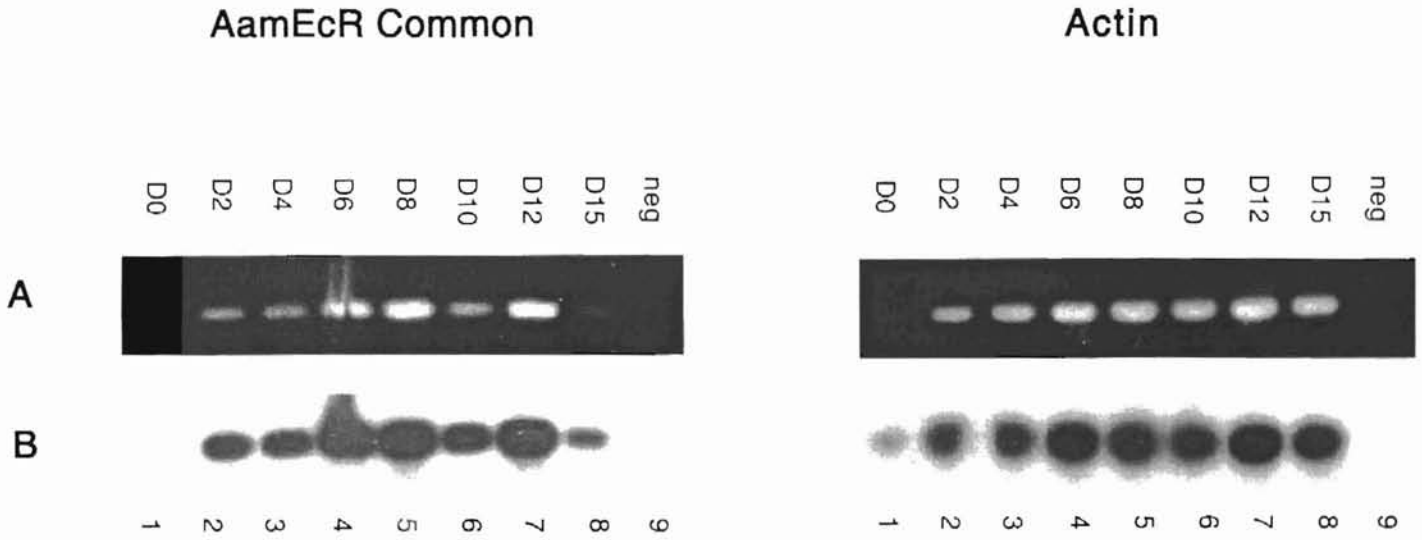

Figure 16. The expression of AamEcR-common and Actin mRNAs in molting larvae of A. americanum. AamEcR-common and Actin mRNA RT-PCR products were electrophoresed on 1.2% agarose gels, visualized by ethidium bromide staining (Panel A, left and right), and hybridized with an AamEcR common or an Actin-specific internal oligonucleotide (Panel B, left and right). Single products of 623 bp (AamEcR-common) and 660 bp (Actin) were detected. D = Day post-feeding from repletion (D0) through ecdysis (D15).

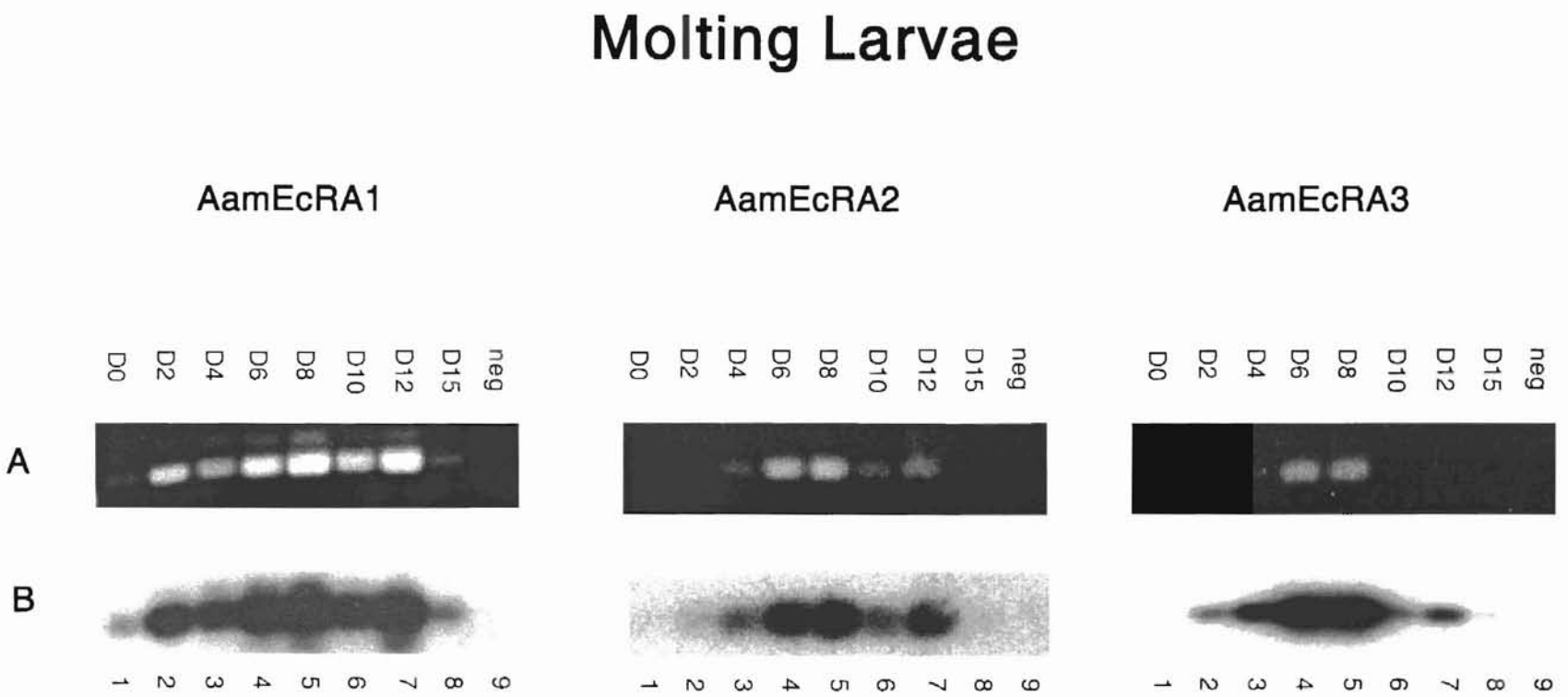

Figure 17. The expression of AamEcR isoform-specific mRNAs in molting larvae of A. americanum. Three AamEcR isoform specific RT-PCR products were electrophoresed on 1.2% agarose gels, visualized by ethidium bromide staining (Panel A, left, middle and right), and hybridized with an AamEcRA1, AamEcRA2 or AamEcRA3-specific internal oligonucleotide (Panel B, left, middle and right). Single products of 530 bp (AamEcRA1), 428 bp (AamEcRA2) and 348 bp (AamEcRA3) were detected. D = Day post-feeding from repletion (D0) through ecdysis (D15).

Molting Larvae

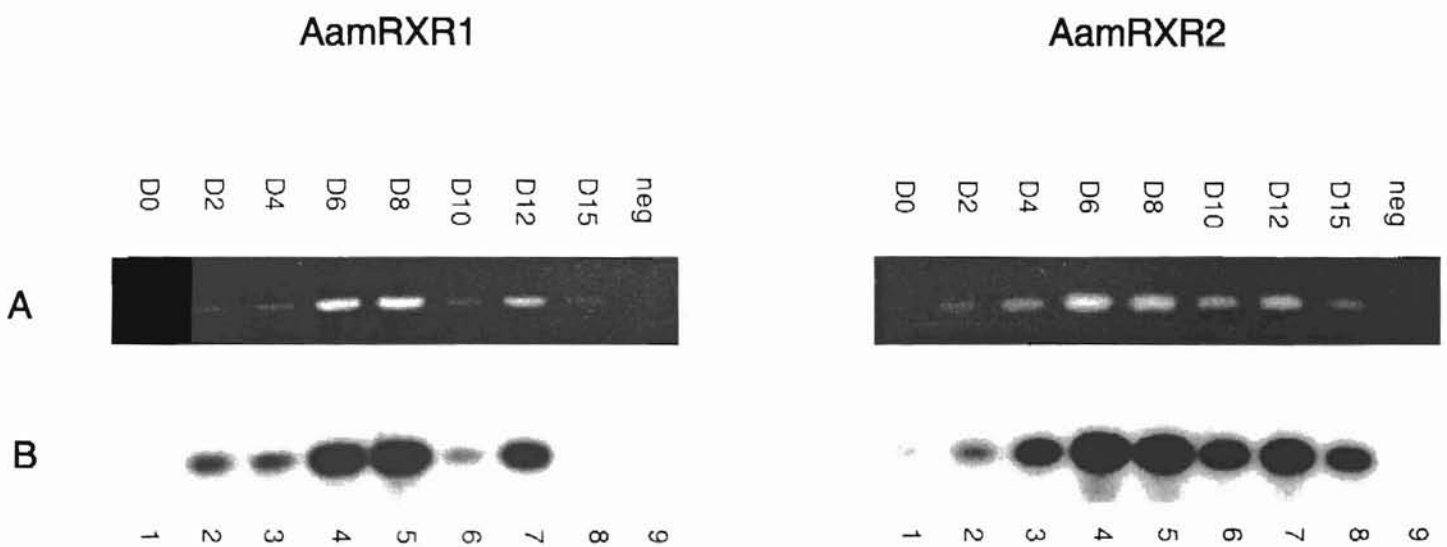

Figure 18. The expression of AamRXR1 and AamRXR2 mRNAs in molting larvae of A. americanum. AamRXR1 and AamRXR2 mRNA RT-PCR products were electrophoresed on 1.2% agarose gels, visualized by ethidium bromide staining (Panel A, left and right), and hybridized with an AamRXR1 or an AamRXR2-specific internal oligonucleotide (Panel B, left and right). Single products of 665 bp (AamRXR1) and 412 bp (AamRXR2) were detected. D = Day post-feeding from repletion (D0) through ecdysis (D15).

			apolysis				ecdysis	
	D0	D2	D4	D6	D8	D10	D12	D15
Actin	+	++	++	+++	+++	+++	+++	+++
AamEcR-common	+/-	++	++	+++	+++	++	+++	+
AamEcRA1	+/-	++	++	+++	+++	++	+++	+
AamEcRA2	-	+/-	++	+++	+++	++	+++	-
AamEcRA3	+/-	++	+++	++++	++++	++	+++	+
AamRXR1	-	+	+	+++	+++	+	++	+/-
AamRXR2	+/-	+	++	+++	+++	++	+++	++

Table VIII. Relative levels of AamEcR, AamRXR and actin mRNAs in molting *A. americanum* larvae.
The symbol "-" and "++++" stand for the lowest and highest expression levels for a given primer set, respectively.
Amplification levels of different primer sets are not directly comparable.

Molting Nymphs

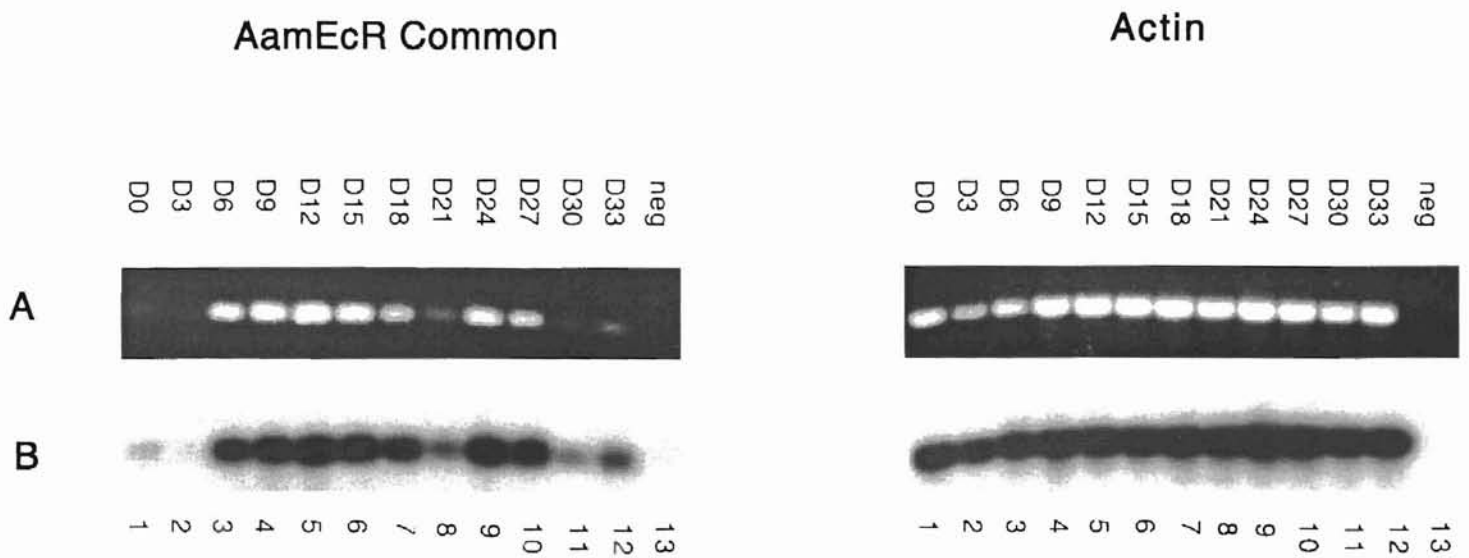

Figure 19. The expression of AamEcR-common and Actin mRNAs in molting nymphs of A. americanum. AamEcR-common and Actin mRNA RT-PCR products were electrophoresed on 1.2% agarose gels, visualized by ethidium bromide staining (Panel A, left and right), and hybridized with an AamEcR-common or an Actin-specific internal oligonucleotide (Panel B, left and right). Single products of 623 bp (AamEcR-common) and 660 bp (Actin) were detected. D = Day post-feeding from repletion (D0) through ecdysis (D33).

Molting Nymphs

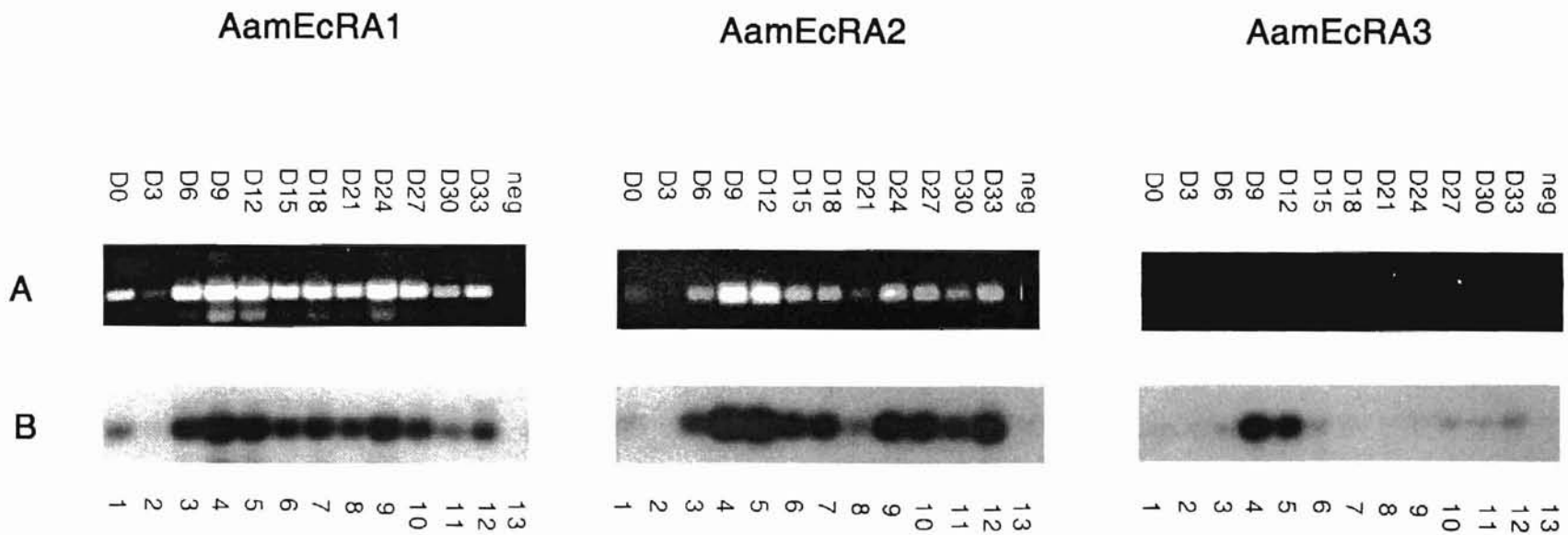

Figure 20. The expression of AamEcR isoform-specific mRNAs in molting nymphs of A. americanum. Three AamEcR isoform-specific RT-PCR products were electrophoresed on 1.2% agarose gels, visualized by ethidium bromide staining (Panel A, left, middle and right), and hybridized with an AamEcRA1, AamEcRA2 or AamEcRA3-specific internal oligonucleotide (Panel B, left, middle and right). Major product of 530 bp for AamEcRA1, 428 bp for AamEcRA2 and 348 bp for AamEcRA3 were detected. D = Day post-feeding from repletion (D0) through ecdysis (D33).

Molting Nymphs

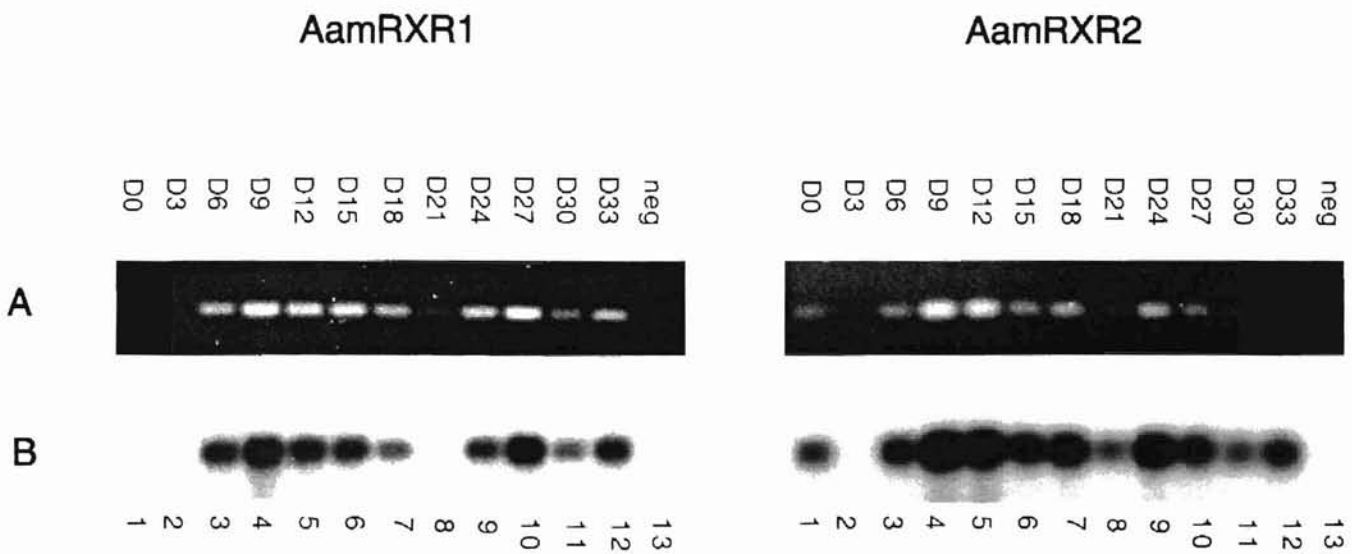

Figure 21. The expression of AamRXR1 and AamRXR2 mRNAs in molting nymphs of A. americanum. AamRXR1 and AamRXR2 mRNA RT-PCR products were electrophoresed on 1.2% agarose gels, visualized by ethidium bromide staining (Panel A, left and right), and hybridized with an AamRXR1 or an AamRXR2-specific internal oligonucleotide (Panel B, left and right). Single products of 665 bp (AamRXR1) and 412 bp (AamRXR2) were detected. D = Day post-feeding from repletion (D0) through ecdysis (D33).

				apolysis						ecdysis		
	D0	D3	D6	D9	D12	D15	D18	D21	D24	D27	D30	D33
Actin	++	+	++	+++	+++	+++	+++	+++	+++	+++	+++	+++
AamEcR-common	+/-	-	+++	+++	+++	+++	+++	+	+++	+++	+	++
AamEcRA1	+	+/-	++	+++	+++	++	++	+	+++	++	+	++
AamEcRA2	+/-	-	++	+++	+++	++	++	+	+++	+++	++	+++
AamEcRA3	+/-	-	+/-	++	++	+	-	-	-	+	+	+
AamRXR1	-	-	++	+++	++	++	+	+/-	++	+++	+	++
AamRXR2	++	-	+++	++++	++++	+++	+++	+	+++	++	+	++

Table IX. Relative levels of AamEcR, AamRXR and actin mRNAs in molting *A. americanum* nymphs.
The symbol "-" and "++++" stand for the lowest and highest expression levels for a given primer set, respectively.
Amplification levels of different primer sets are not directly comparable.

Salivary Glands

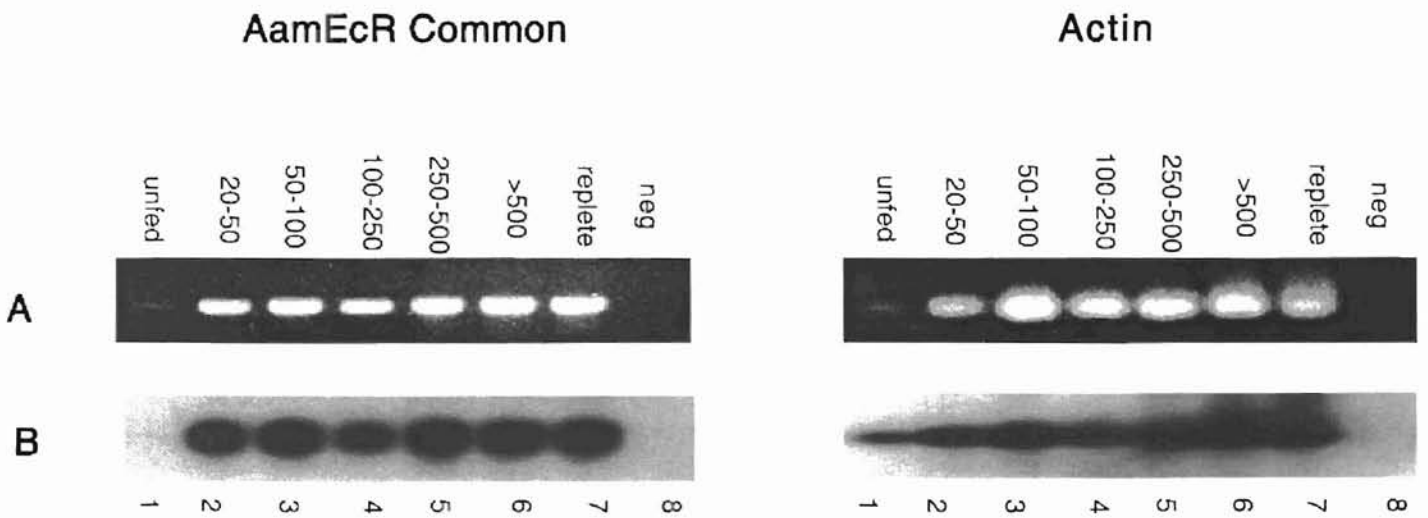

Figure 22. The expression of AamEcR-common and Actin mRNAs in Salivary glands from A. americanum of different weights during feeding. AamEcR-common and Actin RT-PCR products were electrophoresed on 1.2% agarose gels, visualized by ethidium bromide staining (Panel A, left and right), and hybridized with an AamEcR-common or an Actin-specific internal oligonucleotide (Panel B, left and right). Single products of 623 bp (AamEcR common) and 660 bp (Actin) were detected.

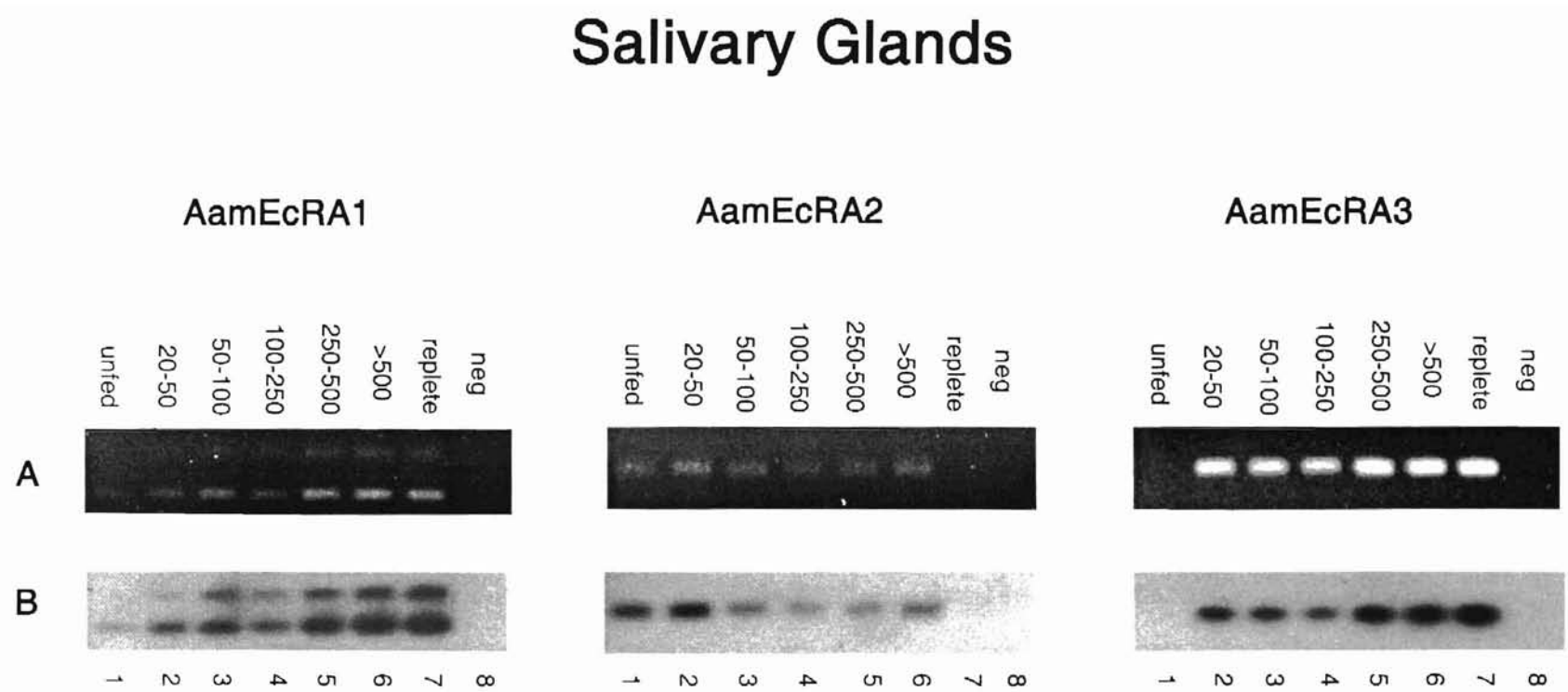

Figure 23. The expression of AamEcR isoform-specific mRNAs in Salivary glands from A. americanum of different weights during feeding. Three AamEcR isoform specific RT-PCR products were electrophoresed on 1.2% agarose gels, visualized by ethidium bromide staining (Panel A, left, middle and right), and hybridized with an AamEcRA1, AamEcRA2 or AamEcRA3-specific internal oligonucleotide (Panel B, left, middle and right). Major products of 530 bp (AamEcRA1), 428 bp (AamEcRA2) and 348 bp (AamEcRA3) were detected. Please note an additional product of 700 bp in AamEcRA1 lanes. This product is a AamEcRA1-specific as evidenced by its hybridization to an internal oligonecleotide. It likely results from secondary structure present in the GC-rich 5' region of AamEcRA1.

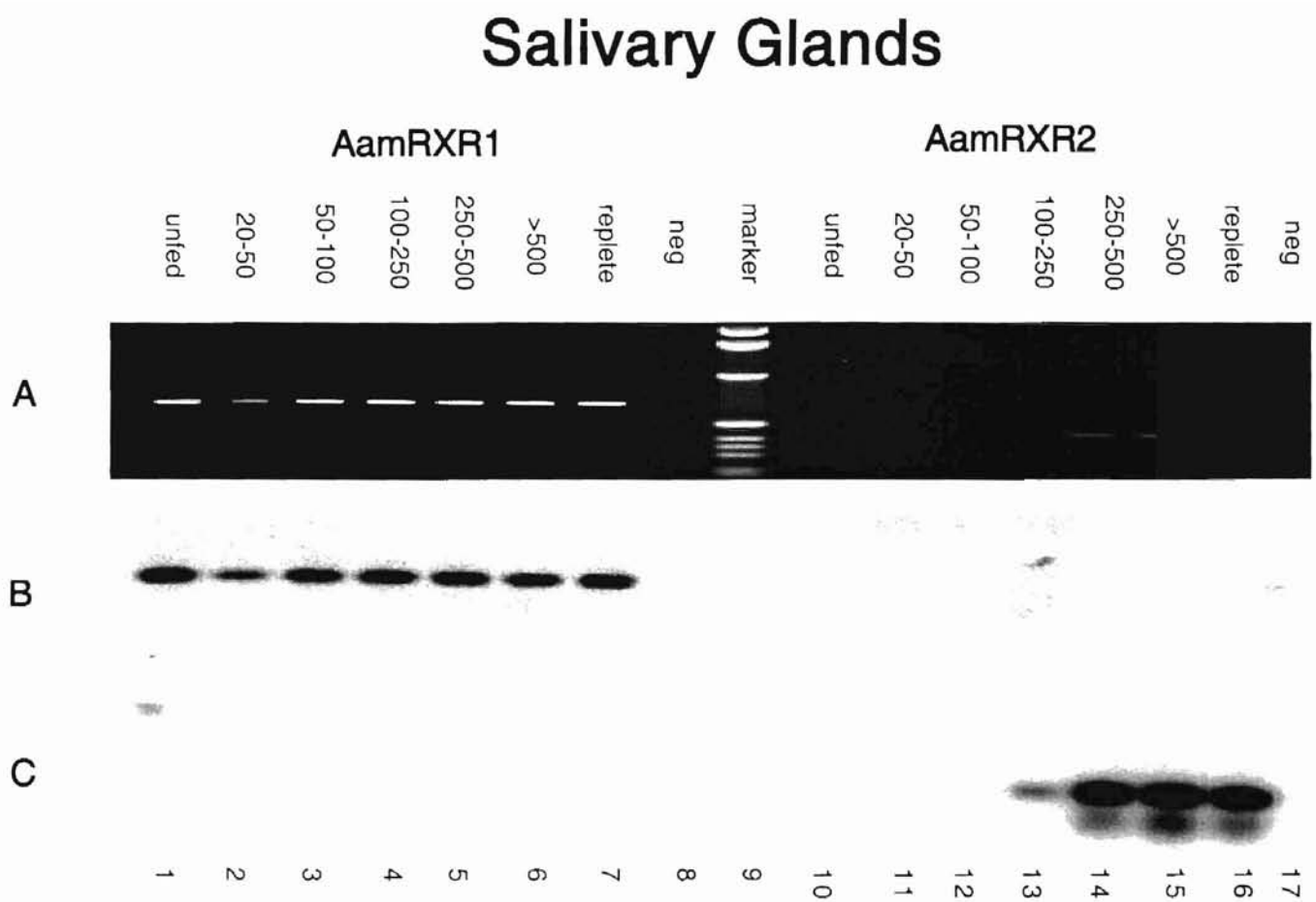

Figure 24. The expression of AamRXR1 and AamRXR2 mRNAs in Salivary glands from A. americanum of different weights during feeding. AamRXR1 and AamRXR2 RT-PCR products were electrophoresed on 1.2% agarose gels, visualized by ethidium bromide staining (Panel A), and hybridized with an AamRXR1 or an AamRXR2-specific internal oligonucleotide (Panel B and C). Single products of 665 bp for AamRXR1 and 412 bp for AamRXR2 were detected.

	unfed	20-50 mg	50-100 mg	100-250 mg	250-500 mg	>500 mg	replete
Actin	+	++	++	++	+++	++++	++++
AamEcR-common	+/-	+++	+++	++	+++	+++	+++
AamEcRA1	+	++	++	++	+++	++++	++++
AamEcRA2	++	++	+	+	+	+	-
AamEcRA3	-	+	+	+	++	++	+++
AamRXR1	++	+	++	++	++	++	++
AamRXR2	-	-	+/-	+	+++	+++	+++

Table X. Relative levels of AamEcR, AamRXR and actin mRNAs in *A. americanum* salivary glands during feeding. The symbol "-" and "++++" stand for the lowest and highest expression levels for a given primer set, respectively. Amplification levels of different primer sets are not directly comparable.

Whole Animal

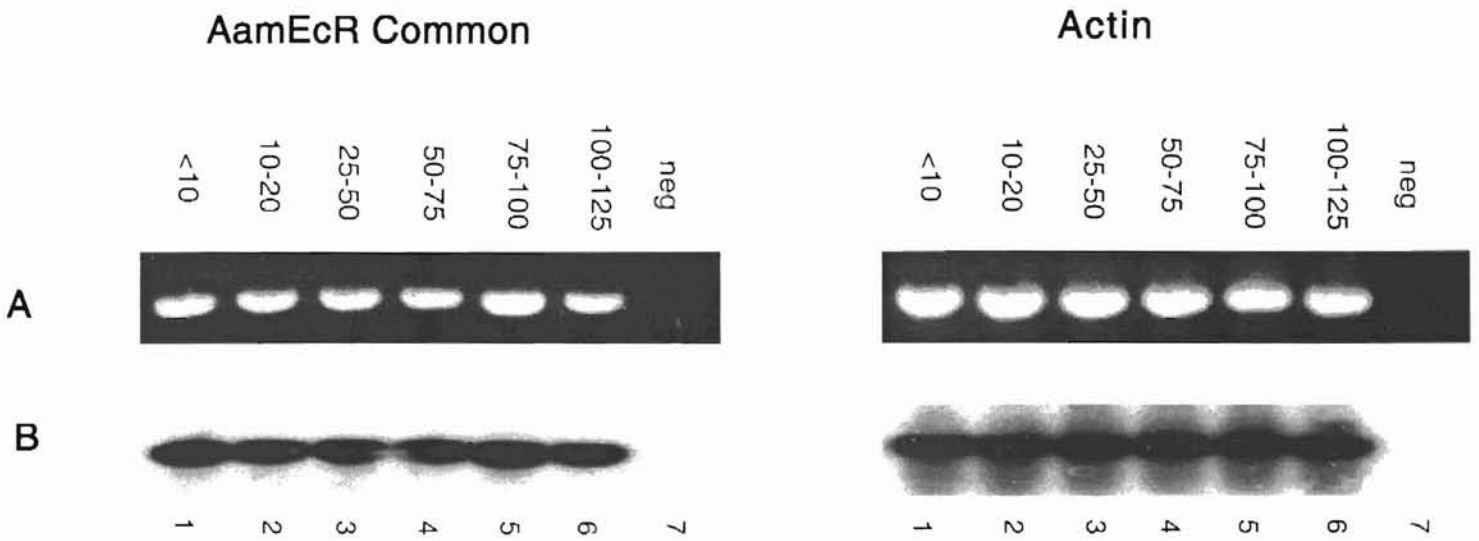

Figure 25. The expression of AamEcR-common and Actin mRNAs from whole animal A. americanum of different weights during feeding. AamEcR-common and Actin RT-PCR products were electrophorese d on 1.2% agarose gels, visualized by ethidium bromide staining (Panel A, left and right), and hybridized with an AamEcR-common or an Actin-specific internal oligonucleotide (Panel B, left and right). Single products of 623 bp (AamEcR common) and 660 bp (Actin) were detected.

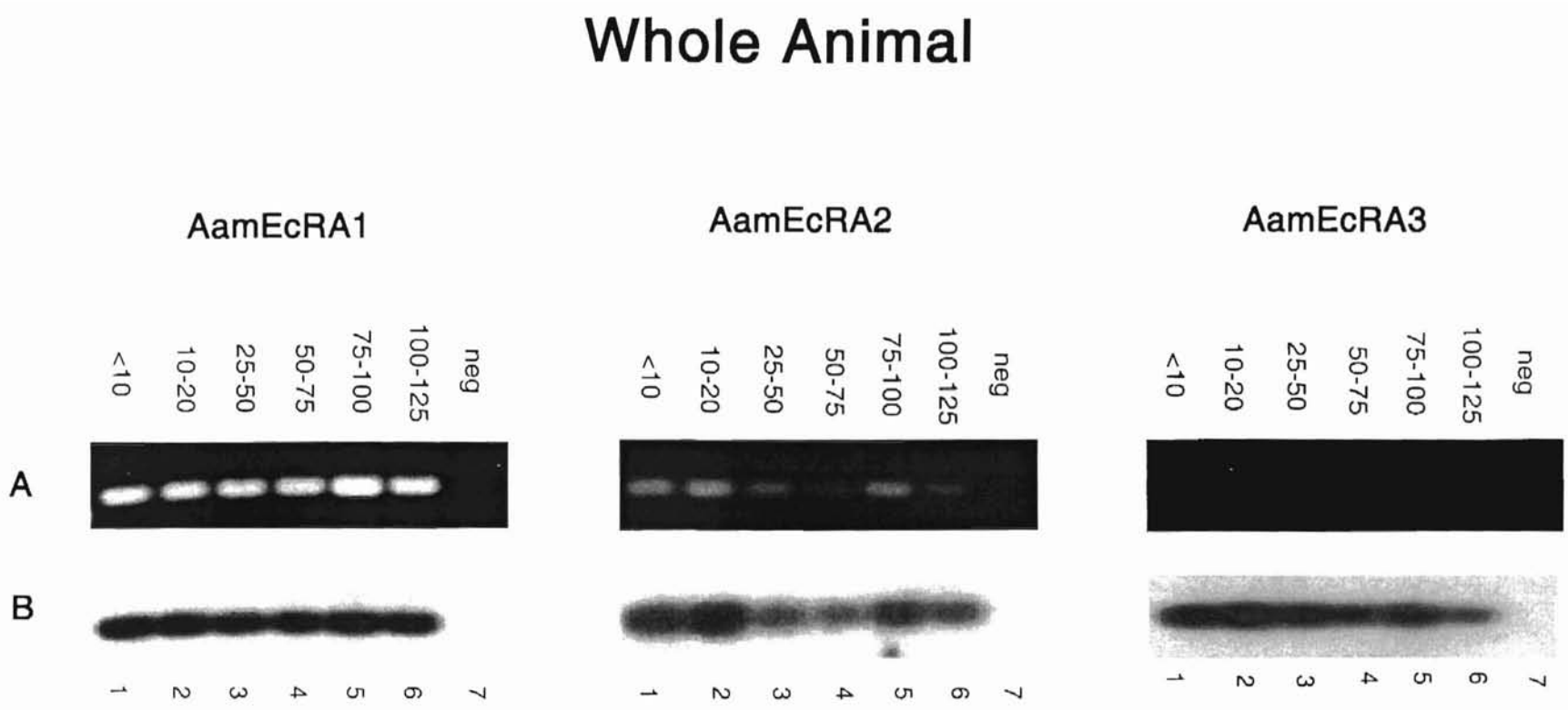

Figure 26. The expression of AamEcR isoform-specific mRNAs from whole animal A. americanum of different weights during feeding. Three AamEcR isoform specific RT-PCR products were electrophoresed on 1.2% agarose gels, visualized by ethidium bromide staining (Panel A, left, middle and right), and hybridized with an AamEcRA1, AamEcRA2 or AamEcRA3-specific internal oligonucleotide (Panel B, left, middle and right). Single products of 530 bp (AamEcRA1), 428 bp (AamEcRA2) and 348 bp (AamEcRA3)were detected.

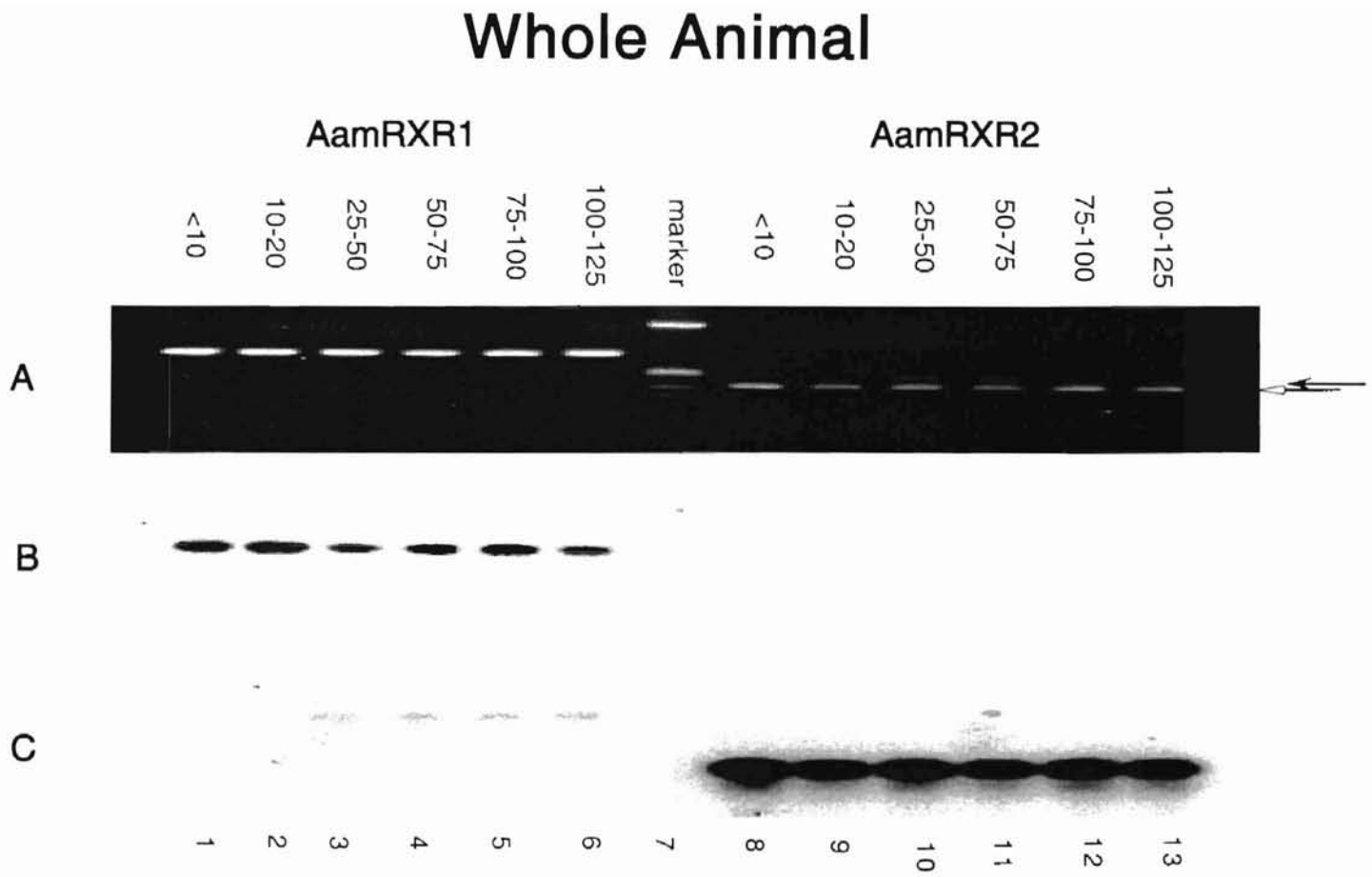

Figure 27. The expression of AamRXR1 and AamRXR2 mRNAs from whole animal A. americanum of different weights during feeding. AamRXR1 and AamRXR2 RT-PCR products were electrophoresed on 1.2% agarose gels, visualized by ethidium bromide staining (Panel A), and hybridized with an AamRXR1 (Panel B) or an AamRXR2-specific internal oligonucleotide (Panel C). Major products of 665 bp (AamRXR1) and 412 bp (AamRXR2) were detected.

	<10 mg	10-20 mg	25-50 mg	50-75 mg	75-100 mg	100-125 mg
Actin	+	+	+	+	+	+
AamEcR-common	+	+	+	+	+	+
AamEcRA1	+	+	+	+	+	+
AamEcRA2	++	++	+	+	++	+
AamEcRA3	+++	+++	+++	++	+++	+
AamRXR1	++	++	+	+	+	+
AamRXR2	+	+	+	+	+	+

Table XI. Relative levels of AamEcR, AamRXR and actin mRNAs from whole *A. americanum* during early feeding. The symbol "-" and "+++" stand for the lowest and highest expression levels for a given primer set, respectively. Amplification levels of different primer sets are not directly comparable.

Ovaries

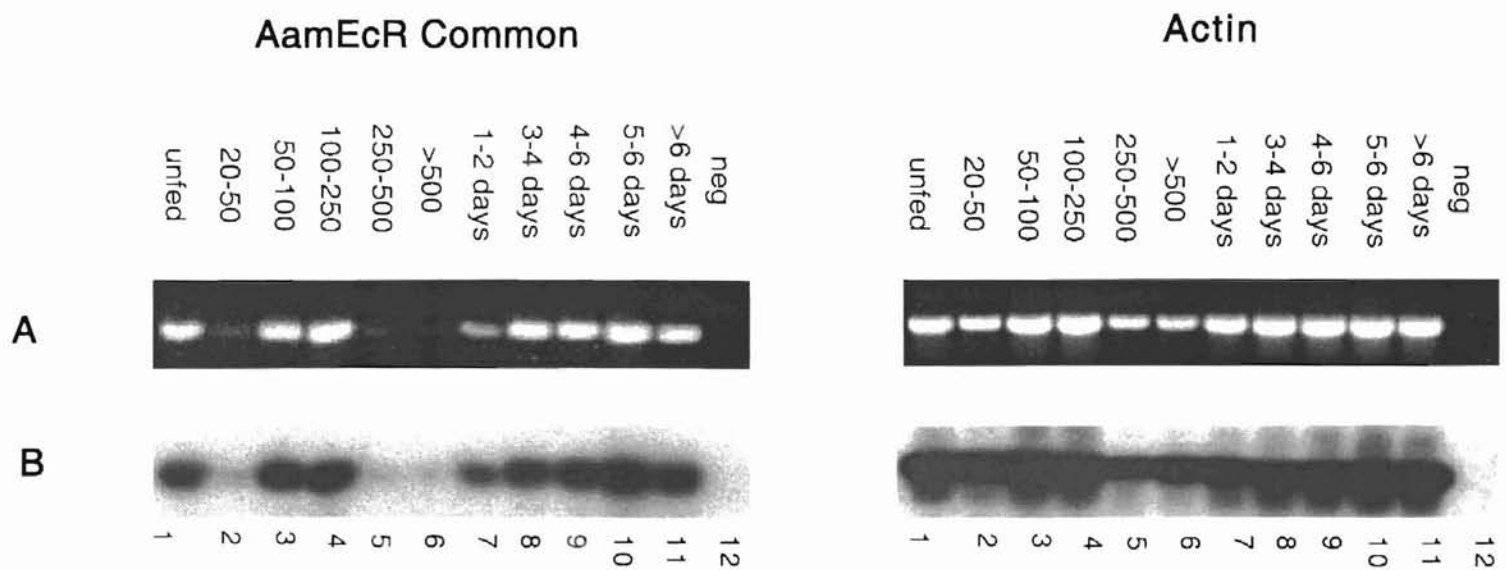

Figure 28. The expression of AamEcR-common and Actin mRNAs in ovaries from A. americanum of different weights during feeding and days following repletion. AamEcR-common and Actin RT-PCR products were electrophoresed on 1.2% agarose gels, visualized by ethidium bromide staining (Panel A, left and right), and hybridized with an AamEcR-common or an Actin-specific internal oligonucleotide (Panel B, left and right). Single product of 623 bp (AamEcR common) and 660 bp ((Actin) were detected.

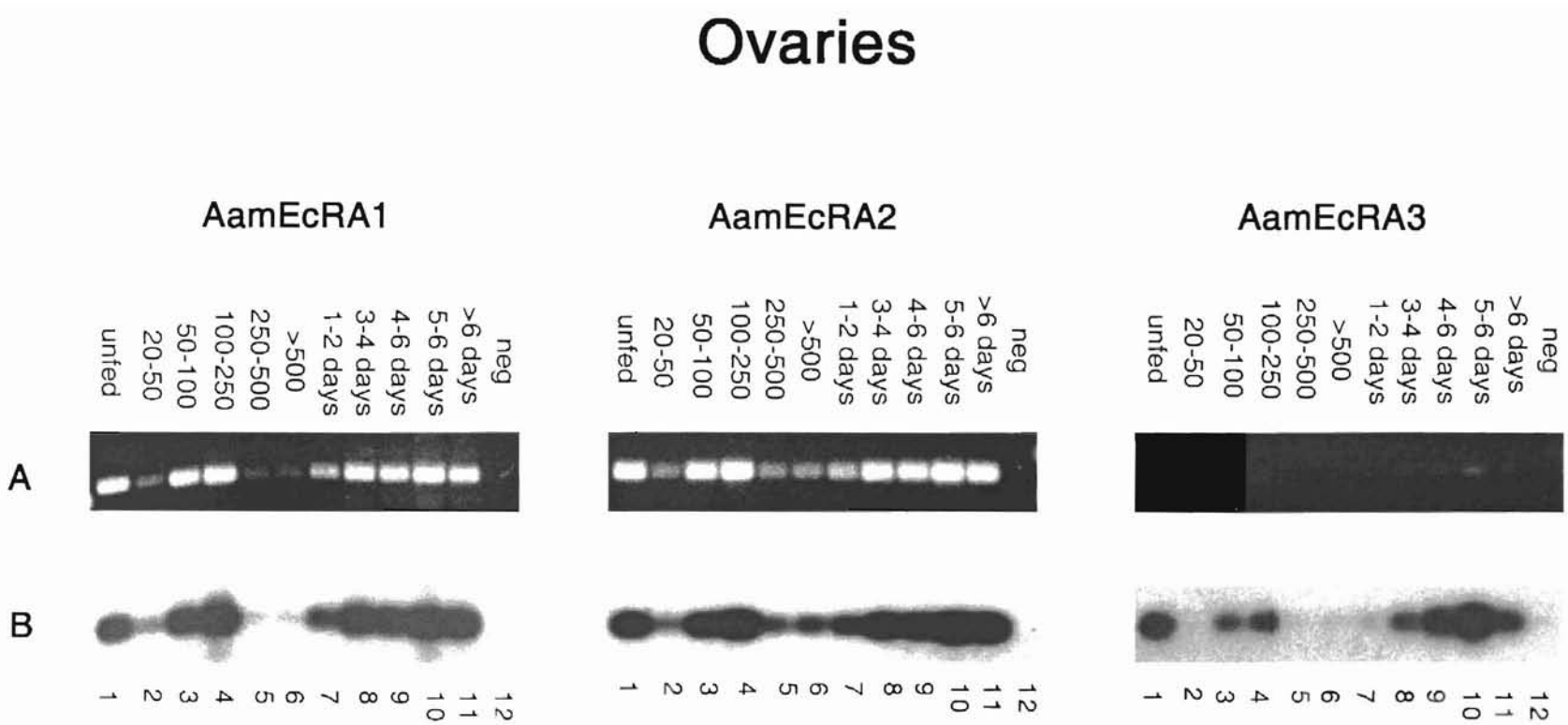

Figure 29. The expression of AamEcR isoform-specific mRNAs in ovaries from A. americanum of different weights during feeding and days following repletion. Three AamEcR isoform specific RT-PCR products were electrophoresed on 1.2% agarose gels, visualized by ethidium bromide staining (Panel A, left, middle and right), and hybridized with an AamEcRA1, AamEcRA2 or AamEcRA3-specific internal oligonucleotide (Panel B, left, middle and right). Single products of 530 bp (AamEcRA1), 428 bp (AamEcRA2) and 348 bp (AamEcRA3) were detected.

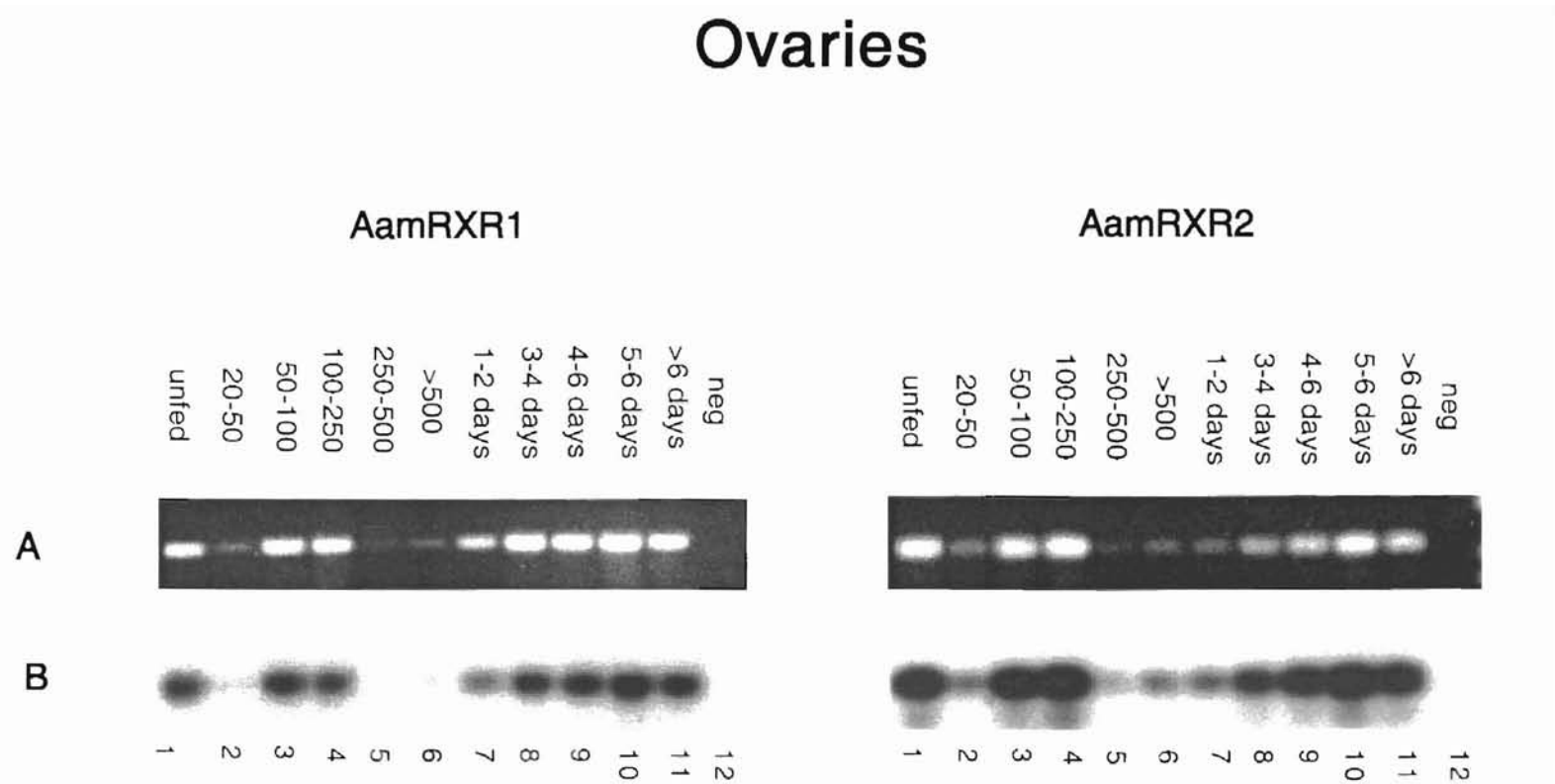

Figure 30. The expression of AamRXR1 and AamRXR2 in ovaries from A. americanum of different weights during feeding and days following repletion. AamRXR1 and AamRXR2 products were electrophoresed on 1.2% agarose gels, visualized by ethidium bromide staining (Panel A, left and right), and hybridized with an AamRXR1 or an AamRXR2-specific internal oligonucleotide (Panel B, left and right). Single products of 665 bp (AamRXR1) and 412 bp (AamRXR2) were detected.

	unfed	20-50 mg	50-100 mg	100-250 mg	250-500 mg	>500 mg	1-2 days	3-4 days	4-6 days	5-6 days	>6 days
Actin	+++	++	+++	+++	+	+	++	++	+++	+++	+++
AamEcR-common	+++	+	+++	+++	+	+	++	++	++	+++	+++
AamEcRA1	+++	+	+++	+++	+	+	++	+++	+++	+++	+++
AamEcRA2	+++	+	+++	+++	+	++	++	+++	+++	+++	+++
AamEcRA3	+++	-	+	+	-	+/-	+/-	+	++	+++	++
AamRXR1	++	+/-	++	++	+/-	+/-	+	++	++	+++	+++
AamRXR2	+++	+	+++	+++	+	+	+	++	++	+++	+++

Table XII. Relative levels of AamEcR, AamRXR and actin mRNAs in *A. americanum* ovaries during feeding and oviposition. The symbol "-" and "+++" stand for the lowest and highest expression levels for a given primer set, respectively. Amplification levels of different primer sets are not directly comparable.

VITA

Xiaojing Jin

Candidate for the degree of

Master of Science

Thesis: EXPRESSION OF ECDYSONE AND RETINOID X RECEPTORS IN THE IXODID TICK, *Amblyomma americanum* (L.)

Major field: Entomology

Biographical:

Personal Data: Born in Tianjin, P. R. China, On May 22, 1966, the daughter of Lingjiao Jin and Mingyu Luo.

Education: Graduated from Nankai Middle School, Tianjin, P. R. China in July 1984; received Bachelor of Science degree in Biomedical Engineering and Instrumentation from Zhejiang University, Hangzhou, Zhejiang, P. R. China in July 1989; completed the requirement for the Master of Science degree in Entomology at Oklahoma State University in December 1998.

Experience: Medical Statistician and Software Programmer at Second Affiliated Hospital of Tianjin Medical University, P. R. China, 1989-1995; Graduate research assistant in Department of Entomology at Oklahoma State University, 1995-1998.

Professional Society: Entomological Society of America